NORSAR

NORSAR Scientific Report No. 1-2011

Semiannual Technical Summary

1 July - 31 December 2010

Frode Ringdal (ed.)

Kjeller, February 2011

REPORT DOCUMENTATION PAGE

Form Approved
OMB No. 0704-0188

1. REPORT DATE *(DD-MM-YYYY)*	2. REPORT TYPE	3. DATES COVERED *(From - To)*
15-02-2011	Semiannual Technical Summary	1 July - 31 December 2010

4. TITLE AND SUBTITLE
Semiannual Technical Summary, 1 July - 31 December 2010

5a. CONTRACT NUMBER
FA2521-06-C-8003

5b. GRANT NUMBER

5c. PROGRAM ELEMENT NUMBER
NDC Support / R&D

6. AUTHOR(S)
Frode Ringdal (Ed.)

5d. PROJECT NUMBER
T/6110

5e. TASK NUMBER
SOW Task 4.2 & 4.3

5f. WORK UNIT NUMBER
CDRL sequence nos. A001-A004

7. PERFORMING ORGANIZATION NAME(S) AND ADDRESS(ES)
Stiftelsen NORSAR
Post Box 53
NO-2027 Kjeller
Norway

8. PERFORMING ORGANIZATION REPORT NUMBER
Scientific Report No. 1-2011

9. SPONSORING/MONITORING AGENCY NAME(S) AND ADDRESS(ES)
AFTAC/TTS, 1030 South Highway A1A MS 1000, Patrick AFB, FL 32925-3002

Army Space and Missile Defense Command , 1515 Wilson Blvd., Suite 720
Arlington, VA 22209

10. SPONSOR/MONITOR'S ACRONYM(S)
AFTAC/TTS & USASMDC

11. SPONSOR/MONITOR'S REPORT NUMBER(S)

12. DISTRIBUTION/AVAILABILITY STATEMENT
Approved for public release; distribution unlimited

13. SUPPLEMENTARY NOTES

14. ABSTRACT

This report describes activities carried out at NORSAR under Contract No. FA2521-06-C-8003 (T/6110) for the period 1 July - 31 December 2010. In addition, it provides summary information on operation and maintenance (O&M) activities at the Norwegian National Data Center (NDC) during the same period. The O&M activities, including operation of transmission links within Norway and to Vienna, Austria, are being funded jointly by the CTBTO/PTS and the Norwegian Government, with the understanding that the funding of O&M activities for primary stations in the International Monitoring System (IMS) will gradually be transferred to the CTBTO/PTS. The O&M statistics presented in this report are included for the purpose of completeness, and in order to maintain consistency with earlier reporting practice. Some of the research activities described in this report are funded by the United States (cont.)

15. SUBJECT TERMS
NORSAR, Norwegian Seismic Array

16. SECURITY CLASSIFICATION OF:			17. LIMITATION OF ABSTRACT	18. NUMBER OF PAGES	19a. NAME OF RESPONSIBLE PERSON
a. REPORT	b. ABSTRACT	c. THIS PAGE			Mr. Kyle S. Roberts, AFTAC/TTX
U	U	U	SAR	71	19b. TELEPHONE NUMBER *(Include area code)* (321) 494-9471

Reset

Standard Form 298 (Rev. 8/98)
Prescribed by ANSI Std. Z39.18

Abstract (cont.)

Government, and the United States also covers the cost of transmission of selected data from the Norwegian NDC to the United States NDC.

The seismic arrays operated by NOR-NDC comprise the Norwegian Seismic Array (NOA), the Arctic Regional Seismic Array (ARCES) and the Spitsbergen Regional Array (SPITS). This report presents statistics for these three arrays as well as for additional seismic stations which through cooperative agreements with institutions in the host countries provide continuous data to NOR-NDC. These additional stations include the Finnish Regional Seismic Array (FINES) and the Hagfors array in Sweden (HFS).

The NOA Detection Processing system has been operated throughout the period with an uptime of 99.998%. A total of 2,038 seismic events have been reported in the NOA monthly seismic bulletin during the reporting period. On-line detection processing and data recording at the NDC of data from ARCES, FINES, SPITS and HFS data have been conducted throughout the period. Processing statistics for the arrays for the reporting period are given.

A summary of the activities at the NOR-NDC and relating to field installations during the reporting period is provided in Section 4. Norway is now contributing primary station data from two seismic arrays: NOA (PS27) and ARCES (PS28), one auxiliary seismic array SPITS (AS72), and one auxiliary three-component station JMIC (AS73). These data are being provided to the IDC via the global communications infrastructure (GCI). Continuous data from the three arrays are in addition being transmitted to the US NDC. The performance of the data transmission to the US NDC has been satisfactory during the reporting period.

So far among the Norwegian stations, the NOA and the ARCES array (PS27 and PS28 respectively), the radionuclide station at Spitsbergen (RN49) and the auxiliary seismic stations on Spitsbergen (AS72) and Jan Mayen (AS73) have been certified. Provided that adequate funding continues to be made available (from the CTBTO/PTS and the Norwegian Ministry of Foreign Affairs), we envisage continuing the provision of data from these and other Norwegian IMS-designated stations in accordance with current procedures. As part of NORSAR's obsolescence management, a recapitalization plan for PS27 and PS28 was submitted to CTBTO/PTS in October 2008, in order to prevent severe degradation of the stations due to lack of spare parts. Testing of new equipment has been done during 2010, and full deployment in the NOA array is expected in 2011.

The IMS infrasound station originally planned to be located near Karasjok (IS37) will need to be moved to another site, since the local authorities have not granted the permissions required for the establishment of the station. Alternative locations have been pursued, and we have identified two alternative sites in northern Norway for possible installation of IS37. Work is progressing towards installation at one of these sites, and the CTBTO PrepCom has approved a corresponding coordinate change for the site.

Summaries of four scientific and technical contributions presented in Chapter 6 of this report are provided below:

Section 6.1 describes the results from an initial phase of a study investigating various approaches to assessing the validity of seismic events defined through automatic phase association at the International Data Center (IDC). The main idea is to develop and test various consistency measures for individual phases associated with a seismic event, using in particular the dynamic phase information (i.e. amplitudes/magnitudes). In this process, we will use the detec-

tion parameters of each station associated with the event as well as the information from non-detecting stations (i.e. stations not listed as associated with the event).

Our approach focuses on developing a procedure to check individual phases of events defined after the Global association (GA) process has been performed and magnitudes have been calculated. The procedure would be particularly suitable for application after the final automatic event list (SEL3) has been produced, but in principle such checks could be applied at any point in the phase association procedure, with feedback to GA for reprocessing as appropriate.

The present contribution is a study of the various body-wave magnitudes calculated routinely by the IDC and published in the Reviewed Event Bulletin (REB) and the Late Event Bulletin (LEB). The IDC routinely computes a number of different magnitude estimates. In this study we have compared four of them, named mb, mb1, mbmle and mb1mle. The mb is the standard body-wave magnitude calculated by averaging the observed magnitudes at all stations in the epicentral distance range 20-100 degrees which detected the event. The magnitude mb1, which is denoted the 'generalized body-wave magnitude' is estimated by using stations in the distance range 2-180 degrees, and includes the station corrections as well as distance weighting factors. The magnitudes mbmle and mb1mle are maximum-likelihood estimates of mb and mb1, respectively.

We note that the magnitude values are fairly consistent, but the two mb1-based magnitudes are on the average about 0.1-0.2 units higher than the corresponding ones based on mb. The difference is largest at the low magnitude end. The maximum-likelihood magnitudes (mbmle and mb1mle) are more mutually consistent than the averaged magnitudes (mb and mb1). This is observed in all regions we have studied. The lower scatter for the maximum-likelihood magnitudes is attributed to the fact that the correction for non-detections reduces the standard deviation of individual network magnitude estimates.

The contribution also provides some initial recommendations to the IDC. The study will continue by including additional information such as the results of the continuous Threshold Monitoring carried out at the IDC.

Section 6.2 is entitled: "Late stages of the Storfjorden, Svalbard, aftershock sequence". On 21 February 2008, a strong earthquake of moment magnitude Mw = 6.1 occurred in the offshore area of Storfjorden, Svalbard. The event was followed by a vast aftershock sequence, recorded by the seismological stations in the broader region, and is still ongoing at the time of this report. The paper analyzes the spatial and temporal distribution of this seismicity based partly on listings of NORSAR's regional, analyst reviewed bulletin, which contains events with an automatic magnitude larger than 2.0. For some of these events, the epicenters are relocated with the use of additional data, different velocity models and/or different phase identification compared to the routine analysis.

Additionally, in order to retrieve information about the distribution of events of smaller magnitude, a waveform cross-correlation detector on the data of the broadband sensor at the Polish Polar station Hornsund (HSPB) has been used. For this cross-correlation, a total of 23 master events from the sequence were selected as templates. These events were distributed troughout the three-year period, and resulted in an increase of observed aftershocks from about 400 to almost 1500. Interestingly, the different templates provided a highly variable number of additional events: ranging from 0 for one of the templates to more than 300 for the 'best' one.

In summary, monitoring of the persisting seismic activity in the area of Storfjorden, Svalbard, leads us to the conclusion that this is a continuation of the February 2008 earthquake series.

However, from autumn 2010 on, the main part of the activity is concentrated in an area SW of the original aftershock region, revealing a new source, either on a different part of the fault that gave the magnitude 6.1 mainshock in 2008 or on a neighboring tectonic structure. A solid conclusion on the characteristics and nature of this source can only be derived from the calculation of focal mechanisms for the largest, most recent events. It is clear though, based on waveform similarity and the spatio-temporal distribution of these late events, that the mechanism behind their occurrence is different than that of the earlier stages of the series. The large magnitudes ($M > 4.0$) observed during this latest stage further suggest that the region is far from reaching equilibrium.

Section 6.3 describes the installation of a new seismic broadband station in Barentsburg, Svalbard. Within the framework of the project 'Cooperative seismological studies on Spitsbergen' (Polar Research program of the Research Council of Norway), NORSAR is expanding its long-standing cooperation with the Kola Regional Seismological Centre (KRSC) in monitoring seismic events in the European Arctic. KRSC has been operating a seismic station in Barentsburg for many years and one of the major goals of the project was to acquire and install a modern broadband instrument. The new station in Barentsburg (BRBA) will improve the monitoring capability of man-made events (e.g., mining blasts, rock bursts), seismic events related to the moving of glaciers (icequakes, calving) and regional and teleseismic earthquakes. It will be a significant supplement to the already existing permanent stations in the Svalbard region in Adventdalen (SPITS), Ny-Ålesund (KBS), Hornsund (HSPB) and Hopen (HOPEN).

The new data acquisition system started up on 13 September 2010 and since then continuous data (3 components at 80 Hz) have been recorded and stored locally on a laptop. We are working on establishing a dedicated internet connection with fixed IP address in order to fully integrate the station into our data storage and processing environment at NORSAR.

The first data from the new broadband station in Barentsburg became available in January 2011 for analysis and quality check. It became very soon clear that the data quality of this station varies significantly with the time of the day. During working hours, the noise level in the high frequency range can be quite high although the man-made noise usually decreases during night time. The station has already recorded many smaller and larger earthquakes in the region. In 2011 we plan installation of a second broadband sensor (BRBB) near Barentsburg, but farther away from the disturbing man-made noise sources.

Section 6.4 describes testing of new hybrid seismometers at NORSAR. In the framework of the recapitalization of the NORSAR arrays NOA and ARCES (primary stations PS27 and PS28, respectively) and a potential modernization of the SPITS array (auxiliary station AS72) we wish to install new digitizers and sensors. One of our goals was to specify one sensor type suitable for all our arrays. Having a uniform sensor at all sites will simplify maintenance and data processing as well as improve the operational readiness, because of the interchangeability of spare parts.

Most of the seismometer systems currently in use at the NORSAR arrays have a response proportional to velocity. However, for two of them the response is proportional to acceleration. In order to decide on a new sensor type we were taking into account the ambient noise conditions and the experiences with our existing systems. Eventually we decided upon a seismic sensor with a newly designed hybrid response. We specified the desired shape and Güralp Systems designed and fabricated the sensor.

NORSAR received two prototypes of the new sensor in early 2010 and five second-generation prototypes in summer 2010. We carried out extensive testing of the new sensors at the NORSAR test facility at the site NC602 of the NOA array. This test facility has a central building (the center of the former NORES regional array) and communication to the nearby subsurface bunker that houses the IMS short-period Teledyne and Güralp instrument. This spacious bunker has three seismometer pits out of which two have been used for testing purposes. Detailed results of the testing is presented in the paper.

In summary, the new hybrid seismic sensors to be installed in the NORSAR arrays will have a transfer function that is designed to be suitable for the ambient noise conditions of our sites and to deliver similar or higher data quality than the existing systems are providing. Additionally, the hybrid response reduces the risk of clipping high-frequency signals from local events, and provides improved sensitivity for long-period signals. The instrument noise of the new hybrid sensors is below the Peterson low noise model for frequencies above 0.03 Hz. The coherency is very good (>0.9) for frequencies between 0.03 Hz and 20 Hz under quiet ambient noise conditions. From direct waveform comparisons we can conclude that we can expand these frequency limits (especially in the high-frequency end) for practical applications, because the waveform similarity is still satisfactory even for coherency values down to 0.6.

AFTAC Project Authorization	:	T/6110
Purchase Request No.	:	F3KTK85290A1
Name of Contractor	:	Stiftelsen NORSAR
Effective Date of Contract	:	1 March 2006
Contract Expiration Date	:	30 September 2011
Amount of Contract	:	$ 1,003,494.00
Project Manager	:	Frode Ringdal +47 63 80 59 00
Title of Work	:	The Norwegian Seismic Array (NORSAR) Phase 3
Period Covered by Report	:	1 July - 31 December 2010

The views and conclusions contained in this document are those of the authors and should not be interpreted as necessarily representing the official policies, either expressed or implied, of the U.S. Government.

Part of the research presented in this report was supported by the Army Space and Missile Defense Command, under contract no. W9113M-05-C-0224. Other activities were supported and monitored by AFTAC, Patrick AFB, FL32925, under contract no. FA2521-06-C-8003. Other sponsors are acknowledged where appropriate.

The operational activities of the seismic field systems and the Norwegian National Data Center (NDC) are currently jointly funded by the Norwegian Government and the CTBTO/PTS, with the understanding that the funding of appropriate IMS-related activities will gradually be transferred to the CTBTO/PTS.

Table of Contents

Page

1 Summary

This report describes activities carried out at NORSAR under Contract No. FA2521-06-C-8003 for the period 1 July - 31 December 2010. In addition, it provides summary information on operation and maintenance (O&M) activities at the Norwegian National Data Center (NOR-NDC) during the same period. The O&M activities, including operation of transmission links within Norway and to Vienna, Austria are being funded jointly by the CTBTO/PTS and the Norwegian Government, with the understanding that the funding of O&M activities for primary stations in the International Monitoring System (IMS) will gradually be transferred to the CTBTO/PTS. The O&M statistics presented in this report are included for the purpose of completeness, and in order to maintain consistency with earlier reporting practice. Some of the research activities described in this report are funded by the United States Government, and the United States also covers the cost of transmission of selected data from the Norwegian NDC to the United States NDC.

The seismic arrays operated by NOR-NDC comprise the Norwegian Seismic Array (NOA), the Arctic Regional Seismic Array (ARCES) and the Spitsbergen Regional Array (SPITS). This report presents statistics for these three arrays as well as for additional seismic stations which through cooperative agreements with institutions in the host countries provide continuous data to NOR-NDC. These additional stations include the Finnish Regional Seismic Array (FINES) and the Hagfors array in Sweden (HFS).

The NOA Detection Processing system has been operated throughout the period with an uptime of 99.998%. A total of 2,038 seismic events have been reported in the NOA monthly seismic bulletin during the reporting period. On-line detection processing and data recording at the NDC of data from ARCES, FINES, SPITS and HFS data have been conducted throughout the period. Processing statistics for the arrays for the reporting period are given.

A summary of the activities at the NOR-NDC and relating to field installations during the reporting period is provided in Section 4. Norway is now contributing primary station data from two seismic arrays: NOA (PS27) and ARCES (PS28), one auxiliary seismic array SPITS (AS72), and one auxiliary three-component station JMIC (AS73). These data are being provided to the IDC via the global communications infrastructure (GCI). Continuous data from the three arrays are in addition being transmitted to the US NDC. The performance of the data transmission to the US NDC has been satisfactory during the reporting period.

So far among the Norwegian stations, the NOA and the ARCES array (PS27 and PS28 respectively), the radionuclide station at Spitsbergen (RN49) and the auxiliary seismic stations on Spitsbergen (AS72) and Jan Mayen (AS73) have been certified. Provided that adequate funding continues to be made available (from the CTBTO/PTS and the Norwegian Ministry of Foreign Affairs), we envisage continuing the provision of data from these and other Norwegian IMS-designated stations in accordance with current procedures. As part of NORSAR's obsolescence management, a recapitalization plan for PS27 and PS28 was submitted to CTBTO/PTS in October 2008, in order to prevent severe degradation of the stations due to lack of spare parts. Testing of new equipment has been done during 2010, and full deployment in the NOA array is expected in 2011.

The IMS infrasound station originally planned to be located near Karasjok (IS37) will need to be moved to another site, since the local authorities have not granted the permissions required for the establishment of the station. Alternative locations have been pursued, and we have identified two alternative sites in northern Norway for possible installation of IS37. Work is pro-

gressing towards installation at one of these sites, and the CTBTO PrepCom has approved a corresponding coordinate change for the site.

Summaries of four scientific and technical contributions presented in Chapter 6 of this report are provided below:

Section 6.1 describes the results from an initial phase of a study investigating various approaches to assessing the validity of seismic events defined through automatic phase association at the International Data Center (IDC). The main idea is to develop and test various consistency measures for individual phases associated with a seismic event, using in particular the dynamic phase information (i.e. amplitudes/magnitudes). In this process, we will use the detection parameters of each station associated with the event as well as the information from non-detecting stations (i.e. stations not listed as associated with the event).

Our approach focuses on developing a procedure to check individual phases of events defined after the Global association (GA) process has been performed and magnitudes have been calculated. The procedure would be particularly suitable for application after the final automatic event list (SEL3) has been produced, but in principle such checks could be applied at any point in the phase association procedure, with feedback to GA for reprocessing as appropriate.

The present contribution is a study of the various body-wave magnitudes calculated routinely by the IDC and published in the Reviewed Event Bulletin (REB) and the Late Event Bulletin (LEB). The IDC routinely computes a number of different magnitude estimates. In this study we have compared four of them, named mb, mb1, mbmle and mb1mle. The mb is the standard body-wave magnitude calculated by averaging the observed magnitudes at all stations in the epicentral distance range 20-100 degrees which detected the event. The magnitude mb1, which is denoted the 'generalized body-wave magnitude' is estimated by using stations in the distance range 2-180 degrees, and includes the station corrections as well as distance weighting factors. The magnitudes mbmle and mb1mle are maximum-likelihood estimates of mb and mb1, respectively.

We note that the magnitude values are fairly consistent, but the two mb1-based magnitudes are on the average about 0.1-0.2 units higher than the corresponding ones based on mb. The difference is largest at the low magnitude end. The maximum-likelihood magnitudes (mbmle and mb1mle) are more mutually consistent than the averaged magnitudes (mb and mb1). This is observed in all regions we have studied. The lower scatter for the maximum-likelihood magnitudes is attributed to the fact that the correction for non-detections reduces the standard deviation of individual network magnitude estimates.

The contribution also provides some initial recommendations to the IDC. The study will continue by including additional information such as the results of the continuous Threshold Monitoring carried out at the IDC.

Section 6.2 is entitled: "Late stages of the Storfjorden, Svalbard, aftershock sequence". On 21 February 2008, a strong earthquake of moment magnitude Mw = 6.1 occurred in the offshore area of Storfjorden, Svalbard. The event was followed by a vast aftershock sequence, recorded by the seismological stations in the broader region, and is still ongoing at the time of this report. The paper analyzes the spatial and temporal distribution of this seismicity based partly on listings of NORSAR's regional, analyst reviewed bulletin, which contains events with an automatic magnitude larger than 2.0. For some of these events, the epicenters are relocated with the use of additional data, different velocity models and/or different phase identification compared to the routine analysis.

Additionally, in order to retrieve information about the distribution of events of smaller magnitude, a waveform cross-correlation detector on the data of the broadband sensor at the Polish Polar station Hornsund (HSPB) has been used. For this cross-correlation, a total of 23 master events from the sequence were selected as templates. These events were distributed troughout the three-year period, and resulted in an increase of observed aftershocks from about 400 to almost 1500. Interestingly, the different templates provided a highly variable number of additional events: ranging from 0 for one of the templates to more than 300 for the 'best' one.

In summary, monitoring of the persisting seismic activity in the area of Storfjorden, Svalbard, leads us to the conclusion that this is a continuation of the February 2008 earthquake series. However, from autumn 2010 on, the main part of the activity is concentrated in an area SW of the original aftershock region, revealing a new source, either on a different part of the fault that gave the magnitude 6.1 mainshock in 2008 or on a neighboring tectonic structure. A solid conclusion on the characteristics and nature of this source can only be derived from the calculation of focal mechanisms for the largest, most recent events. It is clear though, based on waveform similarity and the spatio-temporal distribution of these late events, that the mechanism behind their occurrence is different than that of the earlier stages of the series. The large magnitudes ($M > 4.0$) observed during this latest stage further suggest that the region is far from reaching equilibrium.

Section 6.3 describes the installation of a new seismic broadband station in Barentsburg, Svalbard. Within the framework of the project 'Cooperative seismological studies on Spitsbergen' (Polar Research program of the Research Council of Norway), NORSAR is expanding its long-standing cooperation with the Kola Regional Seismological Centre (KRSC) in monitoring seismic events in the European Arctic. KRSC has been operating a seismic station in Barentsburg for many years and one of the major goals of the project was to acquire and install a modern broadband instrument. The new station in Barentsburg (BRBA) will improve the monitoring capability of man-made events (e.g., mining blasts, rock bursts), seismic events related to the moving of glaciers (icequakes, calving) and regional and teleseismic earthquakes. It will be a significant supplement to the already existing permanent stations in the Svalbard region in Adventdalen (SPITS), Ny-Ålesund (KBS), Hornsund (HSPB) and Hopen (HOPEN).

The new data acquisition system started up on 13 September 2010 and since then continuous data (3 components at 80 Hz) have been recorded and stored locally on a laptop. We are working on establishing a dedicated internet connection with fixed IP address in order to fully integrate the station into our data storage and processing environment at NORSAR.

The first data from the new broadband station in Barentsburg became available in January 2011 for analysis and quality check. It became very soon clear that the data quality of this station varies significantly with the time of the day. During working hours, the noise level in the high frequency range can be quite high although the man-made noise usually decreases during night time. The station has already recorded many smaller and larger earthquakes in the region. In 2011 we plan installation of a second broadband sensor (BRBB) near Barentsburg, but farther away from the disturbing man-made noise sources.

Section 6.4 describes testing of new hybrid seismometers at NORSAR. In the framework of the recapitalization of the NORSAR arrays NOA and ARCES (primary stations PS27 and PS28, respectively) and a potential modernization of the SPITS array (auxiliary station AS72) we wish to install new digitizers and sensors. One of our goals was to specify one sensor type suitable for all our arrays. Having a uniform sensor at all sites will simplify maintenance and

data processing as well as improve the operational readiness, because of the interchangeability of spare parts.

Most of the seismometer systems currently in use at the NORSAR arrays have a response proportional to velocity. However, for two of them the response is proportional to acceleration. In order to decide on a new sensor type we were taking into account the ambient noise conditions and the experiences with our existing systems. Eventually we decided upon a seismic sensor with a newly designed hybrid response. We specified the desired shape and Güralp Systems designed and fabricated the sensor.

NORSAR received two prototypes of the new sensor in early 2010 and five second-generation prototypes in summer 2010. We carried out extensive testing of the new sensors at the NORSAR test facility at the site NC602 of the NOA array. This test facility has a central building (the center of the former NORES regional array) and communication to the nearby subsurface bunker that houses the IMS short-period Teledyne and Güralp instrument. This spacious bunker has three seismometer pits out of which two have been used for testing purposes. Detailed results of the testing is presented in the paper.

In summary, the new hybrid seismic sensors to be installed in the NORSAR arrays will have a transfer function that is designed to be suitable for the ambient noise conditions of our sites and to deliver similar or higher data quality than the existing systems are providing. Additionally, the hybrid response reduces the risk of clipping high-frequency signals from local events, and provides improved sensitivity for long-period signals. The instrument noise of the new hybrid sensors is below the Peterson low noise model for frequencies above 0.03 Hz. The coherency is very good (>0.9) for frequencies between 0.03 Hz and 20 Hz under quiet ambient noise conditions. From direct waveform comparisons we can conclude that we can expand these frequency limits (especially in the high-frequency end) for practical applications, because the waveform similarity is still satisfactory even for coherency values down to 0.6.

Frode Ringdal

2 Operation of International Monitoring System (IMS) Stations in Norway

2.1 PS27 — Primary Seismic Station NOA

The mission-capable data statistics were 99.998%, as compared to 100% for the previous reporting period. The net instrument availability was 99.625%.

There were no outages of all subarrays at the same time in the reporting period.

Monthly uptimes for the NORSAR on-line data recording task, taking into account all factors (field installations, transmissions line, data center operation) affecting this task were as follows:

2010		Mission Capable	Net instrument availability
July	:	100%	98.092%
August	:	100%	95.048%
September	:	99.988%	96.545%
October	:	100%	96.708%
November	:	100%	96.571%
December	:	100%	96.788%

B. Paulsen

NOA Event Detection Operation

In Table 2.1.1 some monthly statistics of the Detection and Event Processor operation are given. The table lists the total number of detections (DPX) triggered by the on-line detector, the total number of detections processed by the automatic event processor (EPX) and the total number of events accepted after analyst review (teleseismic phases, core phases and total).

	Total DPX	Total EPX	Accepted Events		Sum	Daily
			P-phases	Core Phases		
Jul	7,057	846	280	70	350	11.3
Aug	6,938	898	315	80	395	12.7
Sep	8,235	865	239	58	297	9.9
Oct	10,019	808	233	44	277	8.9
Nov	10,786	963	252	65	317	10.6
Dec	13,066	1,178	344	58	402	13.0
	56,101	5.558	1,663	375	2,038	11.1

Table 2.1.1. *Detection and Event Processor statistics, 1 July - 31 December 2010.*

NOA detections

The number of detections (phases) reported by the NORSAR detector during day 182, 2010, through day 365, 2010, was 56,101, giving an average of 305 detections per processed day (184 days processed).

B. Paulsen
U. Baadshaug

2.2 PS28 — Primary Seismic Station ARCES

The mission-capable data statistics were 99.368%, as compared to 99.997% for the previous reporting period. The net instrument availability was 97.859%.

The main outages in the period are presented in Table 2.2.1.

Day	Period
16 Sep	17.24-17.26
17 Sep	06.41-06.43
06 Oct	09.00-00.00
07 Oct	00.00-13.00

Table 2.2.1. *The main interruptions in recording of ARCES data at NDPC, 1 July - 31 December 2010.*

Monthly uptimes for the ARCES on-line data recording task, taking into account all factors (field installations, transmission lines, data center operation) affecting this task were as follows:

2010		Mission Capable	Net instrument availability
July	:	99.991%	97.719%
August	:	99.998%	97.220%
September	:	99.988%	97.211%
October	:	96.235%	95.708%
November	:	100%	99.526%
December	:	99.999%	99.771%

B. Paulsen

Event Detection Operation

ARCES detections

The number of detections (phases) reported during day 182, 2010, through day 365, 2010, was 218,086, giving an average of 1185 detections per processed day (184 days processed).

Events automatically located by ARCES

During days 182, 2010, through 365, 2010, 9,347 local and regional events were located by ARCES, based on automatic association of P- and S-type arrivals. This gives an average of 50.8 events per processed day (184 days processed). 73% of these events are within 300 km, and 91 % of these events are within 1000 km.

U. Baadshaug

2.3 AS72 — Auxiliary Seismic Station Spitsbergen

The mission-capable data for the period were 99.964%, as compared to 98.001% for the previous reporting period. The net instrument availability was 99.945%.

The main outages in the period are presented in Table 2.3.1.

Day	Period
26 Dec	03.40-03.42

Table 2.31. *The main interruptions in recording of Spitsbergen data at NDPC, 1 July - 31 December 2010.*

Monthly uptimes for the Spitsbergen on-line data recording task, taking into account all factors (field installations, transmissions line, data center operation) affecting this task were as follows:

2010		Mission Capable	Net instrument availability
July	:	99.907%	99.905%
August	:	99.999%	99.996%
September	:	99.986%	99.850%
October	:	99.907%	99.995%
November	:	99.995%	99.936%
December	:	99.991%	99.988%

B. Paulsen

Event Detection Operation

Spitsbergen array detections

The number of detections (phases) reported from day 182, 2010, through day 365, 2010, was 419,143, giving an average of 2,278 detections per processed day (184 days processed).

Events automatically located by the Spitsbergen array

During days 182, 2010 through 365, 2010, 34,878 local and regional events were located by the Spitsbergen array, based on automatic association of P- and S-type arrivals. This gives an average of 189.6 events per processed day (184 days processed). 77% of these events are within 300 km, and 91% of these events are within 1000 km.

U. Baadshaug

2.4 AS73 — Auxiliary Seismic Station at Jan Mayen

The IMS auxiliary seismic network includes a three-component station on the Norwegian island of Jan Mayen. The station location given in the protocol to the Comprehensive Nuclear-Test-Ban Treaty is 70.9°N, 8.7°W.

The University of Bergen has operated a seismic station at this location since 1970. A so-called Parent Network Station Assessment for AS73 was completed in April 2002. A vault at a new location (71.0°N, 8.5°W) was prepared in early 2003, after its location had been approved by the PrepCom. New equipment was installed in this vault in October 2003, as a cooperative effort between NORSAR and the CTBTO/PTS. Continuous data from this station are being transmitted to the NDC at Kjeller via a satellite link installed in April 2000. Data are also made available to the University of Bergen.

The station was certified by the CTBTO/PTS on 12 June 2006.

J. Fyen

2.5 IS37 — Infrasound Station at Bardufoss

The IMS infrasound network will, according to the protocol of the CTBT, include a station at Karasjok in northern Norway. The coordinates given for this station are 69.5°N, 25.5°E. These coordinates coincide with those of the primary seismic station PS28.

It has, however, proved very difficult to obtain the necessary permits for use of land for an infrasound station in Karasjok. Various alternatives for locating the station in Karasjok were prepared, but all applications to the local authorities to obtain the permissions needed to establish the station were turned down by the local governing council in June 2007.

In 2008, investigations were initiated to identify an alternative site for IS37 outside Karasjok. Two sites at Bardufoss, at 69.1° N, 18.6° E, are currently being pursued to select one of them for possible installation of IS37. The CTBTO PrepCom has approved a corresponding coordinate change for the station.

J. Fyen

2.6 RN49 — Radionuclide Station on Spitsbergen

The IMS radionuclide network includes a station on the island of Spitsbergen. This station has been selected to be among those IMS radionuclide stations that will monitor for the presence of relevant noble gases upon entry into force of the CTBT.

A site survey for this station was carried out in August of 1999 by NORSAR, in cooperation with the Norwegian Radiation Protection Authority. The site survey report to the PTS contained a recommendation to establish this station at Platåberget, near Longyearbyen. The infrastructure for housing the station equipment was established in early 2001, and a noble gas detection system, based on the Swedish "SAUNA" design, was installed at this site in May 2001, as part of PrepCom's noble gas experiment. A particulate station ("ARAME" design) was installed at the same location in September 2001. A certification visit to the particulate station took place in October 2002, and the particulate station was certified on 10 June 2003. Both systems underwent substantial upgrading in May/June 2006. The equipment at RN49 is being maintained and operated under a contract with the CTBTO/PTS.

S. Mykkeltveit

3 Contributing Regional Seismic Arrays

3.1 NORES

NORES has been out of operation since lightning destroyed the station electronics on 11 June 2002.

B. Paulsen

3.2 Hagfors (IMS Station AS101)

Data from the Hagfors array are made available continuously to NORSAR through a cooperative agreement with Swedish authorities.

The mission-capable data statistics were 100%, as compared to 99.999% for the previous reporting period. The net instrument availability was 99.842%.

There were no outages in this period.

Monthly uptimes for the Hagfors on-line data recording task, taking into account all factors (field installations, transmissions line, data center operation) affecting this task were as follows:

2010		Mission Capable	Net instrument availability
July	:	100%	100%
August	:	100%	99.055%
September	:	100%	100%
October	:	100%	100%
November	:	100%	100%
December	:	100%	100%

B. Paulsen

Hagfors Event Detection Operation

Hagfors array detections

The number of detections (phases) reported from day 182, 2010, through day 365, 2010, was 135,294, giving an average of 735 detections per processed day (184 days processed).

Events automatically located by the Hagfors array

During days 182, 2010, through 365, 2010, 4,177 local and regional events were located by the Hagfors array, based on automatic association of P- and S-type arrivals. This gives an average of 22.7 events per processed day (184 days processed). 75% of these events are within 300 km, and 93% of these events are within 1000 km.

U. Baadshaug

3.3 FINES (IMS station PS17)

Data from the FINES array are made available continuously to NORSAR through a cooperative agreement with Finnish authorities.

The mission-capable data statistics were 99.974%, as compared to 94.662% for the previous reporting period. The net instrument availability was 99.963%.

The main outages in the period are presented in Table 3.3.1.

Day	Period
19 Oct	06.46-07.47

Table 3.3.1. *The main interruptions in recording of FINES data at NDPC, 1 July - 31 December 2010.*

Monthly uptimes for the FINES on-line data recording task, taking into account all factors (field installations, transmissions line, data center operation) affecting this task were as follows:

2010		Mission Capable	Net instrument availability
July	:	100%	99.955%
August	:	99.999%	99.980%
September	:	100%	100%
October	:	99.863%	99.866%
November	:	99.985%	99.979%
December	:	100%	100%

B. Paulsen

FINES Event Detection Operation

FINES detections

The number of detections (phases) reported during day 182, 2010, through day 365, 2010, was 40,839, giving an average of 222 detections per processed day (184 days processed).

Events automatically located by FINES

During days 182, 2010, through 365, 2010, 2,693 local and regional events were located by FINES, based on automatic association of P- and S-type arrivals. This gives an average of 14.6 events per processed day (184 days processed). 91% of these events are within 300 km, and 95% of these events are within 1000 km.

U. Baadshaug

3.4 Regional Monitoring System Operation and Analysis

The Regional Monitoring System (RMS) was installed at NORSAR in December 1989 and has been operated at NORSAR from 1 January 1990 for automatic processing of data from ARCES and NORES. A second version of RMS that accepts data from an arbitrary number of arrays and single 3-component stations was installed at NORSAR in October 1991, and regular operation of the system comprising analysis of data from the 4 arrays ARCES, NORES, FINES and GERES started on 15 October 1991. As opposed to the first version of RMS, the one in current operation also has the capability of locating events at teleseismic distances.

Data from the Apatity array was included on 14 December 1992, and from the Spitsbergen array on 12 January 1994. Detections from the Hagfors array were available to the analysts and could be added manually during analysis from 6 December 1994. After 2 February 1995, Hagfors detections were also used in the automatic phase association.

Since 24 April 1999, RMS has processed data from all the seven regional arrays ARCES, NORES, FINES, GERES (until January 2000), Apatity, Spitsbergen, and Hagfors. Starting 19 September 1999, waveforms and detections from the NORSAR array have also been available to the analyst.

Phase and event statistics

Table 3.5.1 gives a summary of phase detections and events declared by RMS. From top to bottom the table gives the total number of detections by the RMS, the number of detections that are associated with events automatically declared by the RMS, the number of detections that are not associated with any events, the number of events automatically declared by the RMS, and finally the total number of events worked on interactively (in accordance with criteria that vary over time; see below) and defined by the analyst.

New criteria for interactive event analysis were introduced from 1 January 1994. Since that date, only regional events in areas of special interest (e.g, Spitsbergen, since it is necessary to acquire new knowledge in this region) or other significant events (e.g, felt earthquakes and large industrial explosions) were thoroughly analyzed. Teleseismic events of special interest are also analyzed.

To further reduce the workload on the analysts and to focus on regional events in preparation for Gamma-data submission during GSETT-3, a new processing scheme was introduced on 2 February 1995. The GBF (Generalized Beamforming) program is used as a pre-processor to RMS, and only phases associated with selected events in northern Europe are considered in the automatic RMS phase association. All detections, however, are still available to the analysts and can be added manually during analysis.

	Jul 10	Aug 10	Sep 10	Oct 10	Nov 10	Dec 10	Total
Phase detections	138,600	165,868	162,829	157,767	181,772	170,905	977,741
- Associated phases	6,381	7,741	8,544	7,877	7,060	5,952	43,555
- Unassociated phases	132,219	158,127	154,285	149,890	174,712	164,953	934,186
Events automatically declared by RMS	1,274	1,541	1,710	1,540	1,375	1,083	8,523
No. of events defined by the analyst	97	99	97	89	77	67	526

Table 3.5.1. RMS phase detections and event summary 1 July - 31 December 2010.

4 NDC and Field Activities

4.1 NDC Activitities

NORSAR functions as the Norwegian National Data Center (NDC) for CTBT verification. Six monitoring stations, comprising altogether 132 field sensors plus radionuclide monitoring equipment, will be located on Norwegian territory as part of the future IMS as described elsewhere in this report. The four seismic IMS stations are all in operation today, and all of them are currently providing data to the CTBTO on a regular basis. PS27, PS28, AS72, AS73 and RN49 are all certified. Data recorded by the Norwegian stations is being transmitted in real time to the Norwegian NDC, and provided to the IDC through the Global Communications Infrastructure (GCI). Norway is connected to the GCI with a frame relay link to Vienna.

Operating the Norwegian IMS stations continues to require significant efforts by personnel both at the NDC and in the field. Strictly defined procedures as well as increased emphasis on regularity of data recording and timely data transmission to the IDC in Vienna have led to increased reporting activities and implementation of new procedures for the NDC. The NDC carries out all the technical tasks required in support of Norway's treaty obligations. NORSAR will also carry out assessments of events of special interest, and advise the Norwegian authorities in technical matters relating to treaty compliance. A challenge for the NDC is to carry 40 years' experience over to the next generation of personnel.

Verification functions; information received from the IDC

After the CTBT enters into force, the IDC will provide data for a large number of events each day, but will not assess whether any of them are likely to be nuclear explosions. Such assessments will be the task of the States Parties, and it is important to develop the necessary national expertise in the participating countries. An important task for the Norwegian NDC will thus be to make independent assessments of events of particular interest to Norway, and to communicate the results of these analyses to the Norwegian Ministry of Foreign Affairs.

Monitoring the Arctic region

Norway will have monitoring stations of key importance for covering the Arctic, including Novaya Zemlya, and Norwegian experts have a unique competence in assessing events in this region. On several occasions in the past, seismic events near Novaya Zemlya have caused political concern, and NORSAR specialists have contributed to clarifying these issues.

International cooperation

After entry into force of the treaty, a number of countries are expected to establish national expertise to contribute to the treaty verification on a global basis. Norwegian experts have been in contact with experts from several countries with the aim of establishing bilateral or multilateral cooperation in this field. One interesting possibility for the future is to establish NORSAR as a regional center for European cooperation in the CTBT verification activities.

NORSAR event processing

The automatic routine processing of NORSAR events as described in NORSAR Sci. Rep. No. 2-93/94, has been running satisfactorily. The analyst tools for reviewing and updating the solu-

tions have been continually modified to simplify operations and improve results. NORSAR is currently applying teleseismic detection and event processing using the large-aperture NOA array as well as regional monitoring using the network of small-aperture arrays in Fennoscandia and adjacent areas.

Communication topology

Norway has implemented an independent subnetwork, which connects the IMS stations AS72, AS73, PS28, and RN49 operated by NORSAR to the GCI at NOR_NDC. A contract has been concluded and VSAT antennas have been installed at each station in the network. Under the same contract, VSAT antennas for 6 of the PS27 subarrays have been installed for intra-array communication. The seventh subarray is connected to the central recording facility via a leased land line. The central recording facility for PS27 is connected directly to the GCI (Basic Topology). All the VSAT communication is functioning satisfactorily. As of 10 June 2005, AS72 and RN49 are connected to NOR_NDC through a VPN link.

Jan Fyen

4.2 Status Report: Provision of data from Norwegian seismic IMS stations to the IDC

Introduction

This contribution is a report for the period July - December 2010 on activities associated with provision of data from Norwegian seismic IMS stations to the International Data Centre (IDC) in Vienna. This report represents an update of contributions that can be found in previous editions of NORSAR's Semiannual Technical Summary. All four Norwegian seismic stations providing data to the IDC have now been formally certified.

Norwegian IMS stations and communications arrangements

During the reporting interval, Norway has provided data to the IDC from the four seismic stations shown in Fig. 4.2.1. PS27 —NOA is a 60 km aperture teleseismic array, comprised of 7 subarrays, each containing six vertical short period sensors and a three-component broadband instrument. PS28 — ARCES is a 25-element regional array with an aperture of 3 km, whereas AS72 — Spitsbergen array (station code SPITS) has 9 elements within a 1-km aperture. AS73 — JMIC has a single three-component broadband instrument.

The intra-array communication for NOA utilizes a land line for subarray NC6 and VSAT links based on TDMA DVB-S technology for the other 6 subarrays. The central recording facility for NOA is located at the Norwegian National Data Center (NOR_NDC).

Continuous ARCES data are transmitted from the ARCES site to NOR_NDC using TDMA DVB-S technology. The 7 VSAT links share a capacity of 256 Kbits/s.

Continuous SPITS data were transmitted to NOR_NDC via a VSAT terminal located at Platåberget in Longyearbyen (which is the site of the IMS radionuclide monitoring station RN49 installed during 2001) up to 10 June 2005. The central recording facility (CRF) for the SPITS array has been moved to the University of Spitsbergen (UNIS). A 512 bps SHDSL link has been established between UNIS and NOR_NDC. Data from the array elements to the CRF are

transmitted via a 2.4 Ghz radio link (Wilan VIP-110). Both AS72 and RN49 data are now transmitted to NOR_NDC over this link using VPN technology.

A minimum of seven-day station buffers have been established at the ARCES and SPITS sites and at all NOA subarray sites, as well as at the NOR_NDC for ARCES, SPITS and NOA. In addition, each individual site of the SPITS array has a 14-day buffer.

The NOA and ARCES arrays are primary stations in the IMS network, which implies that data from these stations is transmitted continuously to the receiving international data center. Since October 1999, this data has been transmitted (from NOR_NDC) via the Global Communications Infrastructure (GCI) to the IDC in Vienna. Data from the auxiliary array station SPITS — AS72 have been sent in continuous mode to the IDC during the reporting period. AS73 — JMIC is an auxiliary station in the IMS, and the JMIC data have been available to the IDC throughout the reporting period on a request basis via use of the AutoDRM protocol (Kradolfer, 1993; Kradolfer, 1996). In addition, continuous data from all three arrays is transmitted to the US_NDC.

Uptimes and data availability

Figs. 4.2.2 and 4.2.3 show the monthly uptimes for the Norwegian IMS primary stations ARCES and NOA, respectively, for the reporting period given as the hatched (taller) bars in these figures. These barplots reflect the percentage of the waveform data that is available in the NOR_NDC data archives for these two arrays. The downtimes inferred from these figures thus represent the cumulative effect of field equipment outages, station site to NOR_NDC communication outage, and NOR_NDC data acquisition outages.

Figs. 4.2.2 and 4.2.3 also give the data availability for these two stations as reported by the IDC in the IDC Station Status reports. The main reason for the discrepancies between the NOR_NDC and IDC data availabilities as observed from these figures is the difference in the ways the two data centers report data availability for arrays: Whereas NOR_NDC reports an array station to be up and available if at least one channel produces useful data, the IDC uses weights where the reported availability (capability) is based on the number of actually operating channels.

Use of the AutoDRM protocol

NOR_NDC's AutoDRM has been operational since November 1995 (Mykkeltveit & Baadshaug, 1996). The monthly number of requests by the IDC for JMIC data for the period July - December 2010 is shown in Fig. 4.2.4.

NDC automatic processing and data analysis

These tasks have proceeded in accordance with the descriptions given in Mykkeltveit and Baadshaug (1996). For the reporting period NOR_NDC derived information on 525 supplementary events in northern Europe and submitted this information to the Finnish NDC as the NOR_NDC contribution to the joint Nordic Supplementary (Gamma) Bulletin, which in turn is forwarded to the IDC. These events are plotted in Fig. 4.2.5.

Data access for the station NIL at Nilore, Pakistan

NOR_NDC has for many years provided access to the seismic station NIL at Nilore, Pakistan, through a VSAT satellite link between NOR_NDC and Nilore. In late July 2009, the VSAT ground station equipment at Nilore failed, and it turned out that this equipment is obsolete and cannot be repaired. The service provider has proposed the installation of new equipment. Following some technical clarifications, NORSAR will submit to AFTAC a proposal for a new satellite communications system between NOR_NDC and Nilore.

Current developments and future plans

NOR_NDC is continuing the efforts towards improving and hardening all critical data acquisition and data forwarding hardware and software components, so as to meet the requirements related to operation of IMS stations.

The NOA array was formally certified by the PTS on 28 July 2000, and a contract with the PTS in Vienna currently provides partial funding for operation and maintenance of this station. The ARCES array was formally certified by the PTS on 8 November 2001, and a contract with the PTS is in place which also provides for partial funding of the operation and maintenance of this station. The operation of the two IMS auxiliary seismic stations on Norwegian territory (Spitsbergen and Jan Mayen) is funded by the Norwegian Ministry of Foreign Affairs. Provided that adequate funding continues to be made available (from the PTS and the Norwegian Ministry of Foreign Affairs), we envisage continuing the provision of data from all Norwegian seismic IMS stations without interruption to the IDC in Vienna.

The two stations PS27 and PS28 are both suffering from lack of spare parts. The PS27 NOA equipment was acquired in 1995 and it is now impossible to get spare GPS receivers. The PS28 ARCES equipment was acquired in 1999, and it is no longer possible to get spare digitizers. A recapitilization plan for both arrays was submitted to the PTS in October 2008, and installation of new equipment will start in 2011.

U. Baadshaug
S. Mykkeltveit
J. Fyen

References

Kradolfer, U. (1993): Automating the exchange of earthquake information. *EOS, Trans., AGU*, 74, 442.

Kradolfer, U. (1996): AutoDRM — The first five years, *Seism. Res. Lett.*, 67, 4, 30-33.

Mykkeltveit, S. & U. Baadshaug (1996): Norway's NDC: Experience from the first eighteen months of the full-scale phase of GSETT-3. *Semiann. Tech. Summ., 1 October 1995 - 31 March 1996*, NORSAR Sci. Rep. No. 2-95/96, Kjeller, Norway.

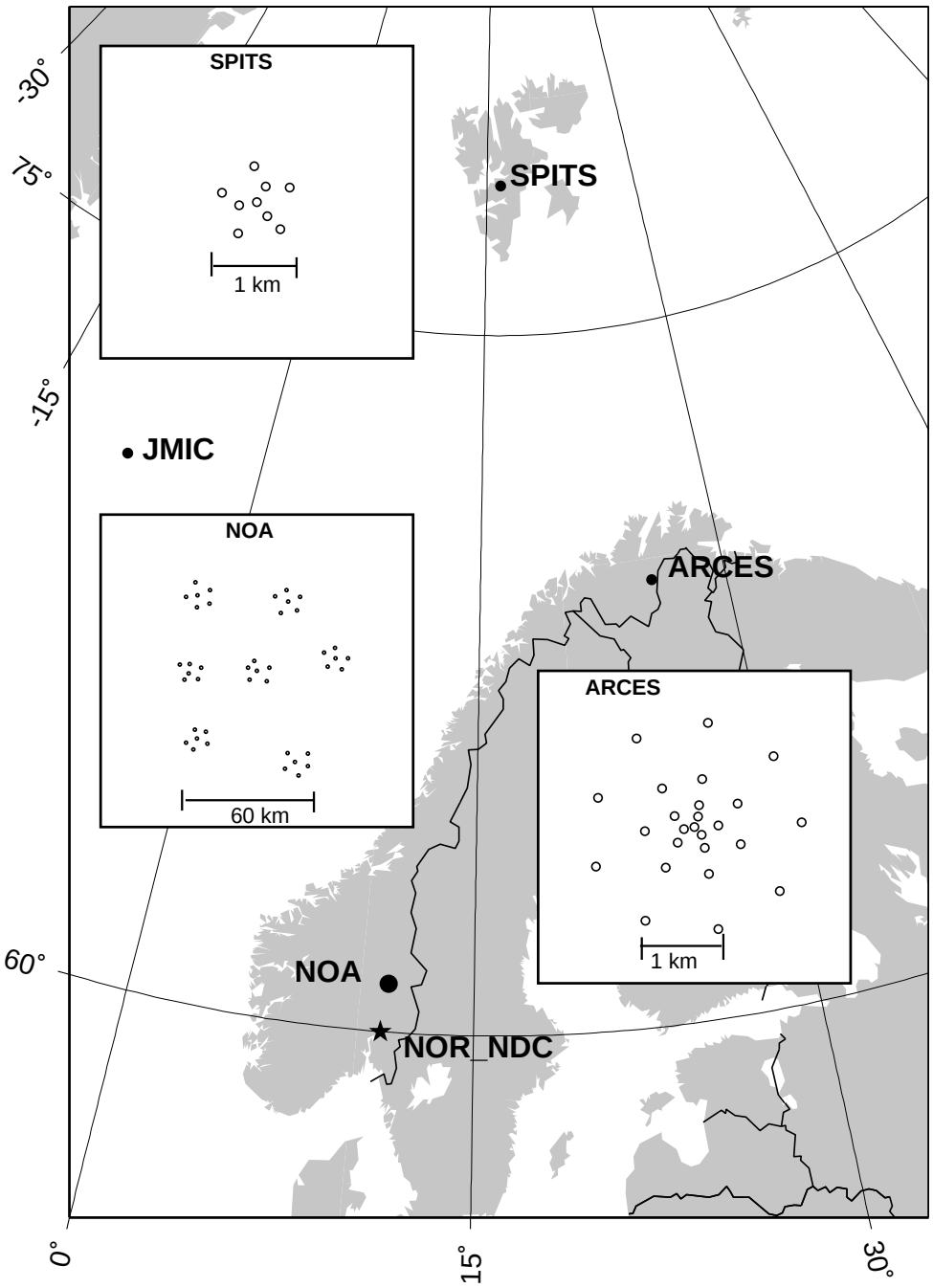

Fig. 4.2.1. The figure shows the locations and configurations of the three Norwegian seismic IMS array stations that provided data to the IDC during the period July - December 2010. The data from these stations and the JMIC three-component station are transmitted continuously and in real time to the Norwegian NDC (NOR_NDC). The stations NOA and ARCES are primary IMS stations, whereas SPITS and JMIC are auxiliary IMS stations.

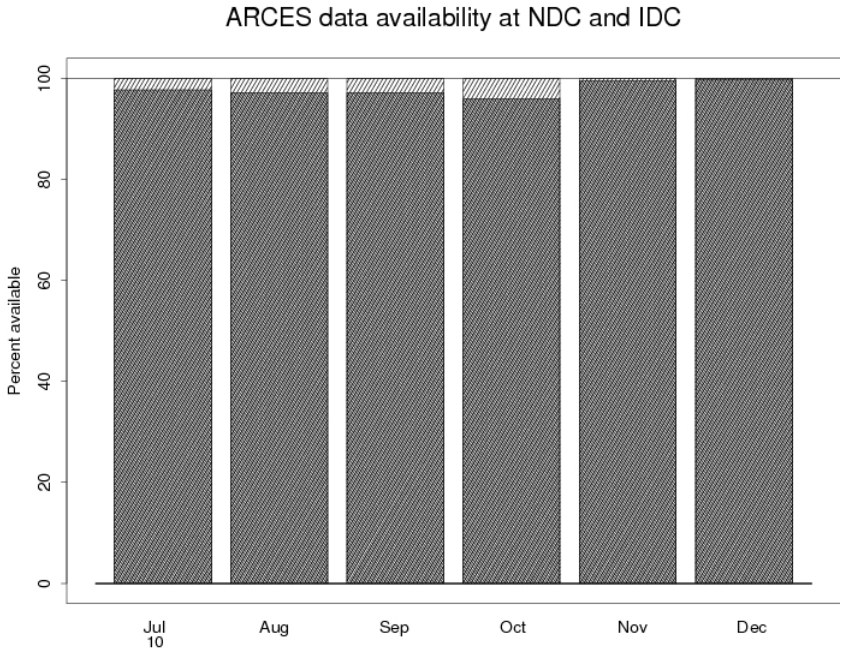

Fig. 4.2.2. The figure shows the monthly availability of ARCES array data for the period July - December 2010 at NOR_NDC and the IDC. See the text for explanation of differences in definition of the term "data availability" between the two centers. The higher values (hatched bars) represent the NOR_NDC data availability.

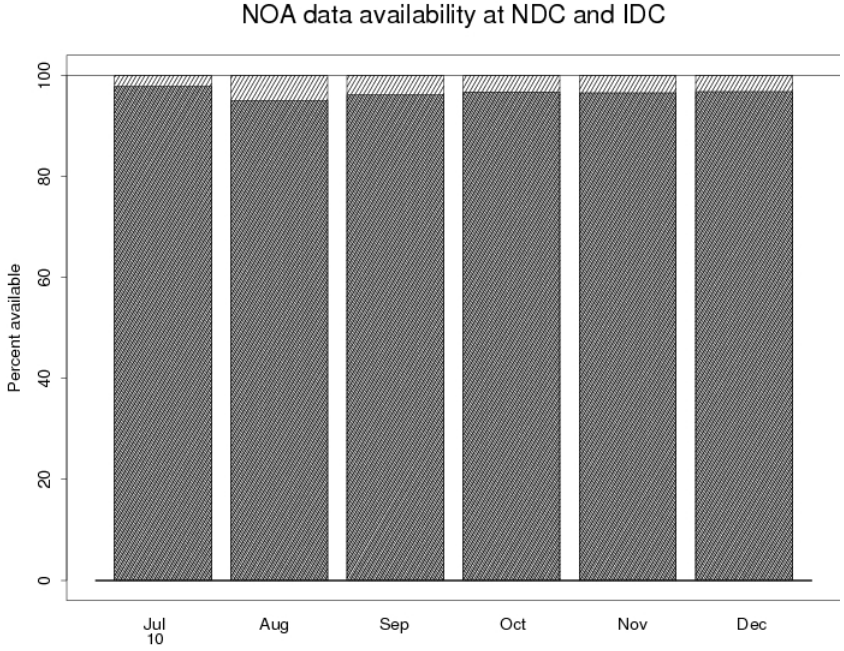

Fig. 4.2.3. The figure shows the monthly availability of NORSAR array data for the period July - December 2010 at NOR_NDC and the IDC. See the text for explanation of differences in definition of the term "data availability" between the two centers. The higher values (hatched bars) represent the NOR_NDC data availability.

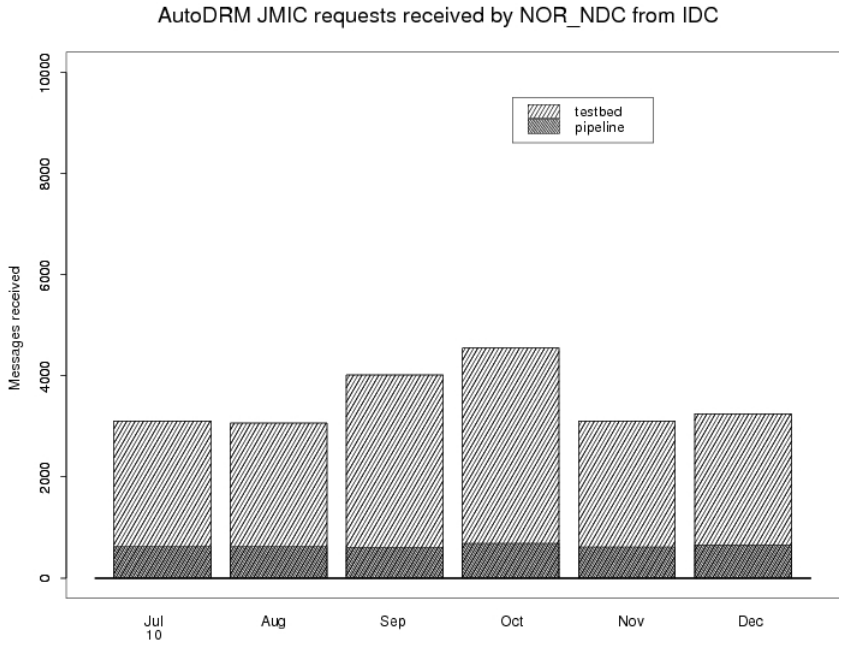

Fig. 4.2.4. The figure shows the monthly number of requests received by NOR_NDC from the IDC for JMIC waveform segments during July - December 2010.

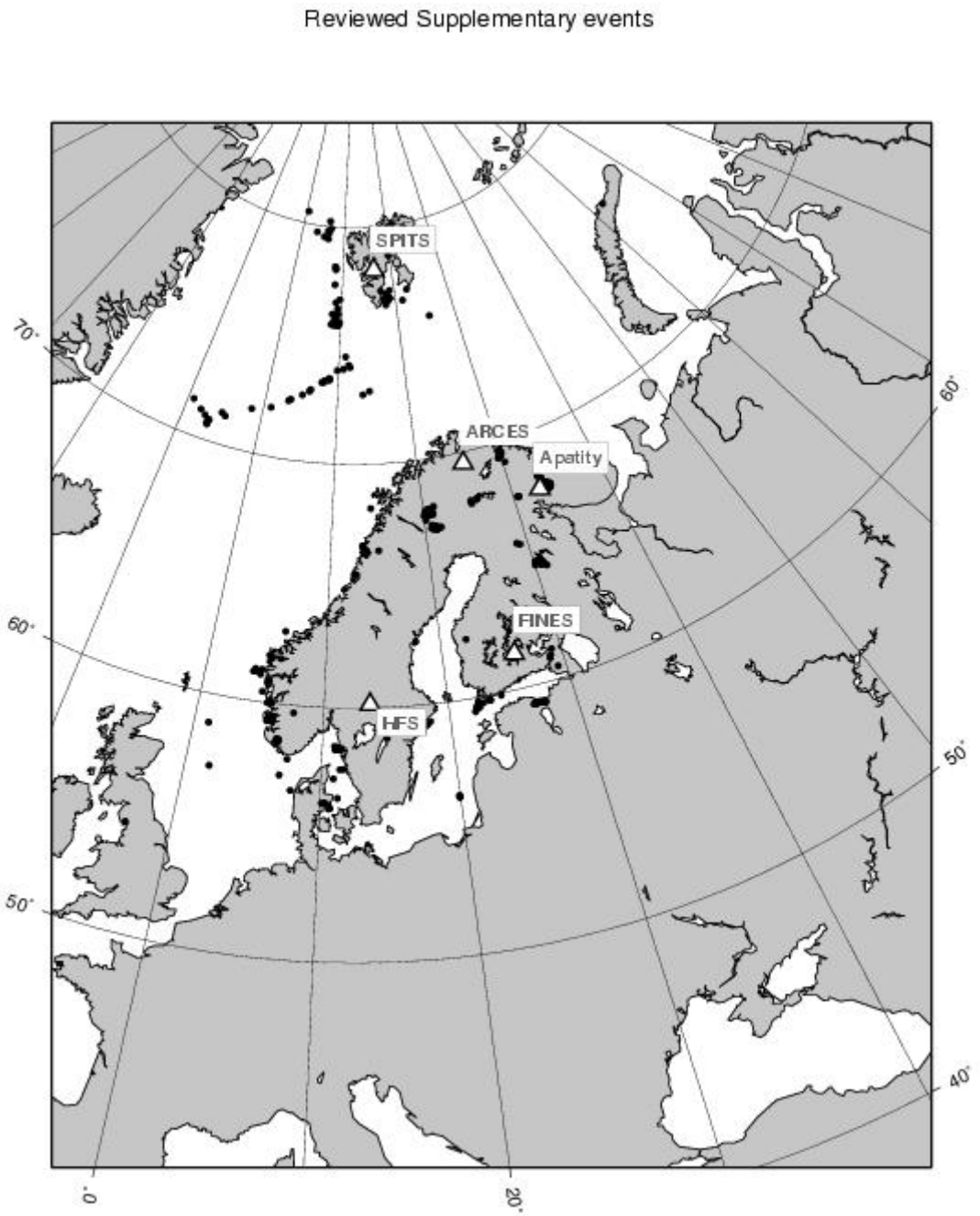

Fig. 4.2.5. The map shows the 525 events in and around Norway contributed by NOR_NDC during July - December 2010 as supplementary (Gamma) events to the IDC, as part of the Nordic supplementary data compiled by the Finnish NDC. The map also shows the main seismic stations used in the data analysis to define these events.

4.3 Field Activities

The activities at the NORSAR Maintenance Center (NMC) at Hamar currently include work related to operation and maintenance of the following IMS seismic stations: the NOA teleseismic array (PS27), the ARCES array (PS28) and the Spitsbergen array (AS72). Some work has also been carried out in connection with the seismic station on Jan Mayen (AS73), the radionuclide station at Spitsbergen (RN49), and preparations for the infrasound station at IS37. NORSAR also acts as a consultant for the operation and maintenance of the Hagfors array in Sweden (AS101).

NORSAR carries out the field activities relating to IMS stations in a manner generally consistent with the requirements specified in the appropriate IMS Operational Manuals, which are currently being developed by Working Group B of the Preparatory Commission. For seismic stations these specifications are contained in the Operational Manual for Seismological Monitoring and the International Exchange of Seismological Data (CTBT/WGB/TL-11/2), currently available in a draft version.

All regular maintenance on the NORSAR field systems is conducted on a one-shift-per-day, five-day-per-week basis. The maintenance tasks include:

- Operating and maintaining the seismic sensors and the associated digitizers, authentication devices and other electronics components.
- Maintaining the power supply to the field sites as well as backup power supplies.
- Operating and maintaining the VSATs, the data acquisition systems and the intra-array data transmission systems.
- Assisting the NDC in evaluating the data quality and making the necessary changes in gain settings, frequency response and other operating characteristics as required.
- Carrying out preventive, routine and emergency maintenance to ensure that all field systems operate properly.
- Maintaining a computerized record of the utilization, status, and maintenance history of all site equipment.
- Providing appropriate security measures to protect against incidents such as intrusion, theft and vandalism at the field installations.

Details of the daily maintenance activities are kept locally. As part of its contract with CTBTO/PTS NORSAR submits, when applicable, problem reports, outage notification reports and equipment status reports. The contents of these reports and the circumstances under which they will be submitted are specified in the draft Operational Manual.

P.W. Larsen
K.A. Løken

5 Documentation Developed

Kværna, T. & F. Ringdal (2011): Study of body-wave magnitudes calculated at the IDC. In: Semiannual Technical Summary, 1 July - 31 December 2010, NORSAR Sci. Rep. 1-2011, Kjeller.

Pirli, M., B. Paulsen & J. Schweitzer (2011): Late stages of the Storfjorden, Svalbard, after-shock sequence. In: Semiannual Technical Summary, 1 July - 31 December 2010, NORSAR Sci. Rep. 1-2011, Kjeller.

Roth, M., M.Pirli, J. Schweitzer & E. Kremenetskaya (2011): Installation of the seismic broadband station in Barentsburg, Svalbard. In: Semiannual Technical Summary, 1 July - 31 December 2011, NORSAR Sci. Rep. 1-2011, Kjeller.

Roth, M., J. Fyen, P.W. Larsen & J. Schweitzer (2011): Test of new hybrid seismometers at NORSAR. In: Semiannual Technical Summary, 1 July - 31 December 2011, NORSAR Sci. Rep. 1-2011, Kjeller.

6 Summary of Technical Reports / Papers Published

6.1 Study of body-wave magnitudes calculated at the IDC

6.1.1 Introduction

We have initiated a study to investigate various approaches to assessing the validity of seismic events defined through automatic phase association at the International Data Center (IDC). The main idea is to develop and test various consistency measures for individual phases associated with a seismic event, using in particular the dynamic phase information (i.e. amplitudes/magnitudes). We will define 'consistency indices' for each phase automatically associated with a given event, and determine empirically a threshold for these indices in order to accept or reject a phase in the event definition. In this process, we will use the detection parameters of each station associated with the event as well as the information from non-detecting stations (i.e. stations not listed as associated with the event).

Our approach focuses on developing a procedure to check individual phases of events defined after the Global association (GA) process has been performed and magnitudes have been calculated. The procedure would be particularly suitable for application after the final automatic event list (SEL3) has been produced, but in principle such checks could be applied at any point in the phase association procedure, with feedback to GA for reprocessing as appropriate.

This contribution is an initial part of developing a procedure as described above, and contains a study of the various body-wave magnitudes calculated routinely by the IDC and published in the Reviewed Event Bulletin (REB) and the Late Event Bulletin (LEB). Our purpose is not to assess the quality of these magnitude calculations, nor do we intend to compare the magnitude values to those produced by other agencies, such as the ISC or USGS. Our focus in this study is to assess the usefulness of the IDC-calculated magnitudes in providing data and criteria for dynamic assessment of the automatic phase association process at the IDC. For this purpose, the important point to study is the consistency of various magnitudes calculated at the IDC, regardless of how well they correspond to external magnitude information.

6.1.2 Body-wave magnitudes calculated at the IDC and used in this study

The IDC routinely computes a number of different magnitude estimates. In this study we have compared four of them, named mb, mb1,mbmle and mb1mle. (Note that in some connections the notations mbmx and mb1mx are used instead of mbmle and mb1mle). The mb is the standard body-wave magnitude calculated by averaging the observed magnitudes at all stations in the epicentral range 20-100 degrees which detected the event. The magnitude mb1, which is denoted the 'generalized body-wave magnitude' by Murphy and Barker (2003) is estimated by using stations in the distance range 2-180 degrees, and includes the station corrections developed by Murphy and Barker (2003) as well as distance weighting factors. The magnitudes mbmle and mb1mle are maximum-likelihood estimates of mb and mb1, respectively, using the formulation of Ringdal (1976).

The differences in the distance correction factors between mb1 and mb are illustrated in Figures 6.1.1 and 6.1.2, which show the attenuation relations as a function of distance for the two magnitude types for events at zero depth.

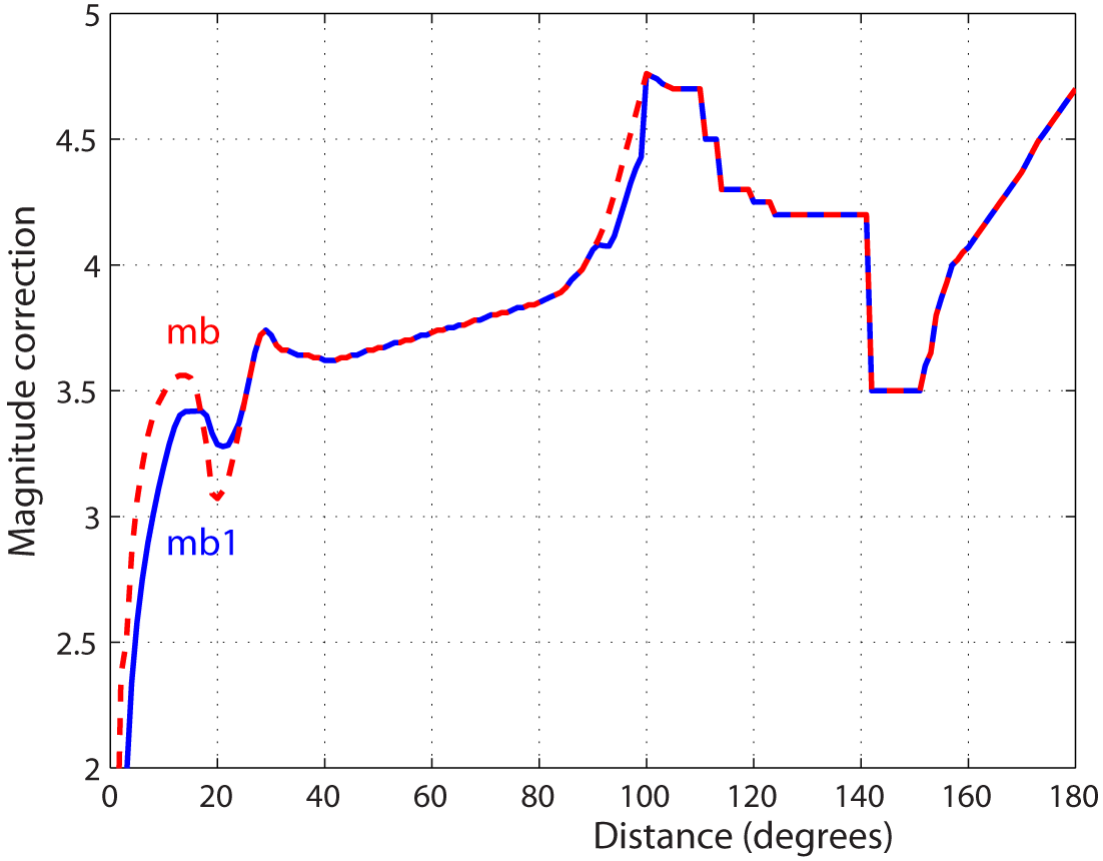

Fig. 6.1.1 Comparison of attenuation relations for mb1 and mb. Note the significant differences at distances less than 25 degrees. Also note that the IDC uses stations in the epicentral distance range 20-100 degrees for calculating REB mb values, whereas REB mb1 values are calculated for stations in the epicentral distance range 2-100 degrees.

6.1.3 Comparison of magnitudes

Figures 6.1.3 and 6.1.4 show relationships between various IDC magnitude measures as a function of event size. Figure 6.1.3 corresponds to the years 2001-2005, whereas Figure 6.1.4 covers 2006-2009. For all the plots in these and other figures in this Appendix, we have included all events in the IDC REB database satisfying the restrictions that mb has been calculated using at least five stations, and that the estimated event depth is less than 50 km.

We first note that Figures 6.1.3 and 6.1.4 are almost identical in appearance, thus indicating that the IDC processing has been very consistent over time. The increase in the IMS network and the ensuing increased number of events reported in the REB appears to have had no significant influence on this type of comparison.

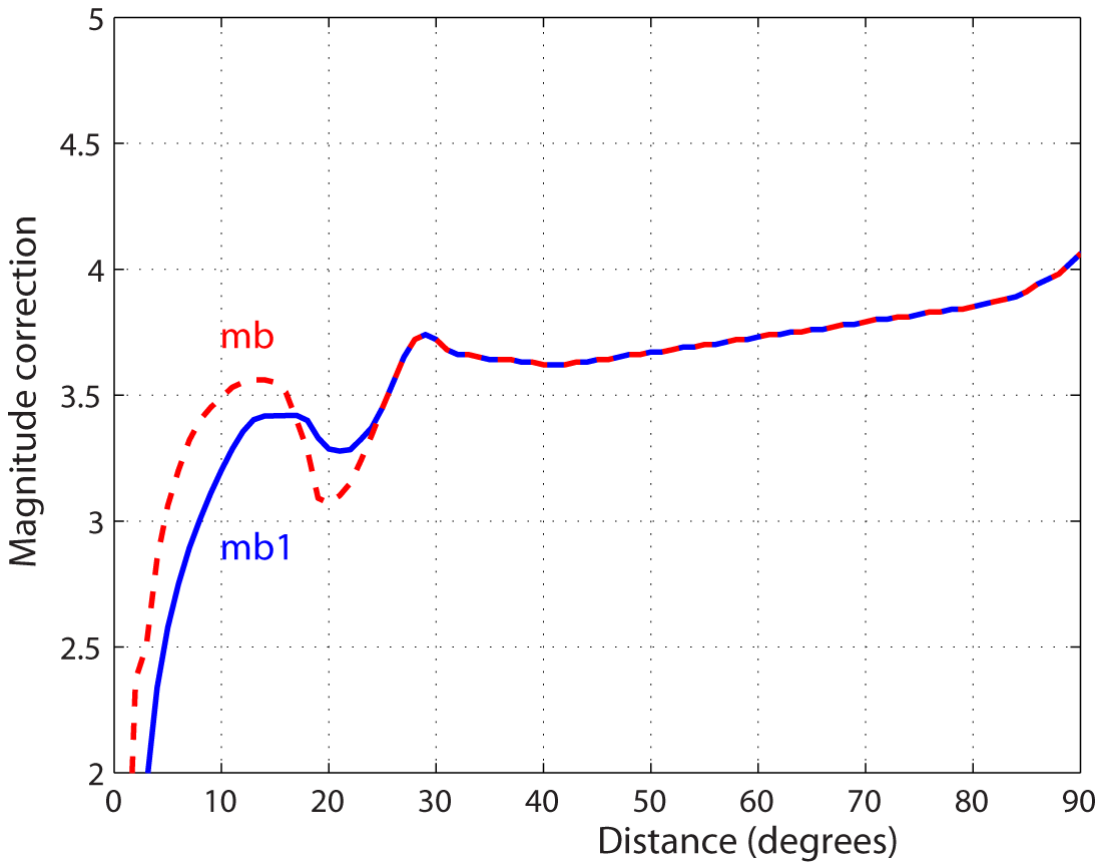

Fig. 6.1.2 Same as Figure 6.1.1, but showing an expanded view of the distance 0-90 degrees.

We further note the clear magnitude dependency, with the mb1-based magnitudes being systematically higher than the mb-based magnitudes at the low magnitude end. This would be partly due to the differences in attenuation curves shown in Figures 6.1.1 and 6.1.2, combined with the inclusion of observations at distances 2-20 degrees for the mb1 values and the weighting procedure that is part of the mb1 calculation. The station corrections could also be contributing, although they have been developed so as to retain overall consistency with the standard mb calculations. It might be interesting to compare the application of the Murphy-Baker station corrections to those developed by Zaslavsky-Paltiel and Steinberg (2008).

Figures 6.1.5 and 6.1.6 show plots similar to Figures 6.1.3 and 6.1.4, but covering only specific regions as indicated in the figure captions. In order to increase the event populations, all years (2001-2009) have been included in these plots. We note that the first of these regions is the region discussed in detail as a case study in the paper by Kværna et al. (2009).

Figures 6.1.5 and 6.1.6 show trends that are very similar to those shown in Figures 6.1.3 and 6.1.4. Other regions that we have studied show the same characteristics, so there appears to be little variation on a regional basis between the magnitude relationships.

The observed inconsistency between the mb and mb1 based magnitudes is an issue of some concern. We intend to use mb1 magnitudes in our further work since they, in contrast to the mb magnitudes, are calculated not only in the distance range 20-100 degrees, but also in the distance range 2-20 degrees. However, the current SEL3 lists include only mb and ML magni-

tudes, and we therefore need to consider carefully how this will influence the consistency indices.

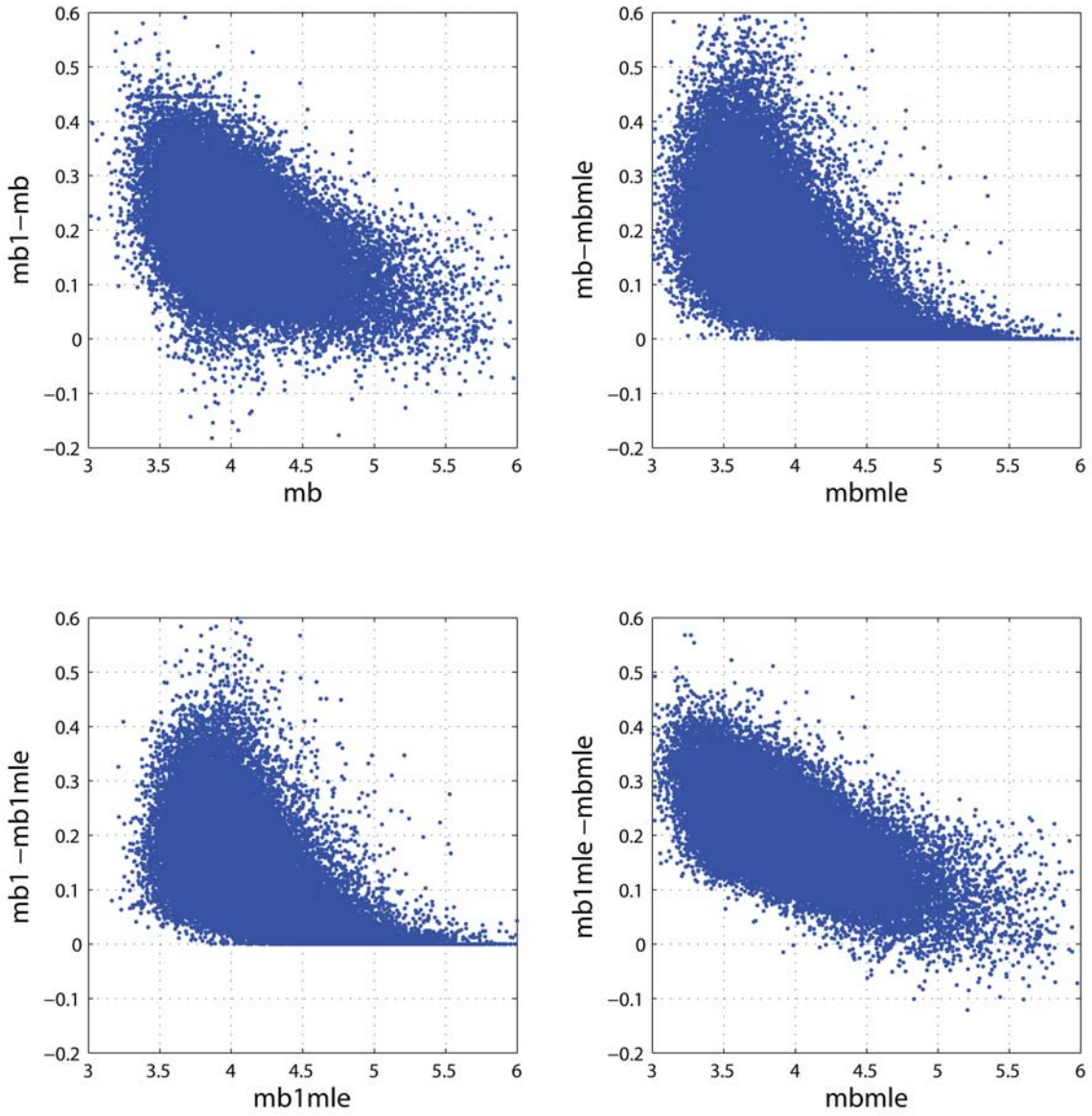

Fig. 6.1.3 Relationships between various IDC magnitude measures as a function of event size. The figure corresponds to the years 2001-2005, and covers all events in the IDC REB database satisfying the restriction that mb has been calculated using at least five stations, and that the estimated event depth is less than 50 km. Note the significant magnitude dependency, with the mb1-based magnitudes being systematically higher than the mb-based magnitudes at the low magnitude end.

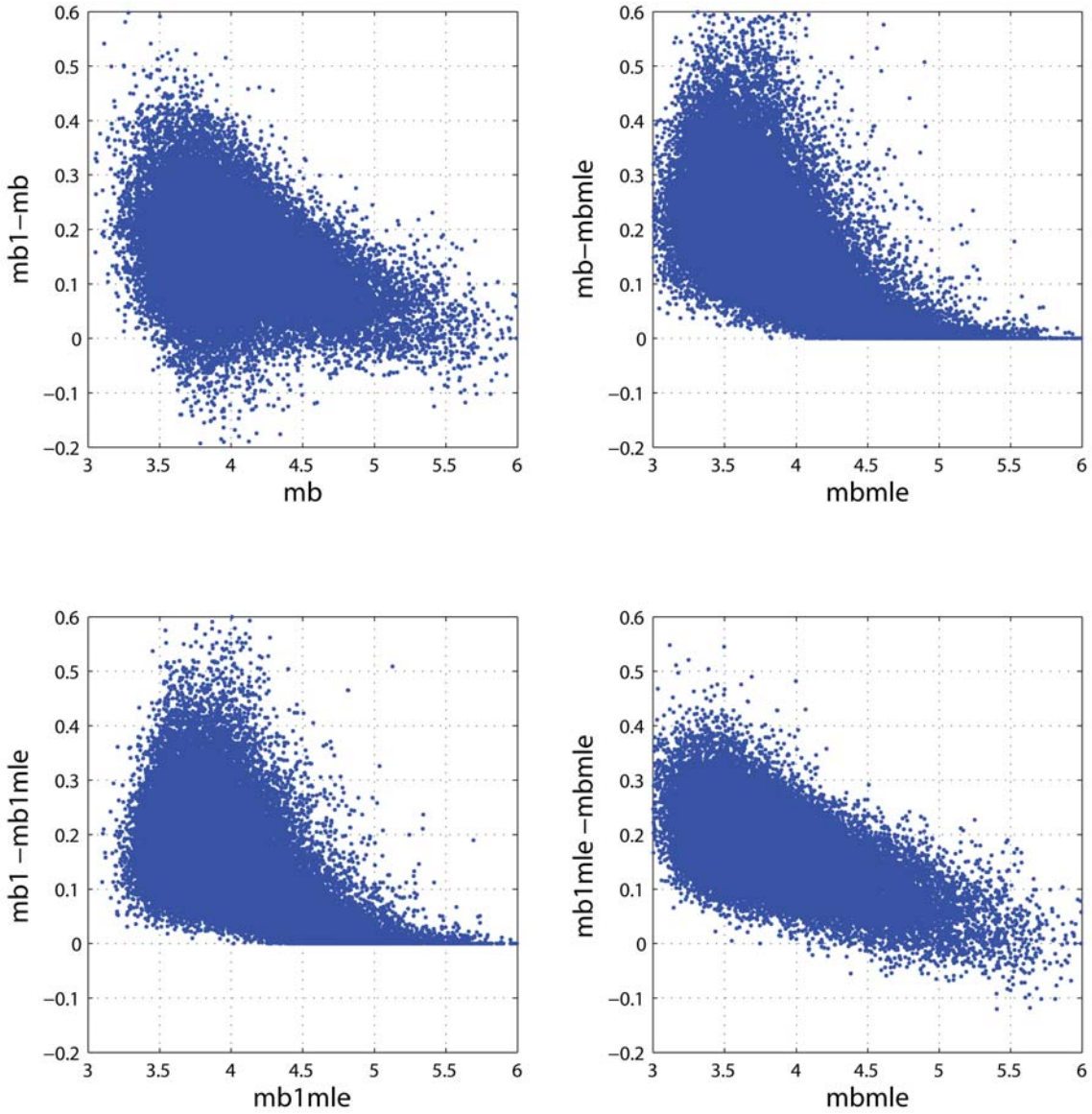

Fig. 6.1.4 Same as Figure 6.1.3, but covering the years 2006-2009. Note the very high similarity to Figure 6.1.3, indicating that the patterns are very consistent over time, even though the IMS network has expanded considerably during the years.

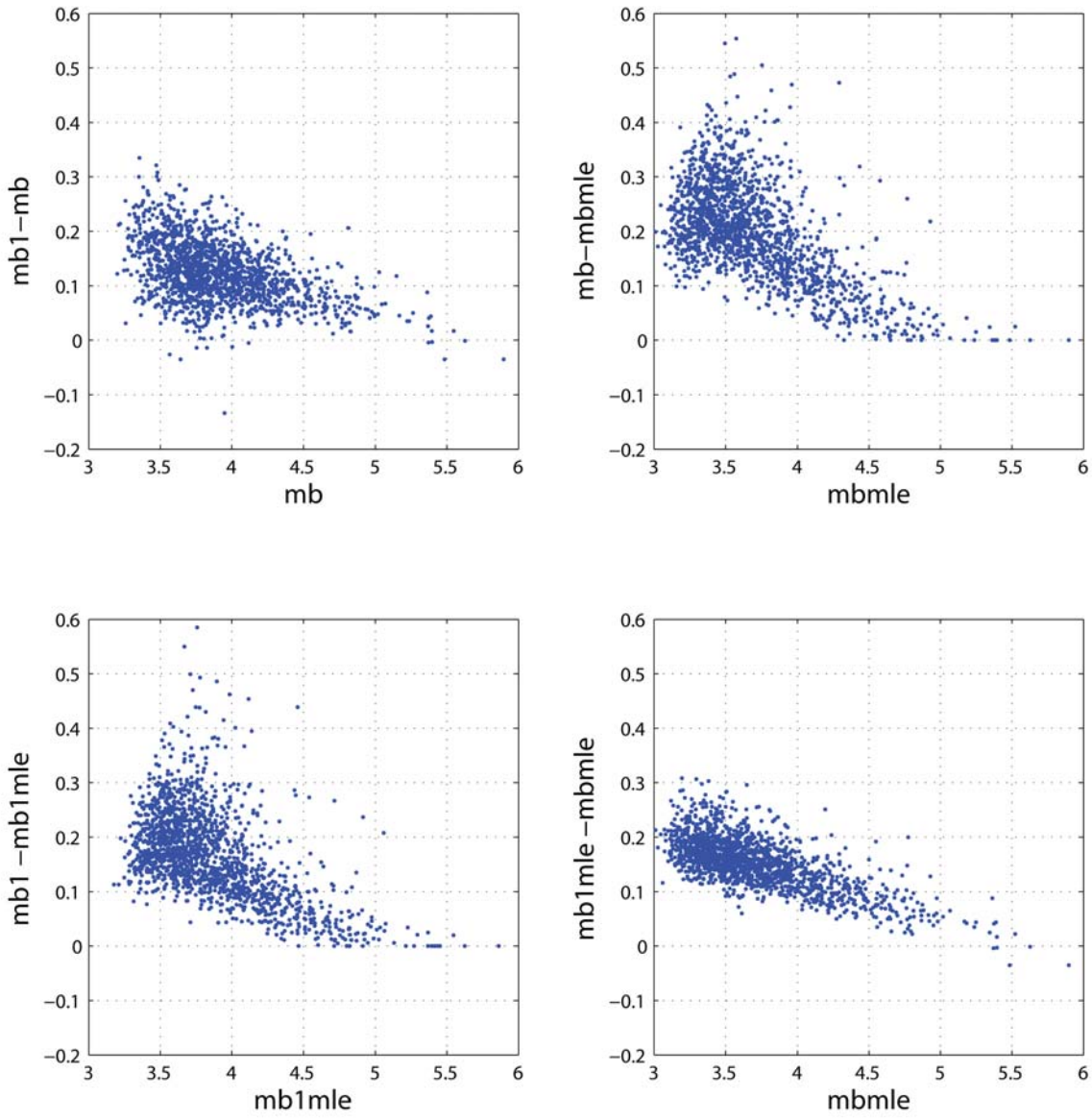

Fig. 6.1.5 Same as Figure 6.1.3, but covering all years 2001-2009 and showing only those REB events which are located within 5 degrees of 32 N, 104 E (China).

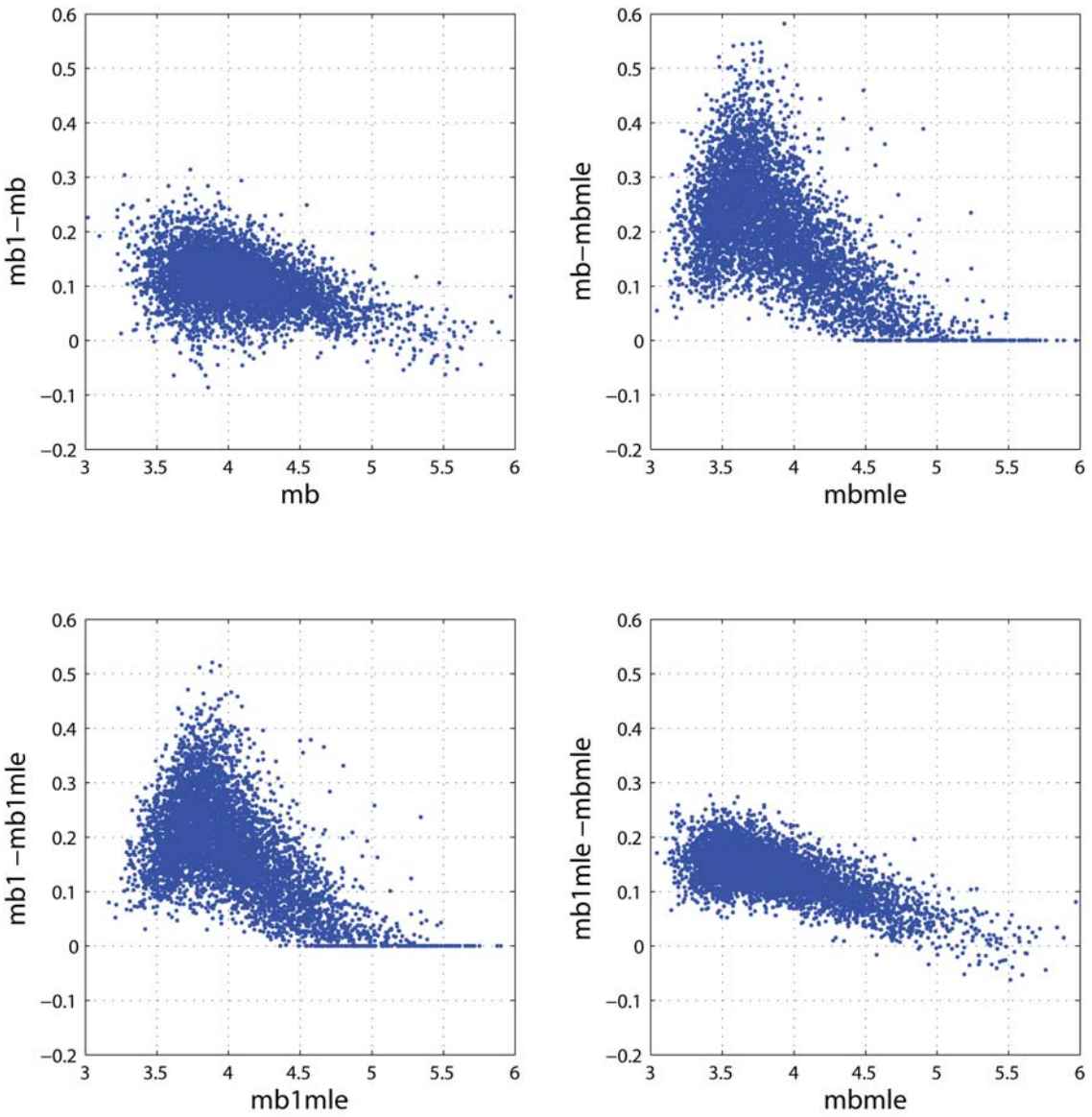

Fig. 6.1.6 Same as Figure 6.1.3, but covering all years 2001-2009 and showing only those REB events which are located within 5 degrees of 0 N, 100 E (Indonesia).

6.1.4 Linear relationships

Figures 6.1.7 through 6.1.9 show illustrations of the linear relationships between the magnitude measures. Figure 6.1.7 covers the entire database 2001-2009 with the same 5-station and 0-50 km depth restrictions as before. Figures 6.1.8 and 6.1.9 cover the two regions discussed earlier with the same restrictions.

We note that the relationships are similar for the global case and the two regions. When comparing mb-based magnitudes (x-axis) and mb1-based magnitudes (y-axis) we see that the slope is systematically less than 1.0, consistent with the previous observation of mb1 being increas-

ingly higher than mb at low magnitudes. This is most clearly observed on the two regional plots (China and Indonesia).

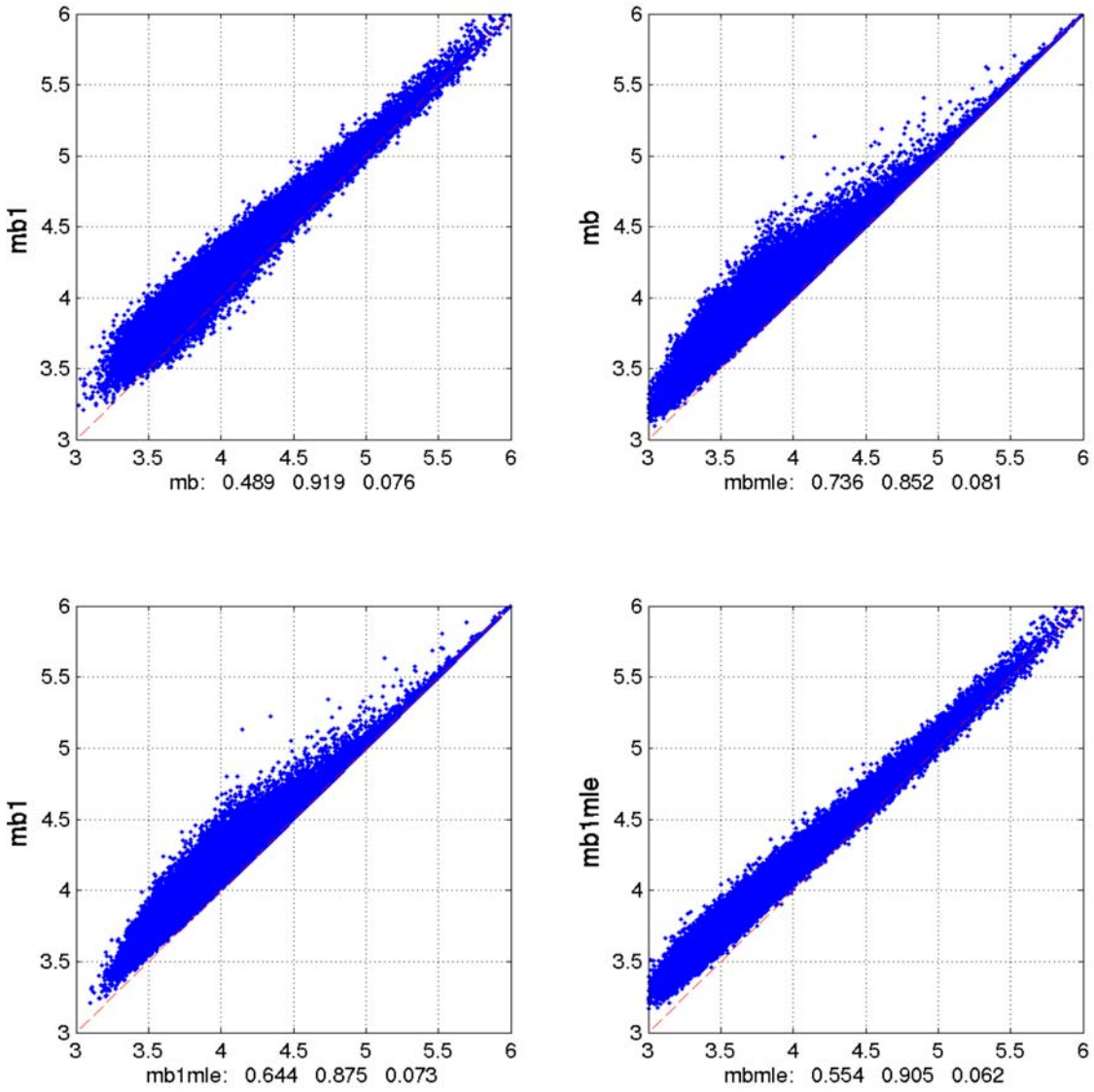

Fig. 6.1.7 Linear relations between various magnitude measures, using data from 2001-2009 from all regions (with restrictions as before). The intercept, slope and standard deviation of each least squares fit is indicated for each subplot.

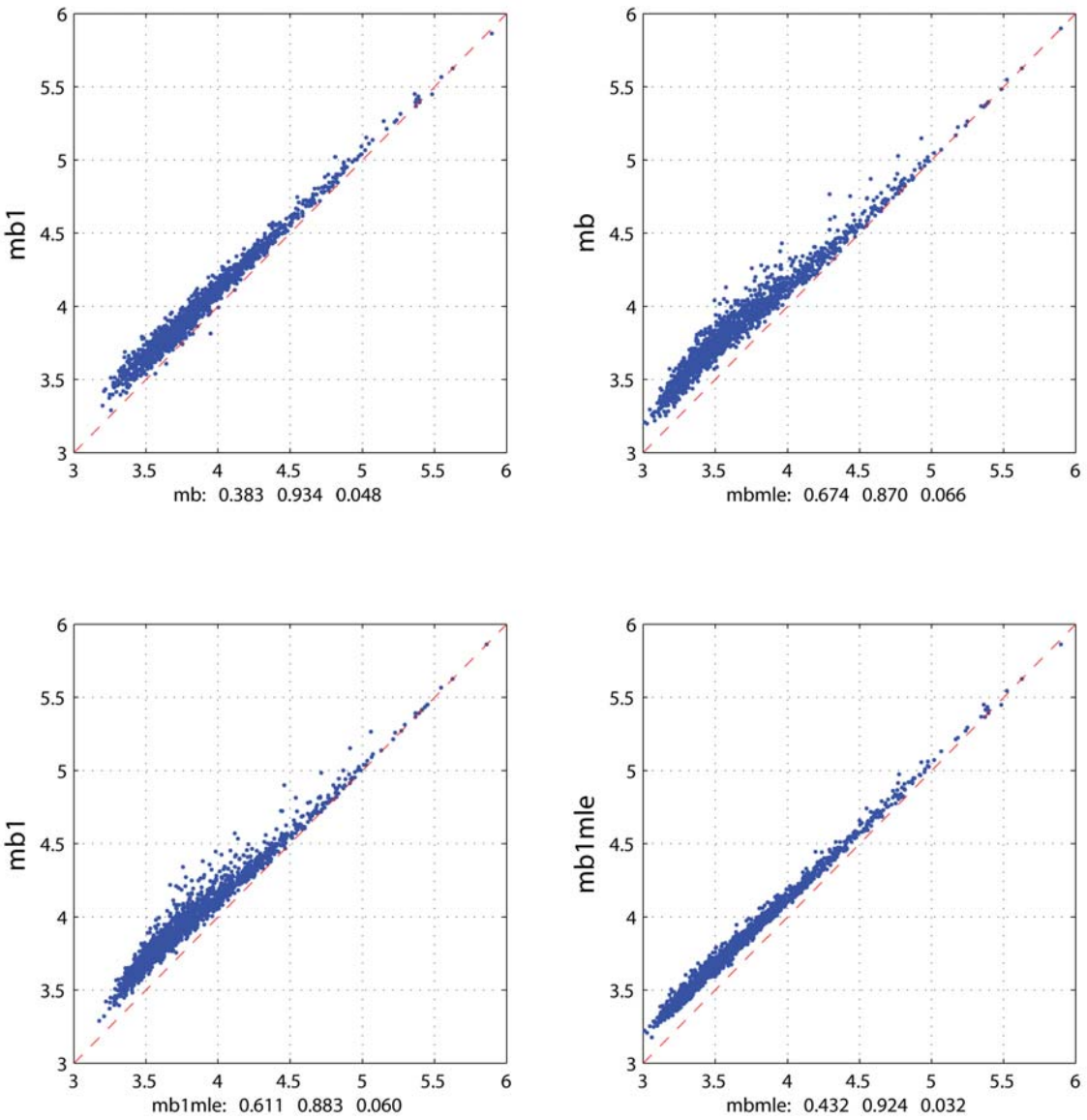

Fig. 6.1.8 Linear relations between various magnitude measures, using data from 2001-2009 (within 5 degrees of 32N, 104E, China). The intercept, slope and standard deviation of each least squares fit is indicated for each subplot.

.

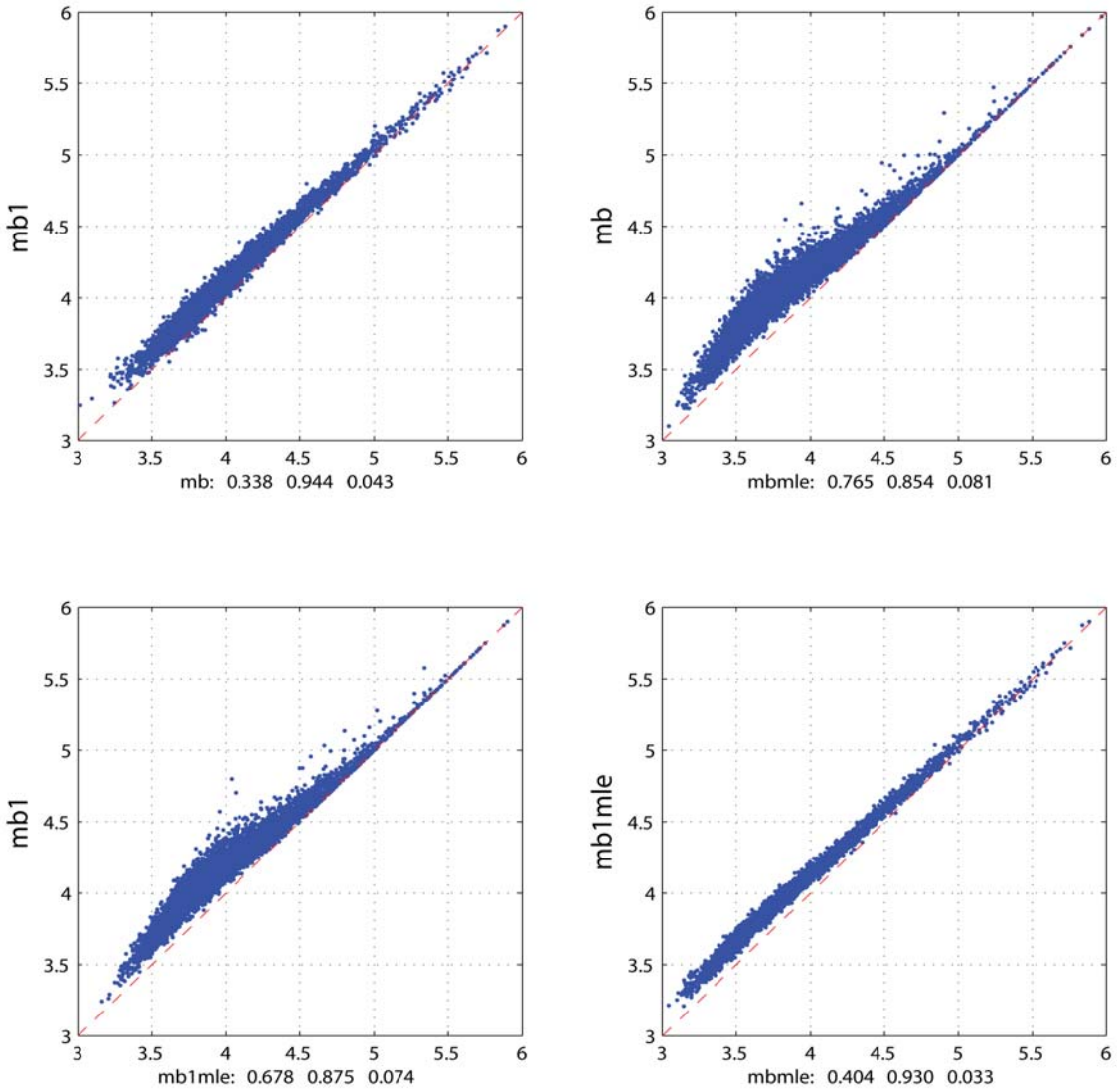

Fig. 6.1.9 Linear relations between various magnitude measures, using data from 2001-2009 (within 5 degrees of 0N, 100E, Indonesia). The intercept, slope and standard deviation of each least squares fit is indicated for each subplot.

6.1.5 Magnitude-frequency relationships

We have also studied the magnitude-frequency relationships for the various magnitude types. These relationships are shown in six figures (Figures 6.1.10-6.1.15), with Figures 6.1.10 and 6.1.11 covering all regions, while Figures 6.1.12 and 6.1.13 cover the region in China and Figures 6.1.14 and 6.1.15 cover the region in Indonesia. The restrictions on the selected events are as before.

A common feature of the plots is that the slopes of the magnitude-frequency relationships are steeper for the mb1-based magnitudes than for the mb-based magnitudes. This is clearly connected with the magnitude dependent bias effects already noted. Furthermore, we observe that (as expected) the slopes for maximum-likelihood magnitudes are less steep than those for the conventional magnitudes.

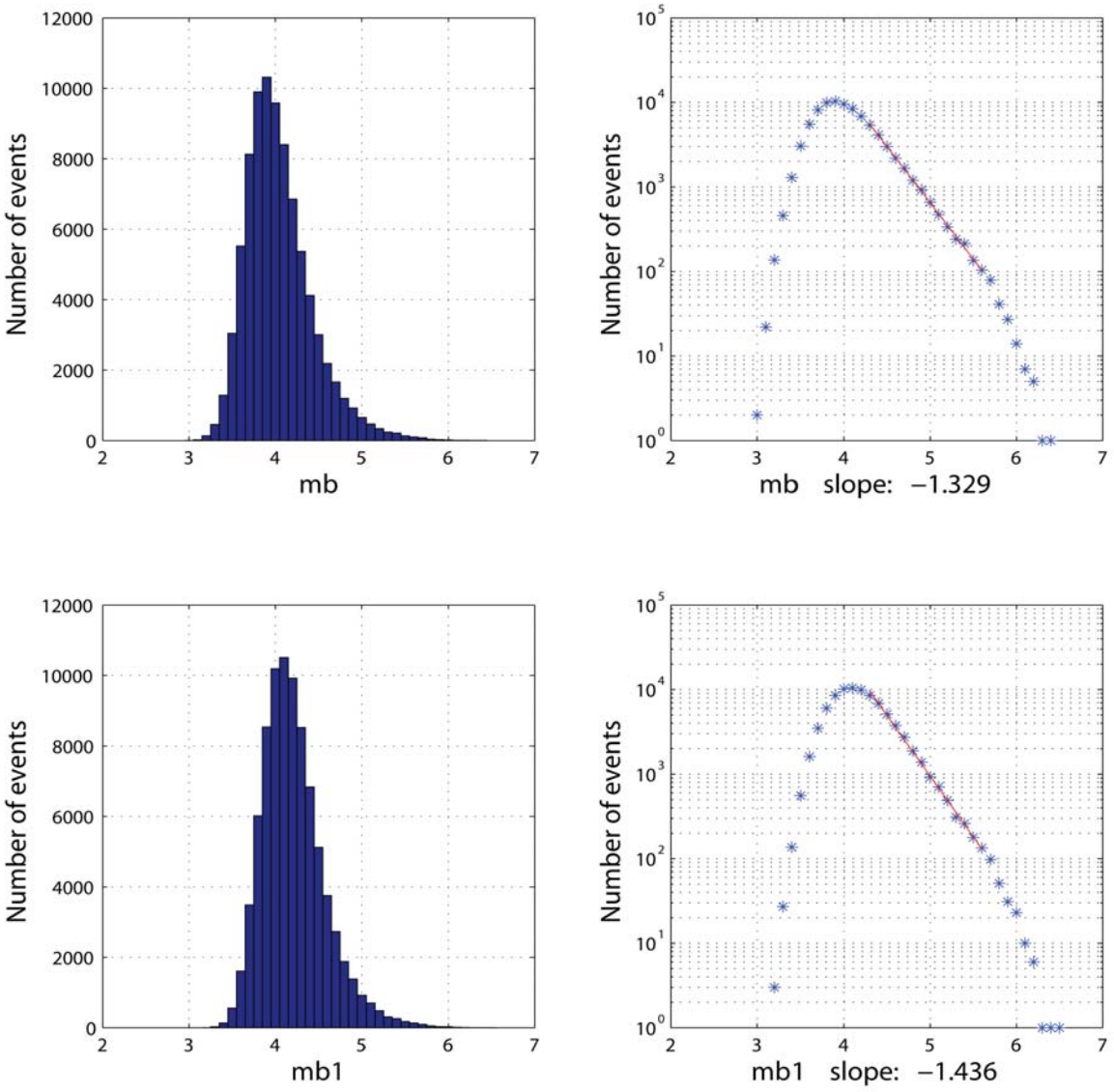

Fig. 6.1.10 Recurrence statistics for mb and mb1 for 2001-2009 (all regions). The estimated slope of the magnitude-frequency relationship (shown in red) is given for each plot.

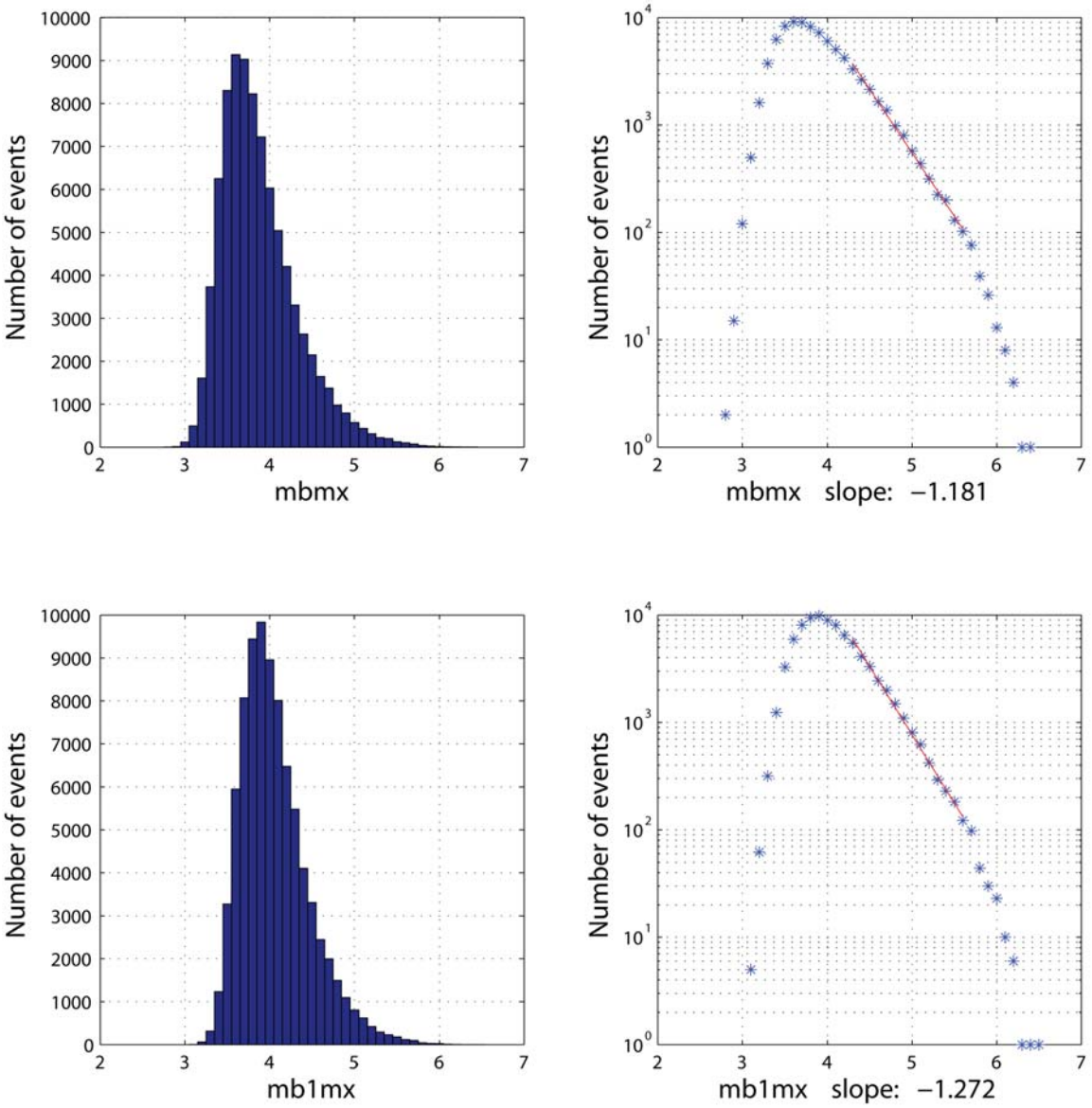

Fig. 6.1.11 Recurrence statistics for mbmx and mb1mx for 2001-2009 (all regions). The estimated slope of the magnitude-frequency relationship (shown in red) is given for each plot.

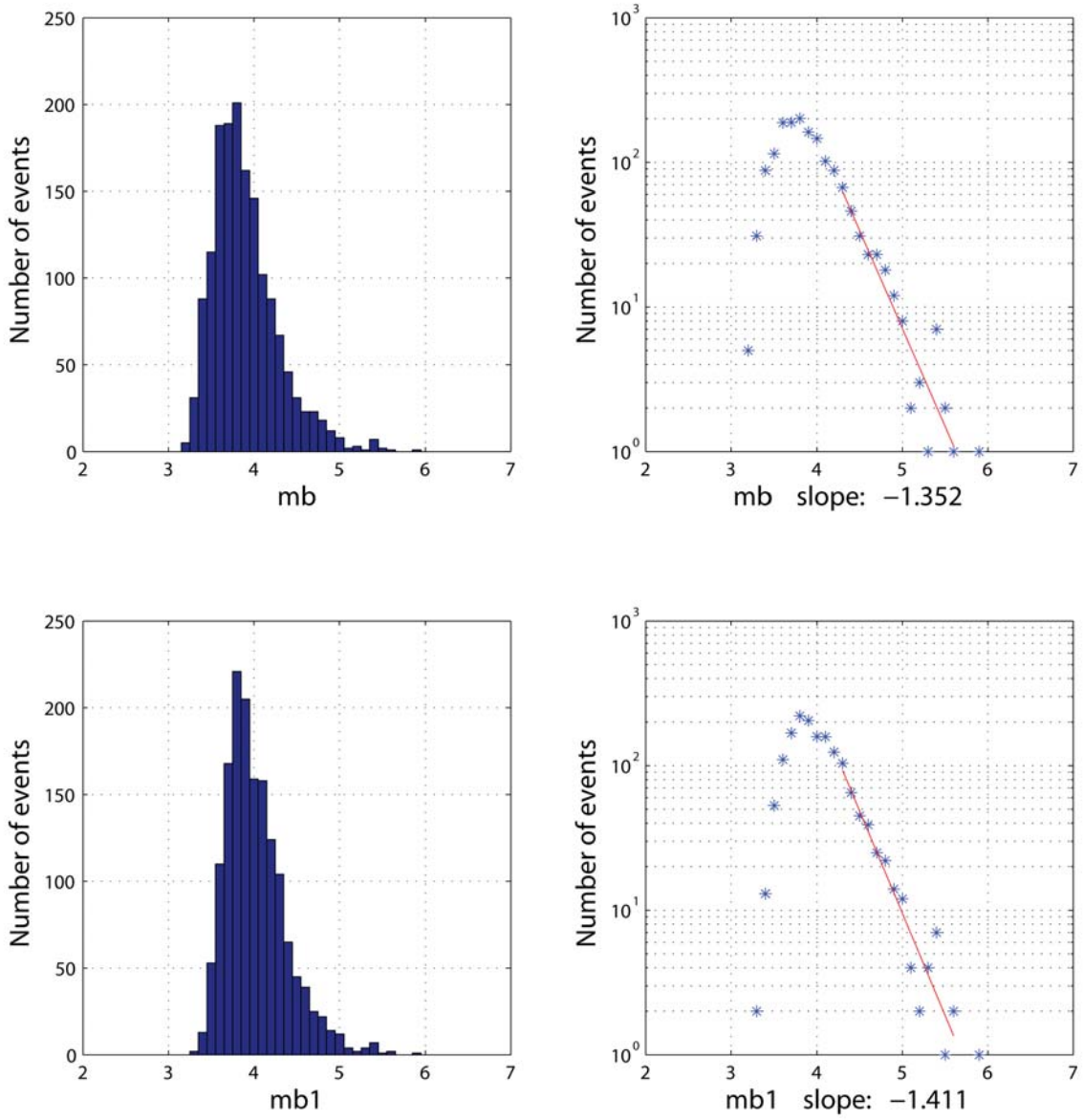

Fig. 6.1.12 Recurrence statistics for mb and mb1 for 2001-2009 (within 5 degrees of 32N, 104E, China). The estimated slope of the magnitude-frequency relationship (shown in red) is given for each plot.

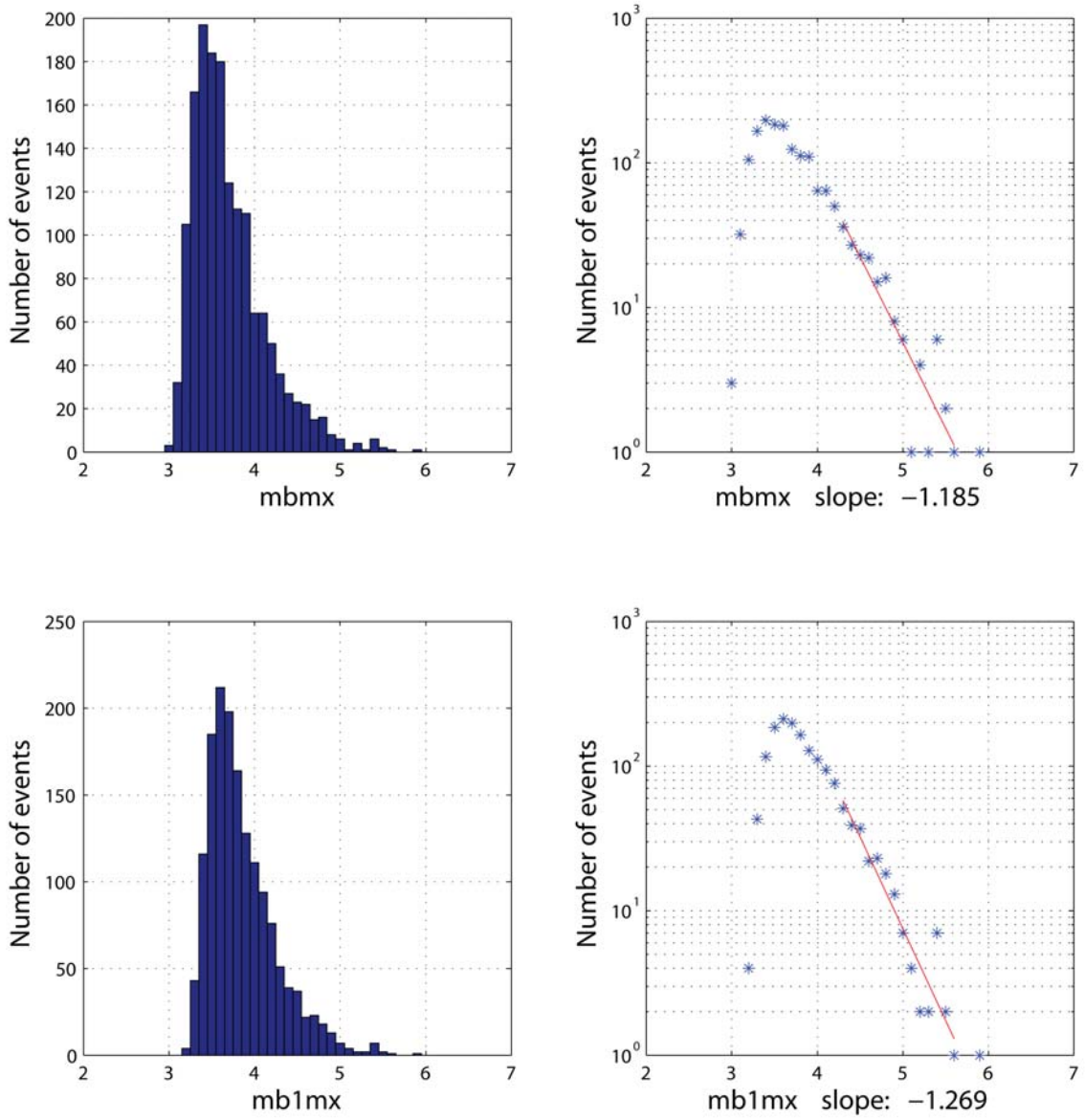

Fig. 6.1.13 Recurrence statistics for mbmx and mb1mx for 2001-2009 (within 5 degrees of 32N, 104E, China). The estimated slope of the magnitude-frequency relationship (shown in red) is given for each plot.

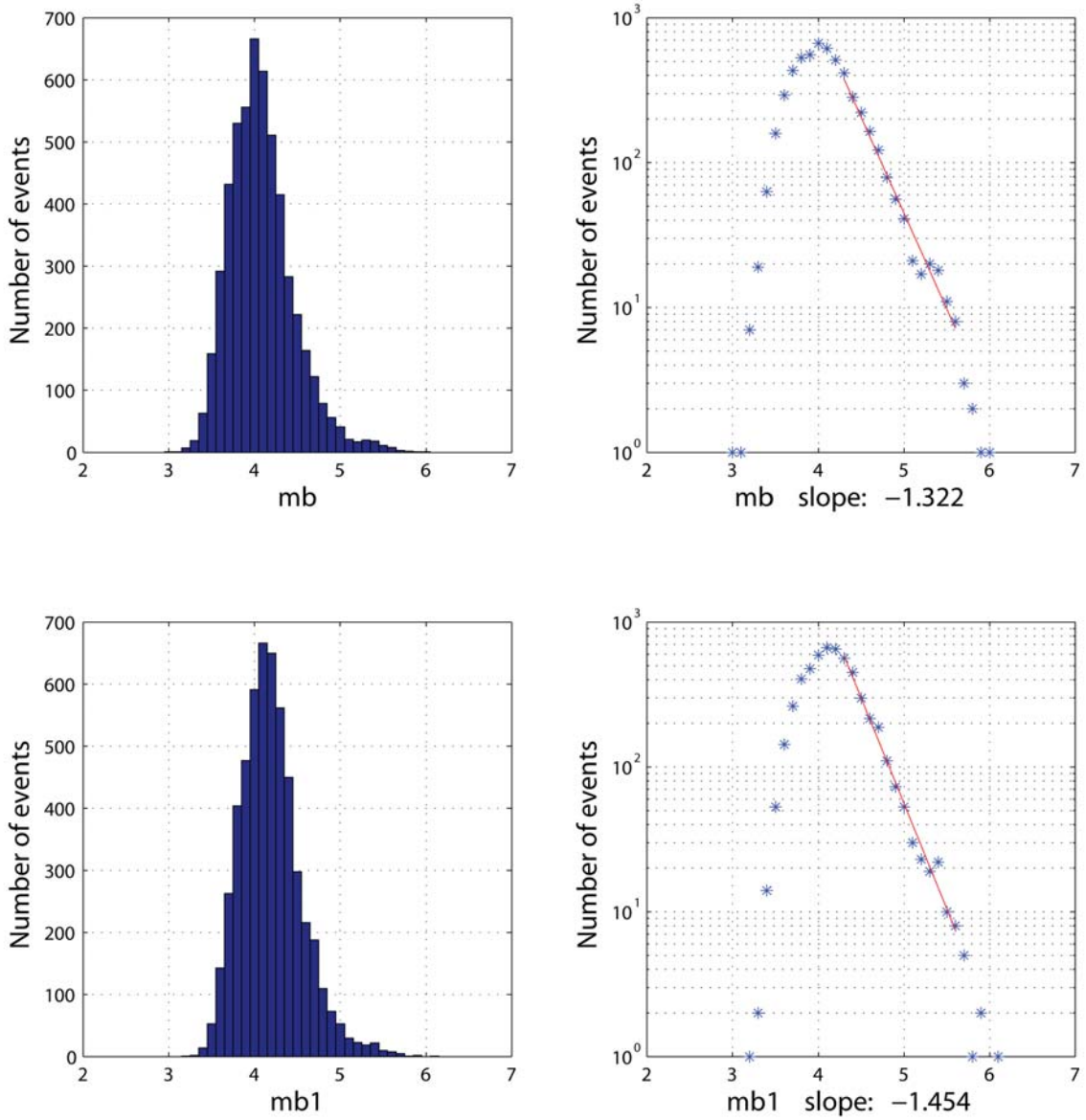

Fig. 6.1.14 Recurrence statistics for mb and mb1 for 2001-2009 (within 5 degrees of 0N, 100E, Indonesia). The estimated slope of the magnitude-frequency relationship (shown in red) is given for each plot.

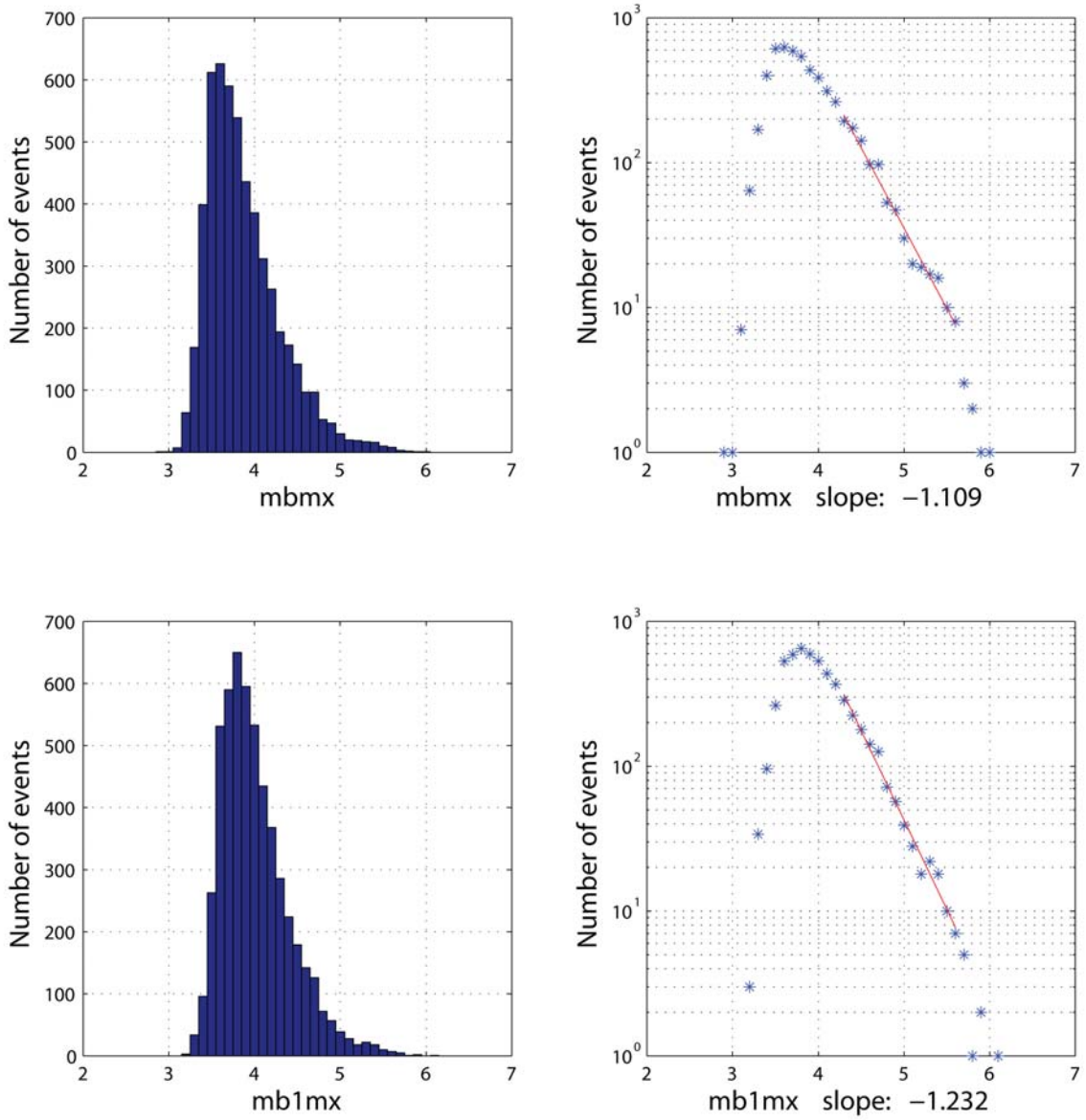

Fig. 6.1.15 Recurrence statistics for mbmx and mb1mx for 2001-2009 (within 5 degrees of 0N, 100E, Indonesia). The estimated slope of the magnitude-frequency relationship (shown in red) is given for each plot.

6.1.6 Conclusions and recommendations

We note the following observations:

- The magnitude values are fairly consistent, but the two mb1-based magnitudes are on the average about 0.1-0.2 units higher than the corresponding ones based on mb. The difference is largest at the low magnitude end.
- When comparing mb-based magnitudes (x-axis) and mb1-based magnitudes (y-axis) we see that the slope is systematically less than 1.0, consistent with the previous observation of mb1 being increasingly higher than mb at low magnitudes. This appears in all the regions we have studied. One major contributing factor here would be the significant

differences in the attenuation curves between 20 and 25 degrees (Figures 6.1.1 and 6.1.2). However, the inclusion of regional data (2-20 degrees) in the mb1 computations, the associated station corrections and the weighting procedure employed in computing mb1 would be likely to play a role as well.

- The maximum-likelihood magnitudes (mbmle and mb1mle) are more mutually consistent than the averaged magnitudes (mb and mb1). Again, this is observed in all regions we have studied.

The lower scatter for the maximum-likelihood magnitudes is attributed to the fact that the correction for non-detections reduces the standard deviation of individual network magnitude estimates.

We note that by definition the maximum-likelihood magnitudes are always lower than (or equal to) the corresponding average magnitudes. This is because the maximum-likelihood procedure is designed to eliminate or reduce positive magnitude bias due to ignoring the non-detections. In the choice between the two different types of maximum likelihood magnitudes, we plan to use the mb1mle estimates as reference event magnitude. The reason for choosing mb1mle rather than mbmle is that, for this magnitude measure, individual event magnitudes for detecting stations are included in the database also for stations within 2-20 degrees of the epicenter, which is not the case for mbmle. We note, however, that in neither case is information on non-detections reported for epicentral distances within 20 degrees, and that, for auxiliary stations, no information on non-detections is reported at any distance.

We recommend that the IDC consider the following possible actions for the near term:

1. For the dynamic validation of events and associated phases, the magnitude information should be as complete as possible, already at the SEL3 stage. Currently, the SEL3 includes only mb and ML. We suggest that mb1 be computed as well, even if the event is "unreasonable". It would also be an advantage, if practicable, to compute the maximum likelihood magnitudes (and the noise levels) for inclusion in the SEL3. In fact, in order to identify bogus events in SEL3, the most important information is precisely those magnitude values and detection/non-detection patterns that appear to be unreasonable.
2. Both previous studies and our initial studies under this project have confirmed the importance of having complete statistics on station uptimes. Clearly, it is meaningless to apply dynamic criteria if a key station is down during an event, and this station is counted as non-detecting because station downtime has not been recorded. During the further work in this study, we plan to use the Threshold Monitoring data to help identify the outages. Nevertheless, it would be an advantage to keep an independent record of the station downtimes (a downtime for a station being defined in conjunction with SEL3 as a time period for which data from that station has not been available to produce the SEL3). Note that the TM processing is not applied to auxiliary stations, so the downtime statistics for those stations must be made available by some other means – otherwise the usefulness of auxiliary stations for dynamic checking will be very limited.

References

Kværna, T., F. Ringdal and U. Baadshaug (2009): Detection Capability of IMS Primary and Auxiliary Seimic Stations. *in* Semiannual Technical Summary, January-June 2009, NORSAR Sci. Rep. 2-2009, Kjeller, Norway.

Murphy, J. R. and B. W. Baker (2003): Revised Distance and Depth Corrections for Use in the Estimation of Short-Period P-Wave Magnitudes, *Bull. Seism. Soc. Am.*, 93, 1746-1764.

Ringdal, F. (1976): Maximum likelihood estimation of seismic magnitude, *Bull. Seism. Soc. Am.*, 66, 789-802.

Zaslavsky-Paltiel, I. and D. M. Steinberg (2008): Comparison of Methods for Estimating Station Magnitude Corrections for Improved Seismologic Monitoring of the Comprehensive Nuclear-Test-Ban Treaty, *Bull. Seism. Soc. Am.*, 98, 1-17.

Tormod Kværna
Frode Ringdal

6.2 Late stages of the Storfjorden, Svalbard, aftershock sequence

6.2.1 Introduction

On 21st February 2008, a strong earthquake of moment magnitude Mw = 6.1 occurred in the offshore area of Storfjorden, Svalbard. The event was followed by a vast aftershock sequence, recorded by the seismological stations in the broader region. A special investigation of the first seven months of this earthquake sequence was facilitated by the coinciding conduction of an International Polar Year (IPY) project (Schweitzer et al., 2008), which included the deployment of several temporary installations in the region. This study (Pirli et al., 2010), which involved the location of a large number of aftershocks and the calculation of moment tensors for the main event, showed that the seismic rupture occurred on an unmapped, oblique-normal fault, probably of NE-SW trend and steep SSE dip (Regional and Teleseismic MTs in Fig. 6.2.1). It also revealed strong indications of secondary activations within the same aftershock volume, suggested by the spatial distribution of the events and waveform similarity.

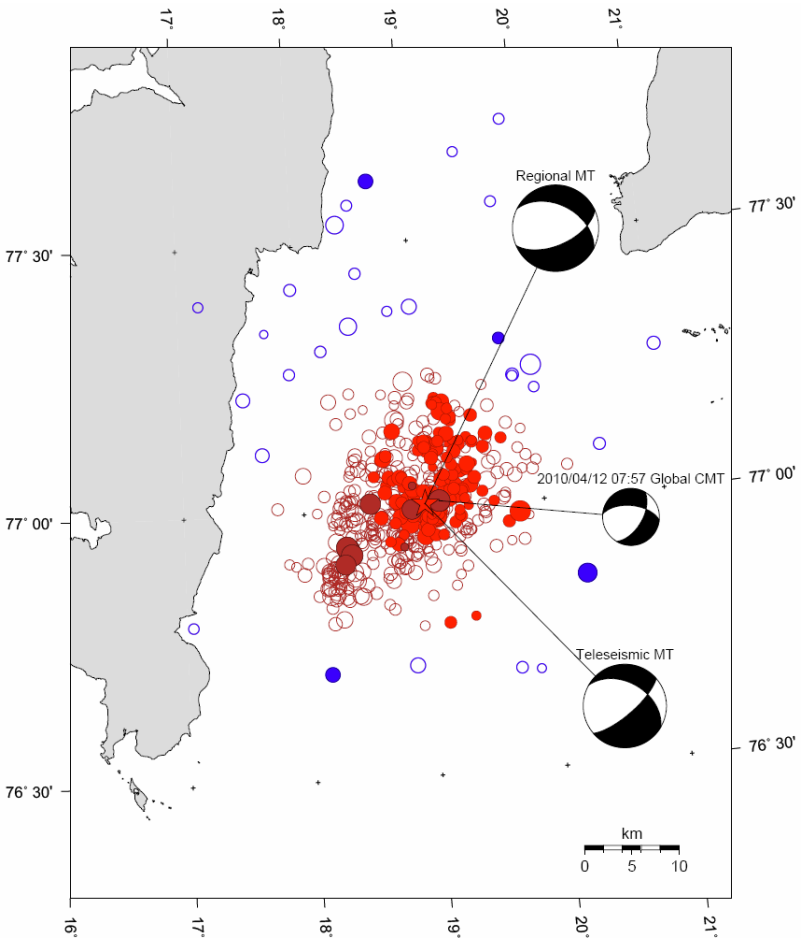

Fig. 6.2.1. Spatial distribution of events in Storfjorden, from the 21st February 2008 mainshock (red star) to the end of November 2010, and focal mechanisms from Pirli et al., 2010. The focal mechanism of the 2010/04/12 07:57 event is calculated by the Global CMT Project. NORSAR reviewed bulletin solutions are shown as open circles, while filled circles denote relocated epicentres. Red circles are relocated events from Pirli et al. (2010), dark red are relocated events after October 2008, and blue colour is used to note events that lie outside the main aftershock volume.

6.2.2 Spatio-temporal evolution of the sequence after October 2008

Although most of the IPY related installations were demobilised in autumn 2008, the area remained under focus within the framework of routine seismic monitoring of the European Arctic. This revealed persistent seismic activity in Storfjorden on an almost continuous basis, still ongoing at the time when this report is being composed. The spatial distribution of this seismicity is displayed in Fig. 6.2.1. The image is based partly on the listings of NORSAR's regional, analyst reviewed bulletin (http://www.norsardata.no/NDC/bulletins/regional/), which contains events with an automatic magnitude larger than 2.0 (open circles of any colour), and partly on the results of Pirli et al., 2010 (red circles) for events up to the end of September 2008. Relocated epicentres for events after this time interval, which were derived with the use of additional data, different velocity models and/or different phase identification compared to the routine analysis, are noted in dark red. A different colour (blue) is used to indicate seismic events that fall outside the main aftershock volume. The most interesting feature of the map is the abundance of epicentres SW of the volume located by Pirli et al. (2010). In addition to the epicentre distribution, the focal mechanism of the 2010/04/12 07:57 M 4.9 event is shown, as determined by the Global CMT Project (http://www.globalcmt.org/). Although this event occurred during the later stages of the sequence, it is located very close to the epicentre of the mainshock and has a focal mechanism which describes very similar faulting.

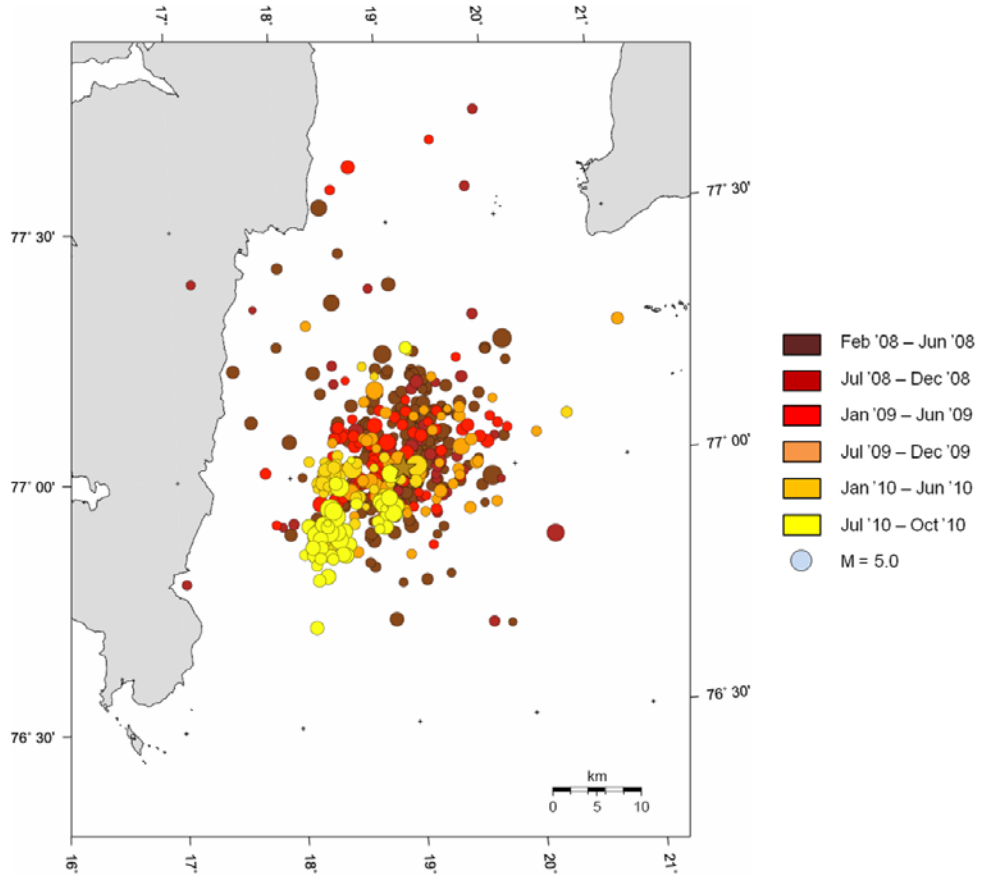

Fig. 6.2.2. Spatiotemporal distribution of events in Storfjorden between 21/02/2008 and 30/11/2010, based on the listings of NORSAR's regional reviewed bulletin and Pirli et al., 2010. The mainshock is noted by a star, while aftershock epicentres are scaled according to magnitude.

A colour scale is used in Fig. 6.2.2 to map the spatiotemporal distribution of the events shown previously in Fig. 6.2.1. It is clearly obvious that while seismic activity in the area of the 21st February 2008 main event persists, the main volume of activity within the year 2010 and in particular its second half, is concentrated in an area SW of the previous aftershock volume. This reveals the existence of a new source of activity, which lies either on the south-westerly extension of the seismogenic fault suggested by Pirli et al. (2010) or a neighbouring tectonic structure.

The distribution of the number N of seismic events per day is shown in Fig. 6.2.3, expressed in days after the occurrence of the February 2008 main event. Alternatively, time is shown in years, and the distribution of observed event magnitudes M with time is additionally plotted. The distribution is again based on NORSAR's regional reviewed bulletin and Pirli et al., 2010. The daily number of events decreases very rapidly already in the early stages of the aftershock sequence, however the activity persists on a low level. Outbursts can be observed in 2009 and a larger activation is observed within the second half of 2010. It is also notable that this late activity is characterised by larger average magnitude levels compared to the time before late spring 2010. This is demonstrated clearly by the fact that excepting the February 2008 main-shock, only 12 aftershocks of magnitude larger than 4.0 were observed until summer 2010, whereas the same number of events within the same magnitude range was observed during the remaining 5 months of 2010.

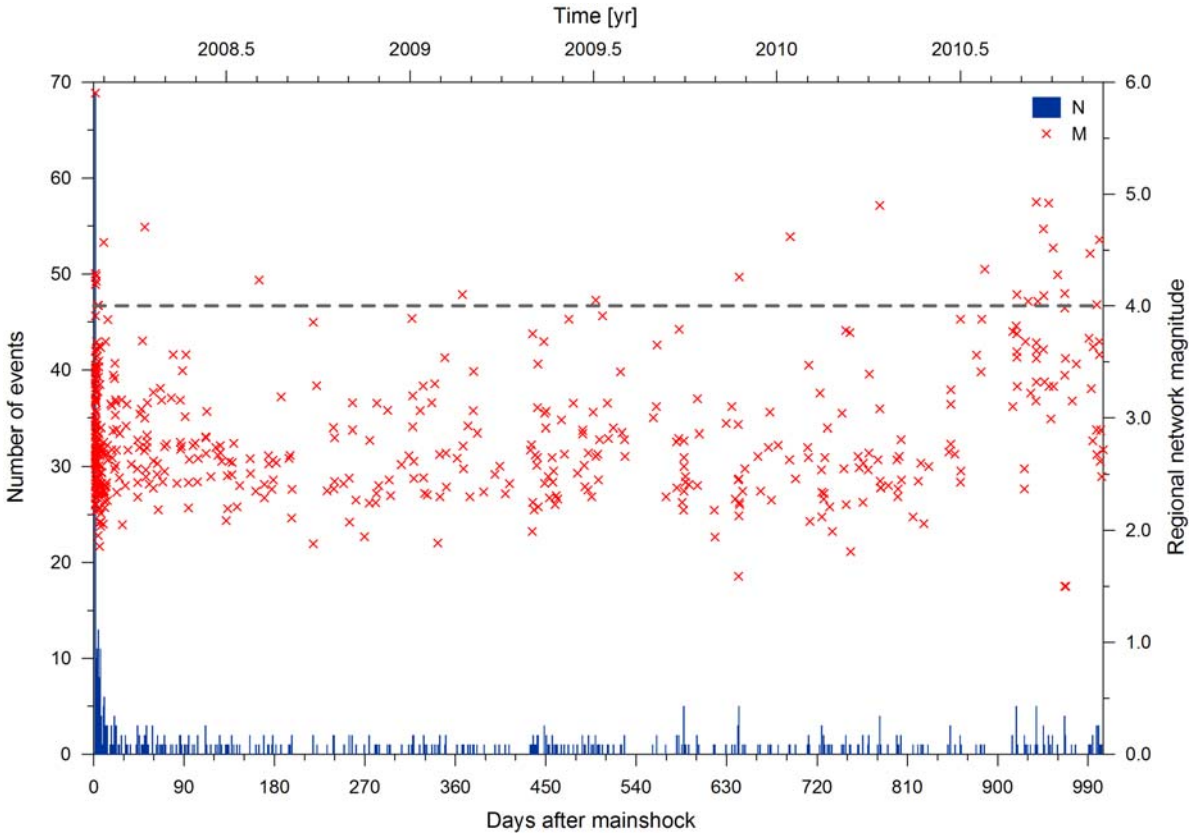

Fig. 6.2.3. Number of events per day after the occurrence of the 21st February 2008 mainshock and event magnitude distribution in time, based on the listings of NORSAR's reviewed bulletin and Pirli et al., 2010. The dashed line marks the magnitude 4.0 threshold.

6.2.3 Waveform cross-correlation detector results

An alternative image of the evolution of the sequence is provided in Fig. 6.2.4 (light coloured line). Since NORSAR's reviewed bulletin has a magnitude threshold of 2.0, this image of the sequence is incomplete. To retrieve information about the distribution of events of smaller magnitude, a waveform cross-correlation detector (Gibbons and Ringdal, 2006) on the data of the broadband sensor at the Polish Polarstation Hornsund (HSPB) was used. A number of events spanning the entire length of the sequence (master events) were selected to detect other similar events. Information about these 23 events can be found in Table 6.2.1. The result of the use of the employed master events (red stars in Fig. 6.2.4) is the dark coloured line, which clearly demonstrates the much larger number of events associated with this activity in Storfjorden than revealed from the listings of NORSAR's reviewed bulletin. The step-like jumps in the distribution correspond to rapid increases in the number of earthquakes, the most striking of them being the one observed at about 780 days after the magnitude 6.1, February 2008 mainshock (spring 2010). Changes in the slope of the "linear" part of the curve indicate distinct branches of activity. Four main branches can be discerned after day 200 from the occurrence of the mainshock, with the following approximate definitions: one from day 200 to day 270 (end of August 2008 to mid November 2008), one from day 270 to day 500 (July 2009), a third one from day 500 to day 900 (August 2010) and a fourth one from day 900 on.

Table 6.2.1. The master events used for aftershock detection

origin time	latitude (°)	longitude (°)	M	N detections
2008-052:02.53	77.072	18.008	3.6	2
2008-053:04.24	77.195	19.138	2.7	151
2008-057:15.56	76.977	19.093	2.9	88
2008-060:13.04	77.042	18.911	< 2.0	65
2008-071:06.05	77.134	19.215	3.4	11
2008-162:04.43	77.099	19.210	2.8	5
2008-333:03.29	77.050	19.095	3.1	36
2009-002:16.52	77.057	18.588	3.2	103
2009-063:08.44	77.038	19.048	3.4	84
2009-133:19.58	77.074	18.412	3.0	35
2009-180:17.38	77.026	18.890	2.3	4
2009-327:04.22	76.986	19.501	2.5	15
2010-030:16.04	76.950	18.794	2.7	28
2010-103:10.59	76.950	18.847	2.4	304
2010-234:17.46	76.943	18.787	3.8	117
2010-270:12.09	76.919	18.379	4.9	Itself
2010-270:22.11	76.899	18.309	3.3	7
2010-275:01.34	76.998	18.896	4.5	4
2010-275:01.47	76.936	18.798	3.3	7
2010-286:08.39	76.907	18.309	< 2.0	5
2010-287:18.09	76.929	18.815	< 2.0	20
2010-320:22.46	76.879	18.191	3.7	12
2010-320:23.59	76.883	18.192	3.6	2

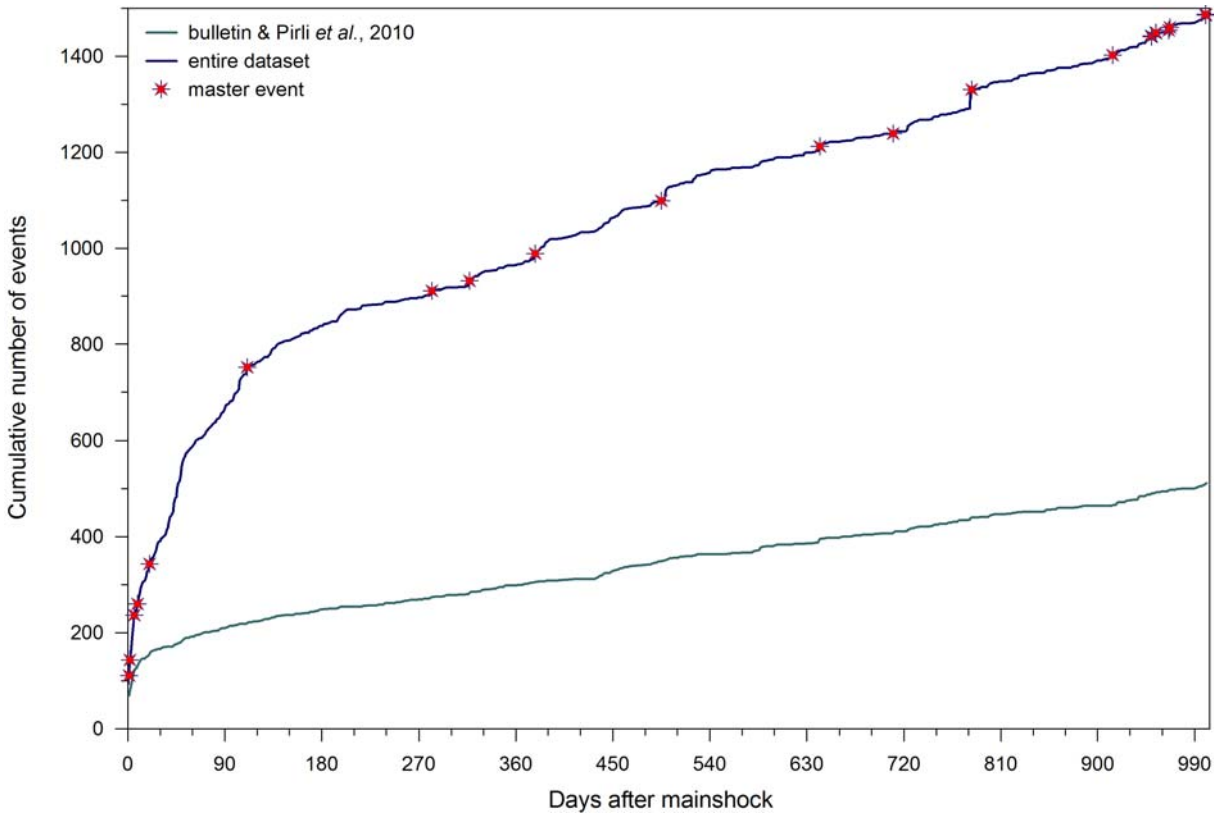

Fig. 6.2.4. Cumulative number of events for the activity in Storfjorden, Svalbard, against time in days after the 21st February 2008 mainshock, for the dataset of located earthquakes (NORSAR's reviewed bulletin and Pirli et al., 2010) – light coloured line – and for a dataset resulting from the use of a waveform cross-correlation detector, with 23 master events so far – dark coloured line. The approximate time of occurrence of the selected master events is noted with red stars.

A more detailed image is provided in Fig. 6.2.5, which is the corresponding distribution to that of Fig. 6.2.3, this time based on the entire dataset associated with the Storfjorden activity, which includes NORSAR's regional bulletin and Pirli et al. (2010) data, as well as the events identified by the cross-correlation detector. The obtained image of aftershock occurrence rate is quite different to that of Fig. 6.2.3, especially for the first 120 days of the series, when many more events have been recovered. The remaining time interval, which exceeds two years, is again characterised by the appearance of short-lived peaks that are, in most cases, related to aftershocks of larger magnitude. The most striking of them is the peak observed 780 days after the February 2008 event, in April 2010. It is associated with the 12th April event of magnitude 4.9 (see Fig. 6.2.1 for focal mechanism) and its aftershocks, however, the rate of event occurrence resumes its previous levels almost immediately after the two-day increase. Another interesting feature of the distribution, which was already apparent in Fig. 6.2.3, is the activity after August 2010. Despite the fact that several master events from this time interval were used, they yielded very few detections; almost none in some cases. Thus, we can safely conclude that during this latest stage the character of the activity is significantly changing, with the occurrence of many small distinct branches, which contain mainly higher magnitude members.

It should be stressed here that the obtained image is a direct consequence of a number of parameters. The most decisive is the number and character of the selected master events, since not all of them are equally productive and/or representative of the diversity of waveforms

within the sequence, as shown in this case by Table 6.2.1. The SNR threshold used for the detection process and the minimum acceptable cross-correlation coefficient, chosen to ensure the validity of the results, may also cause some loss of information, however a balance has been sought between discarding true detections and eliminating the false ones. In addition, all the above points are strongly influenced by the noise conditions at HSPB. Thus, the event catalogue consisting of the achieved detections is not complete, however care was taken that it is representative for the wide variety of waveforms observed throughout the Storfjorden activity, so some safe conclusions can be derived for the overall distribution.

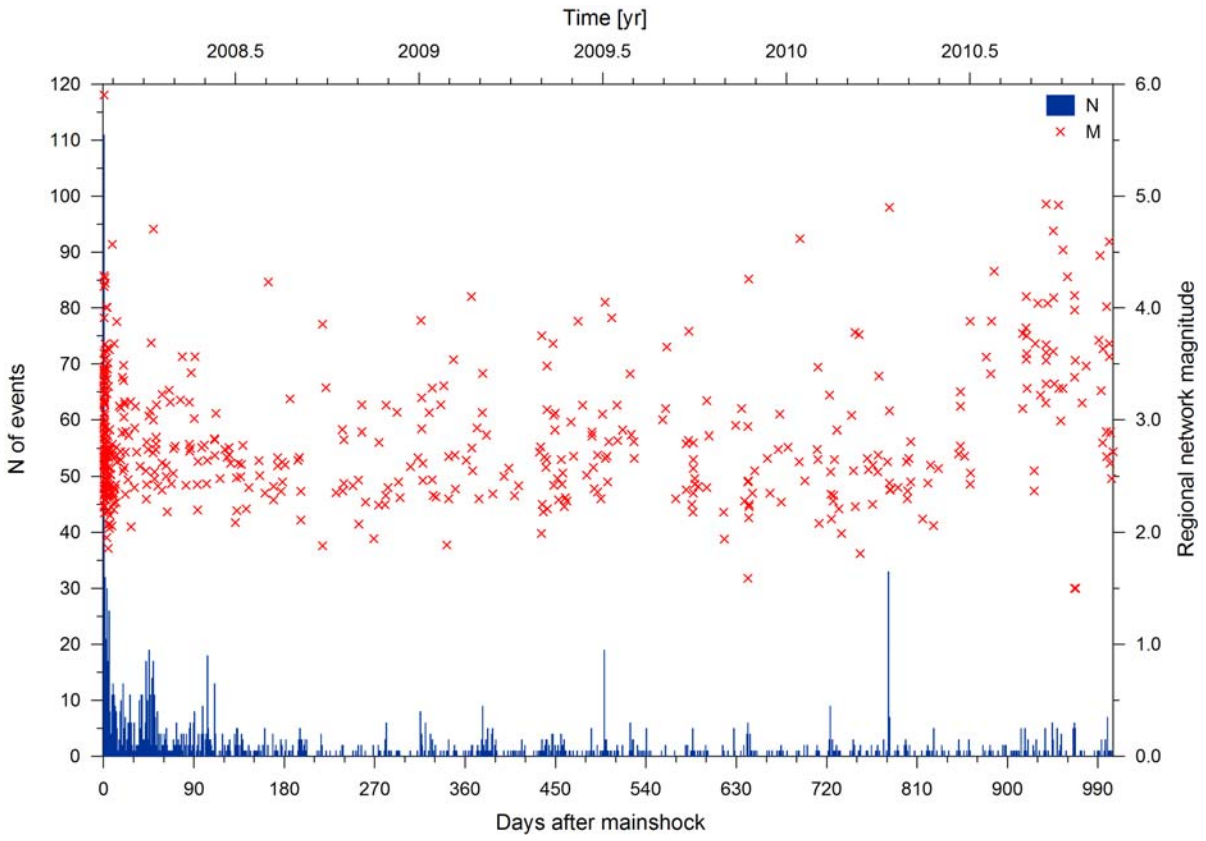

Fig. 6.2.5. Number of events per day after the occurrence of the 21st February 2008 mainshock, based on the listings of NORSAR's reviewed bulletin, Pirli et al. (2010) and the results of the waveform cross-correlation detector. In addition, event magnitude distribution in time is shown for events in NORSAR's bulletin and Pirli et al., 2010.

The three consecutive panels of Fig. 6.2.6 (one for each year) show the distribution with time of the waveform cross-correlation (CC) coefficient for those master events that provided detections. After some visual inspection of detector results, a CC-coefficient of 0.60 was decided as a threshold to eliminate erroneous detections. The time scale is uniform to facilitate a meaningful comparison between the three distributions, while different symbols are used for the detections of different master events. Three main time intervals can be distinguished, based on the "universality" of the employed master events: (a) the early stages of the sequence, represented by master events in 2008, which yield detections almost exclusively within the same time period, (b) a long time interval including 2009 and 2010 until autumn, when employed templates produce detections from almost the entire time length under discussion, and (c) the last two months when master events appear to be associated with only a very small number of earthquakes spaced closely around them in time.

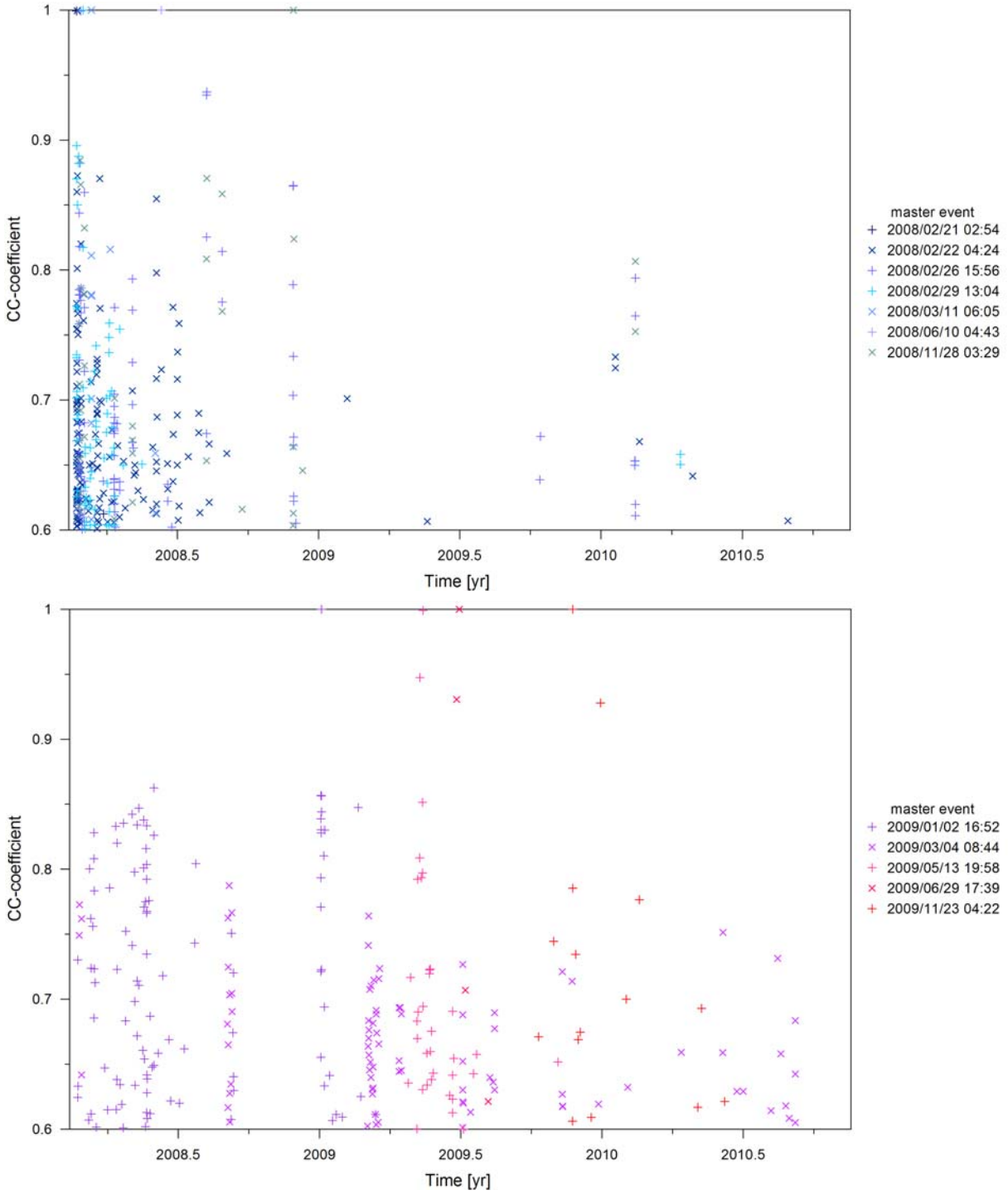

Fig. 6.2.6. Temporal distribution of the waveform CC-coefficient for the 22 of the 23 master events used within this study that yielded detections. A threshold of 0.60 was applied to ensure the validity of the results. Top diagram shows the 2008, at bottom the 2009 and on top on the next page the 2010 master events. Each master event is shown with a different symbol.

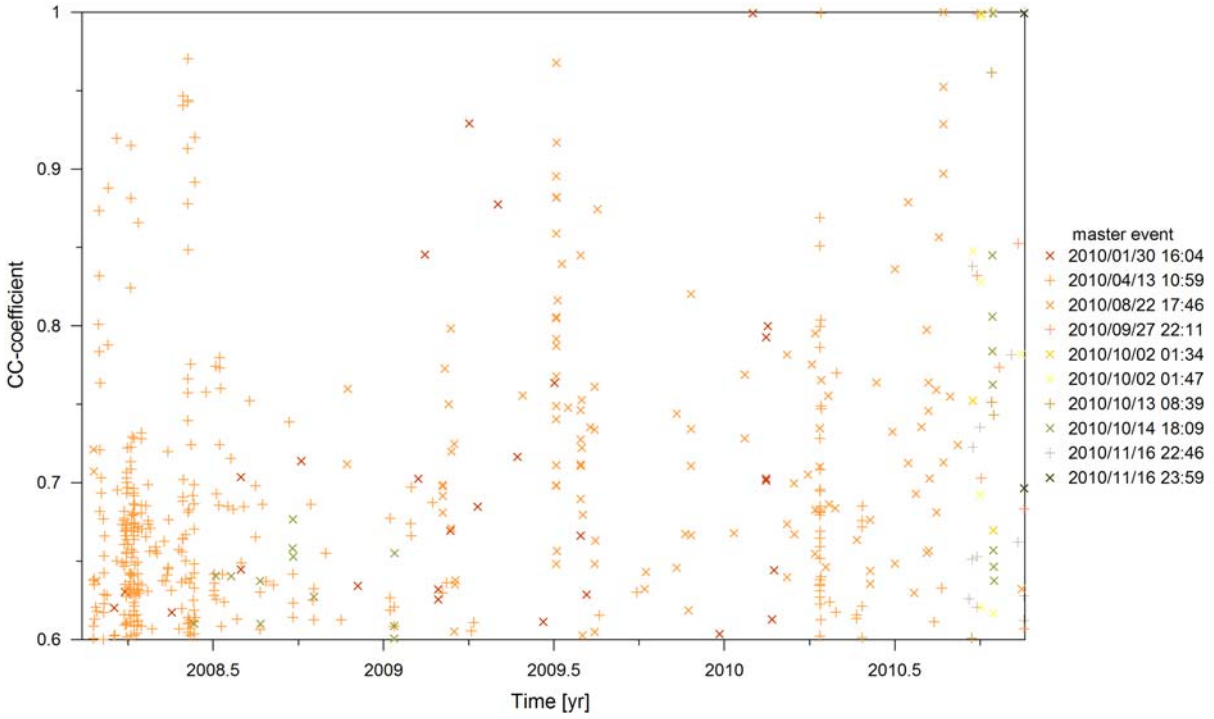

Fig. 6.2.6 Continuation from the previous page.

A closer look into the distributions of Fig. 6.2.6 reveals some expected and some more unusual features. Larger magnitude (e.g., M > 4.0) events are known to be non productive templates and this is verified here. The reason for their selection was to investigate their similarity to other events of the same magnitude order within the sequence; all of the larger events (M > 4.5) appear to be unrelated, suggesting a strong fragmentation of the aftershock region. The first master event (see Table 6.2.1), which is the first significant aftershock of the entire series, is similar only to one more event, a fact that should not be attributed exclusively to its size, but most probably to the conditions and operating mechanisms during the very initial stages of the sequence. The rest of the early master events are quite productive, but only for a limited time interval. What is quite unusual is the very small number of similar events detected by most of the latest templates (from October 2010 on). The fact that they do not correlate with any earlier activity is hardly surprising, since these events are located SW of the main aftershock volume (see Fig. 6.2.2). However, even when their own time period is considered, only very few low magnitude events were detected, suggesting that the image of the activity obtained in Fig. 6.2.5 is quite accurate. Those of the latest master events that share some similarity with the earlier activity, are the ones located within the initial aftershock region (see Fig. 6.2.1 for distribution in Pirli et al., 2010). So, the combination of the spatiotemporal distribution of the events and waveform similarity information provides a good overview of the evolution of the series.

At this point it should be stressed that the observed dissimilarity between the events latest in the series and the rest of the activity is not attributed solely to a difference in the S-P arrival time difference (note that entire waveforms are used for detection purposes). This can be demonstrated by Fig. 6.2.7, where entire waveforms for the three components of station HSPB are shown, band-pass filtered between 3 and 8 Hz. There are three waveform groups, sorted by component, while events are sorted with time, starting with the February 2008 main event on top of each group. The second event is the 12th April 2010, magnitude 4.9 event, followed by

events on 15th September 2010 05:56, 27th September 2010 12:09 and 6th October 2010 09:43. Besides the obvious S-P time difference between the upper two and the lower three events, it is obvious that the two groups contain different phases, while variations in the radiation pattern are also suggested by the different amplitude levels for P-type phases on the horizontal components. It is unclear whether this signifies a larger diversity in focal mechanism, which would point to a tectonic structure of different geometry to that of the seismogenic fault, or this is an effect of the different location and/or probable difference in focal depth between the two groups.

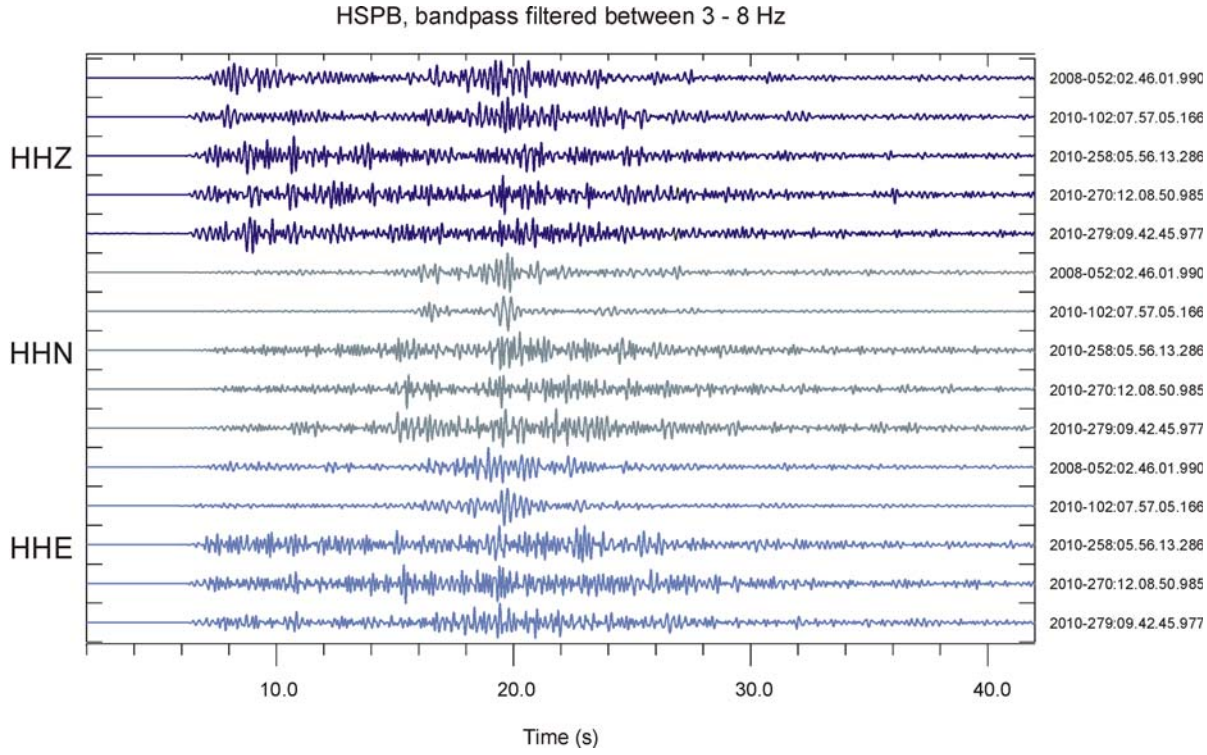

Fig. 6.2.7. Waveforms of Storfjorden events as recorded at HSPB, band-pass filtered between 3 and 8 Hz. The events pictured here are the 21st February 2008 mainshock (2008-052 02:46, Mw 6.1), the 12th April 2010 event (2010-102 07:57, M 4.9), the 15th September 2010 event (2010-258 05:56, M 4.9), the 27th September 2010 event (2010-270 12:09, M 4.9) and the 6th October 2010 (2010-279 09:43, M 4.3) event.

6.2.4 Conclusions

Summarising all the points made above, monitoring of the persisting seismic activity in the area of Storfjorden, Svalbard, leads us to the conclusion that this is a continuation of the February 2008 earthquake series. However, from autumn 2010 on, the main part of the activity is concentrated in an area SW of the original aftershock region, revealing a new source, either on a different part of the fault that gave the magnitude 6.1 mainshock in 2008 or on a neighbouring tectonic structure. A solid conclusion on the characteristics and nature of this source can only be derived from the calculation of focal mechanisms for the largest, most recent events. It

is clear though, based on waveform similarity and the spatio-temporal distribution of these late events, that the mechanism behind their occurrence is different than that of the earlier stages of the series. The large magnitudes (M > 4.0) observed during this latest stage further suggest that the region is far from reaching equilibrium.

Myrto Pirli
Berit Paulsen
Johannes Schweitzer

References

Gibbons, S.J. and F. Ringdal (2006). The detection of low magnitude seismic events using array-based waveform correlation. Geophys. J. Int., **165**, 149-166.

Pirli, M., J. Schweitzer, L. Ottemöller, M. Raeesi, R. Mjelde, K. Atakan, A. Guterch, S.J. Gibbons, B. Paulsen, W. Dębski, P. Wiejacz and T. Kværna (2010). Preliminary analysis of the 21 February 2008, Svalbard (Norway), seismic sequence. Seism. Res. Lett., **81**,(1), 63-75, doi:10.1785/gssrl.81.1.63.

Schweitzer J. and the IPY Project Consortium Members (2008). The International Polar Year 2007-2008 Project "The Dynamic Continental Margin between the Mid-Atlantic-Ridge System (Mohns Ridge, Knipovich Ridge) and the Bear Island Region". NORSAR Sci. Rep., **1-2008**, 53-63.

6.3 Installation of the seismic broadband station in Barentsburg, Svalbard

6.3.1 Background

Within the framework of the project 'Cooperative seismological studies on Spitsbergen' (Polar Research program of the Research Council of Norway), NORSAR is expanding its long-standing cooperation with the Kola Regional Seismological Centre (KRSC) in monitoring seismic events in the European Arctic. KRSC has been operating a seismic station in Barentsburg for many years and one of the major goals of the project was to acquire and install a modern broadband instrument. The new station in Barentsburg (BRBA) will improve the monitoring capability of man-made events (e.g., mining blasts, rock bursts), seismic events related to the moving of glaciers (icequakes, calving) and regional and teleseismic earthquakes. It will be a significant supplement to the already existing permanent stations in the Svalbard region (Fig. 6.3.1) in Adventdalen (SPITS), Ny-Ålesund (KBS), Hornsund (HSPB) and Hopen (HOPEN).

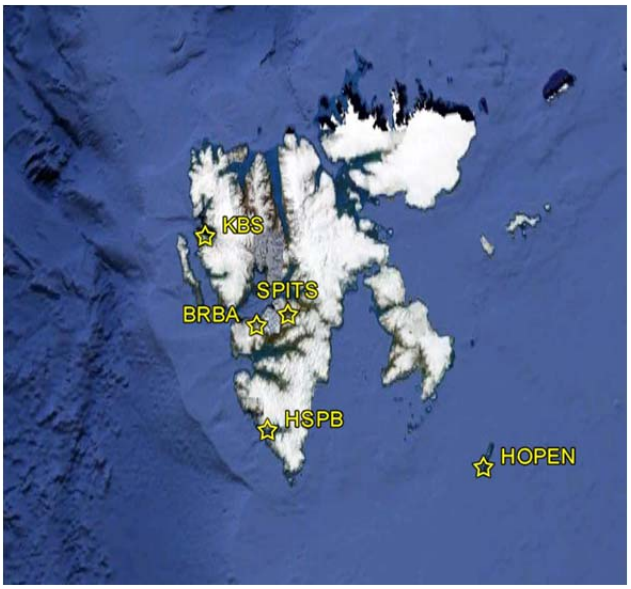

Fig. 6.3.1. The seismic stations SPITS, KBS, HSPB and HOPEN are providing continuous data in near real-time to NORSAR. The new station BRBA currently stores data locally, but it will be connected to the Internet in the near future.

The Svalbard region shows a much higher seismicity than the Norwegian mainland (Fig. 6.3.2). Heerland in the southern part and Nordaustlandet in the northeastern part are the most active earthquake regions. In the West and South-West there is significant seismic activity along the Mid-Atlantic Ridge (Knipovich Ridge and Mohns Ridge) and in the South-East seismicity is found in the Barents Sea around Hopen. On 21 February 2008, one of the largest instrumentally recorded earthquakes in the Spitsbergen region occurred. The epicenter was in the Storfjorden area, and the magnitude 6.1 earthquake was followed by several thousand aftershocks. Fortunately, it occurred offshore, and neither injuries nor damage to structures were reported. The aftershock sequence is today (February 2011) still ongoing (Pirli et al., 2010; 2011).

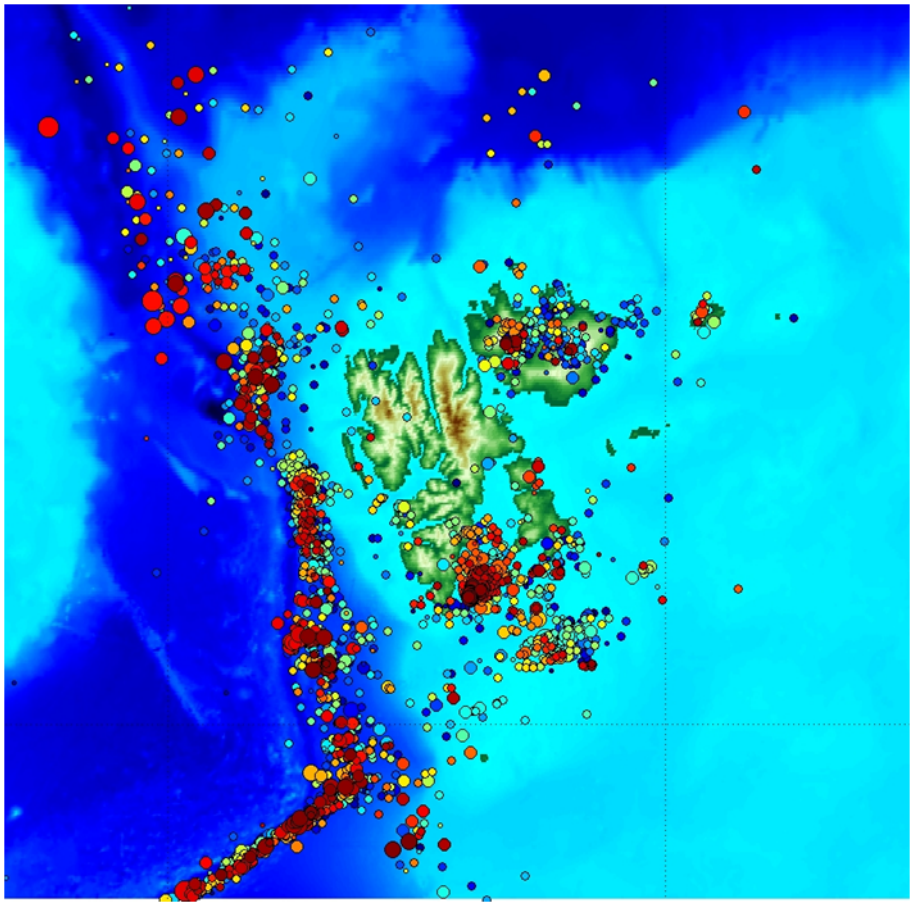

Fig. 6.3.2. Seismicity on and around Svalbard. The map shows about 2700 seismic events for the time period Sep 1998 – Nov 2010 (NORSAR Reviewed Regional Seismic Bulletin). The size of the symbol indicates the event magnitude and the color indicates the origin time (blue: old, yellow/green: intermediate, red: recent events).

The areas around the coal mines on Svalbard also show some seismic activity. A particularly strong earthquake in 1976 caused significant damage to the (now abandoned) Soviet mine in Pyramiden. In general, however, the events within the mining areas are small compared to the known seismicity in the region. The most significant seismic hazard to the mining activity are the numerous rock bursts that are induced by the mining itself, especially in the Barentsburg coal mine. This mine is operated by the Russian company Trust Arktikugol, which has suffered several accidents caused by rock bursts and gas explosions. Larger earthquakes on Svalbard are reported by the Norwegian National Seismic Network (NNSN), and are routinely included in international seismic bulletins. However, until today there is no systematic and detailed monitoring and location of the smaller seismic events that often occur in the mining areas.

In December 2000, KRSC, in cooperation with NORSAR, installed an experimental short-period GeoSig system in Barentsburg (BRB) at about 5 km distance from the mines (Fig. 6.3.3). The intention was to acquire more knowledge about the increasing number of rock bursts in the mines near Barentsburg.

During a time period of 4 months (1 December 2000 to 25 March 2001) when the mine was in full operation, a large number of rock bursts (magnitude typically between 0 and 1) could be recorded (Fig. 6.3.3, left). On 25 March 2001 a particularly large rock burst (magnitude 2.5)

occurred, and for safety reasons the mining was discontinued for about one month. The rock burst activity ceased immediately after the stop of the mining activity (Fig. 6.3.3, right)

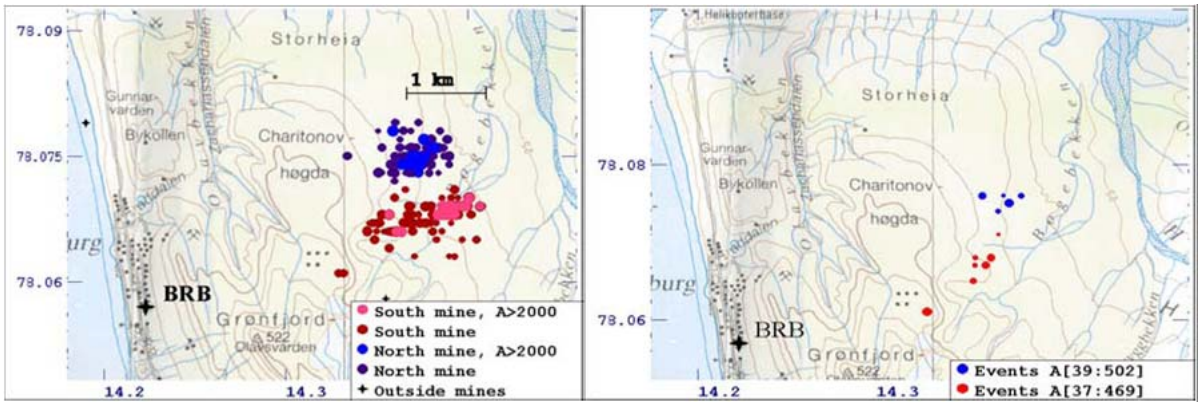

Fig. 6.3.3. Locations of seismic events in the Barentsburg area for the time period 1 December 2000 to 25 March 2001(left) and 26 March to 19 April 2001 (right). The blue symbols show events in the northern mine, while red symbols show events in the southern mine. The largest events have lighter colors. The Barentsburg seismic station (BRB) is shown by the large cross (from Kremenetskaya et al., 2001).

6.3.2 Details and installation of the new station BRBA

The BRBA site (78.0588N 14.2191E, 70 m asl) is in the Barentsburg settling in about 50 meters distance from the 'Research Station Barentsburg', in which KRSC has its rooms (Fig. 6.3.4). The site is sheltered by a wooden barrack, and buried cables between the buildings provide power and communication. The broadband sensor is placed on top of a concrete pillar inside the wooden shed.

Fig. 6.3.4. The seismic station BRBA is in the wooden shed on the left hand side. The 'Research Station Barentsburg' is the yellow brick building in the background.

This pillar (Fig. 6.3.5) reaches several meters down into the permafrost and it is decoupled from the building. In order to monitor both regional and local seismicity, we chose a Güralp broadband instrument (Fig. 6.3.5) with a frequency range from 1/60 – 50 Hz. Taking into account the environmental conditions, we opted for a so-called Polar-version that remains operational for temperatures down to -40 deg Celsius. The matching digitizer module is a Güralp DM24. With the accompanying software it is possible to connect to the system remotely in order to adjust sampling parameters and select data streams, to check the state-of-health (timing, mass position, etc.), to center the instrument and to transmit data. The station is powered by a 12 V DC battery, which in turn is connected to a conventional charger using 220 V AC. The communication between the digitizer and an acquisition laptop in the main building is through a modem connection.

Fig. 6.3.5. Inside the BRBA site. The broadband sensor in the middle of the concrete pillar (dark grey cylinder) is replacing the three obsolete analog short-period Kirnos sensors (grey covers) and the experimental short-period GeoSig systems (blue boxes).

The new data acquisition system with the broadband sensor of BRBA started up on 13 September 2010 and since then continuous data (3 components at 80 Hz) have been recorded and stored locally on the laptop. The laptop is connected to the Internet over a conventional ADSL box and we can access it remotely for state-of-health checks and maintenance. The Internet connection is the only one in the research station. It has a limited capacity and it is shared with other groups. For this reason real-time continuous data transmission is currently not feasible. We can download data for single events of interest, but the main bulk of the data is copied to USB-disks by the local operator and sent to KRSC in Apatity and to NORSAR. We are working on establishing a dedicated Internet connection with fixed IP address in order to fully integrate the station into our data storage and processing environment at NORSAR.

6.3.3 Instrument response of the new broadband recording system at BRBA

As already mentioned, the broadband station BRBA at Barentsburg is equipped with a three-component CMG-3ESPC seismometer and a CMG-DM24 digitizer by Güralp Systems Ltd. The seismometer has the serial number # T35444 and the digitizer the serial number # B212 and their response characteristics (i.e., poles/zeros, sensitivities) are provided by the manufacturer and are listed below:

T35444 Poles [Hz]:
(-11.78 x 10-3) ± j(11.78 x 10-3), -160, -80, -180
Zeros [Hz]:
0.0, 0.0
Sensitivities:
Z: 2 x 988 V/m/s, NS: 2 x 988 V/m/s, EW: 2 x 991

B212 Velocity channel sensitivities:
Z: 3.176 µV/count, NS: 3.190 µV/count, EW: 3.175 µV/count

Two different channel configurations were outputted from the station since its initial installation: 80 sps (HHZ, HHN, HHE channels) and 4 sps (MHZ, MHN, MHE channels) streams for the first hours of operation, and 80 sps and 1 sps (LHZ, LHN, LHE channels) streams from then on. This required a change in the FIR filter cascade employed by the digitizer to decimate down from the input rate of 512 kHz to the outputted data sampling rates (Güralp Systems, 2006). The two filter cascades (TTL = 86 for 80 sps and 4 sps and TTL = 90 for 80 sps and 1 sps) are identical down to the 80 sps tap, so the response of the HH channels has remained unchanged throughout the station's operation. The TTL = 90 FIR cascade is shown below (Cirrus Logic, 2001; Güralp Systems, 2006):

FIR filter SINC-1 (asymmetric) with 18 coefficients, decimating by 8 down to 64 kHz from an input rate of 512 kHz.
FIR filter SINC-2-stage-3 (asymmetric) with 3 coefficients, decimating by 2
FIR filter SINC-2-stage-4 (symmetric) with 7 coefficients, decimating by 2
filter FIR-1-set0 (asymmetric) with 24 coefficients, decimating by 4
filter FIR-2-set0 (asymmetric) with 63 coefficients, decimating by 2
filter DM24-tap0 (symmetric) with 501 coefficients, decimating by 5
filter DM24-tap1 (symmetric) with 501 coefficients, decimating by 5 down to the desired sampling rate of 80 sps (HH channels)
filter DM24-tap0 (symmetric) with 501 coefficients, decimating by 4
filter DM24-tap0 (symmetric) with 501 coefficients, decimating by 2
filter DM24-tap0 (symmetric) with 501 coefficients, decimating by 5
filter DM24-tap2 (symmetric) with 501 coefficients, decimating by 2 down to the desired sampling rate of 1 sps (LH channels)

The BRBA station's configuration described above and the corresponding Respid flags (Pirli, 2010) are listed in Table 6.3.1. The displacement amplitude and phase response curves are shown in Fig. 6.3.6 for the vertical channel.

Table 6.3.1. The instrument configuration of the BRBA station

Time	Installation Name	System Components	Calib [nm/ count]	Calper [s]
2010/09/13 - …	Current HH BRBAHH1 BRBAHH2 BRBAHH3	CMG-3ESPC CMG-DM24 digitizer	Z: 0.25581 NS: 0.25694 EW: 0.25495	1.00
2010/09/13	Initial MH BRBAMH1 BRBAMH2 BRBAMH3	CMG-3ESPC CMG-DM24 digitizer TTL 86 FIR cascade	Z: 0.25581 NS: 0.25694 EW: 0.25495	1.00
2010/09/13 - …	Current LH BRBALH1 BRBALH2 BRBALH3	CMG-3ESPC CMG-DM24 digitizer TTL 90 FIR cascade	Z: 0.25581 NS: 0.25694 EW: 0.25495	1.00

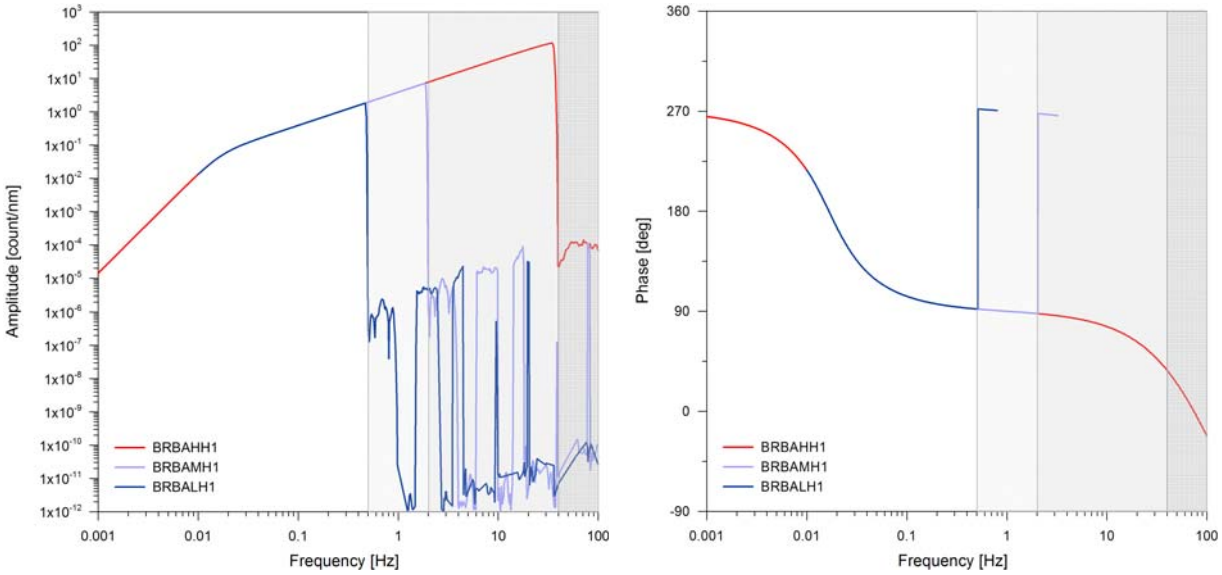

Fig. 6.3.6. Displacement amplitude (left) and phase (right) response for the vertical component of the different configurations of station BRBA. Respids are used to link each curve to the corresponding configuration listed in Table 6.3.1. Shaded areas represent the range beyond the Nyquist frequency (40 Hz for HH, 2 Hz for MH and 0.5 Hz for LH channels.

6.3.4 First data analysis

Since January 2011, the first seismic data from the new broadband station in Barentsburg are available for analysis and quality check. It became very soon clear that the data quality of this station varies signifcantly with the time of the day. During working hours, the noise level in the high frequency range can be quite high (see e.g., http://www.norsardata.no/cgi-bin/ spdatashow.cgi ?sta=BRB&year=2011&doy=038), although the man-made noise is not constant and may disapear for some time. The man-made noise usually decreases during night time. The station has already recorded many smaller and larger earthquakes in the region. For long period data the noise level is on the same level as at the other broadband stations on Spits-

bergen (HSPB or KBS), see e.g.,
http://www.norsardata.no/cgi-bin/lpdatashow.cgi?sta=BRB&year=2011&doy=033.

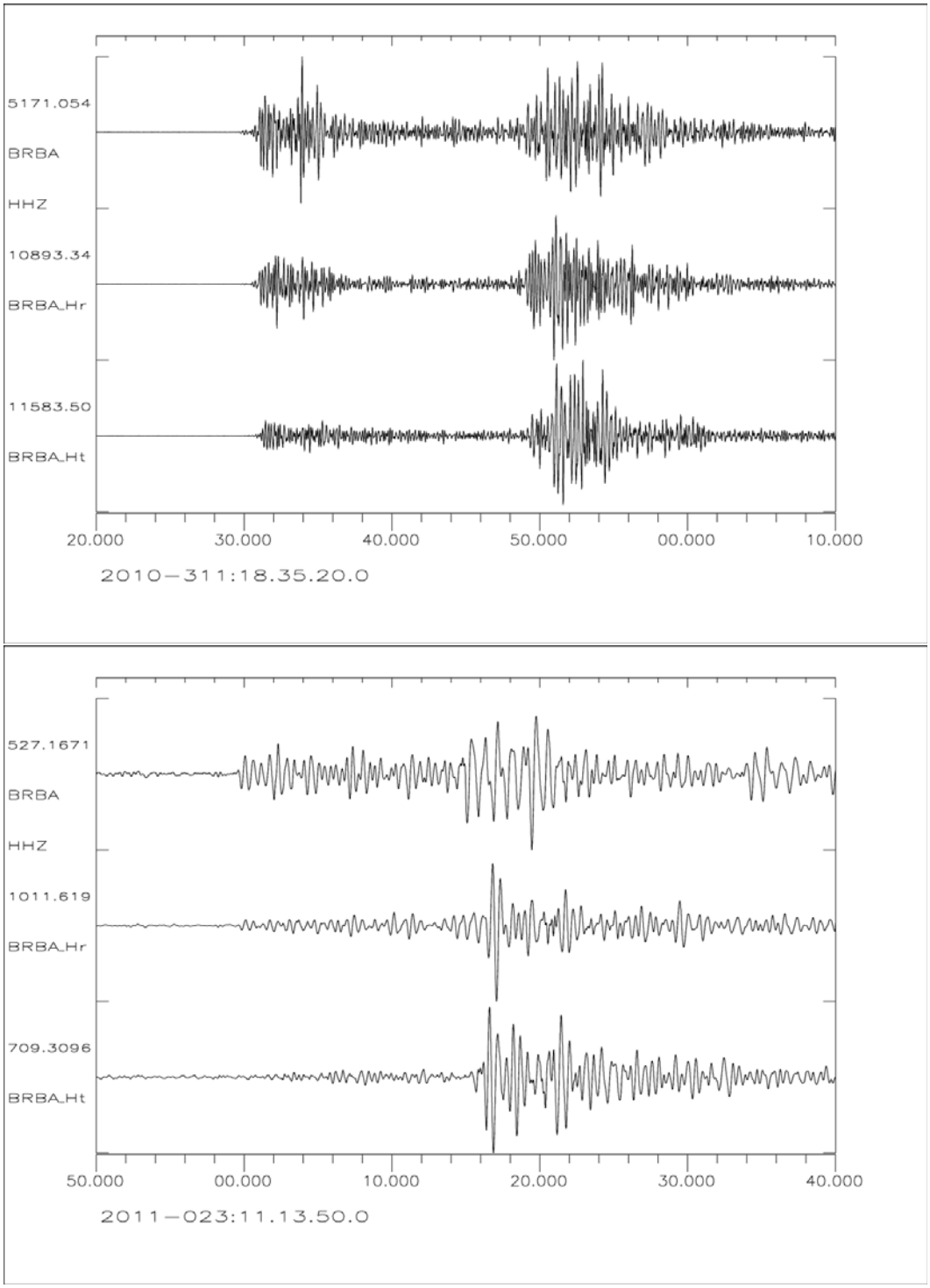

Fig. 6.3.7. Two earthquakes recorded with the new broadband station in Barentsburg. On top we see the data from one of the larger aftershocks of the Storfjorden sequence (Pirli et al., 2010; 2011) at a distance of about 158 km (Butterworth bandpass 3 - 8 Hz) and at the bottom the data from a smaller event on the Knipovich Ridge at a distance of about 133 km (Butterworth bandpass 1 - 3 Hz). For further details, see text.

In Fig. 6.3.7 we show two examples of earthquake records at the new broadband station BRBA in Barentsburg. The first earthquake (Fig. 6.3.7, top) is a magnitude 4.5 event from the Storfjorden aftershock sequence (Pirli et al., 2010; 2011). BRBA is located about 158 km from the source region (2010-311:18.35.04, 76.98 N, 18.43 E, NORSAR Reviewed Bulletin). The vertical and the backazimuth rotated horizontal radial and transverse components are shown. The second example (Fig. 6.3.7, bottom) shows the data for a much smaller earthquake (magnitude 2.3), which occured at the Knipovich Ridge, West of Svalbard (2011-023:11.13.37, 77.76 N, 8.72 E, NORSAR Reviewed Bulletin). BRBA is located about 133 km from the earthquake and again the vertical and horizontally rotated components are shown.

For 2011 the installation of a second broadband sensor nearby Barentsburg (BRBB), but farther away from the dirsturbing man-made noise sources, is planned. In addition, we plan also to establish a stable online data transmission from both stations to KRSC and NORSAR.

Michael Roth
Myrto Pirli
Johannes Schweitzer
Elena Kremenetskaya, KRSC

Acknowledgements

Purchase and installation of the new broadband station in Barentsburg was mainly financed by the Research Council of Norway (Project number 196157/S30). Fig. 6.3.1was made with the help of Google Earth.

References

Cirrus Logic (2001). Crystal CS5376 Low Power Multi-Channel Decimation Filter. DSA0072869.pdf, Cirrus Logic Inc., Austin, Texas, 122 pp.

Güralp Systems (2006). CMG-DM24 Mk3 Digitizer Operator's Guide. MAN-D24-0004, Güralp Systems Ltd., Aldermaston, England, 122 pp.

Kremenetskaya, E., S. Baranov, Y. Filatov, V.E. Asming and F. Ringdal (2001). Study of the seismicity near the Barentsburg mine (Spitsbergen). NORSAR Sci. Rep., **1-2001**, 114-121.

Pirli, M. (2010). NORSAR System Responses Manual, 2nd Edition. NORSAR, Kjeller, Norway. 180 pp.

Pirli, M., J. Schweitzer, L. Ottemöller, M. Raeesi, R. Mjelde, K. Atakan, A. Guterch, S.J. Gibbons, B. Paulsen, W. Dębski, P. Wiejacz and T. Kværna (2010). Preliminary analysis of the 21 February 2008, Svalbard (Norway), seismic sequence. Seism. Res. Lett., **81**,(1), 63-75, doi:10.1785/gssrl.81.1.63.

Pirli, M., B. Paulsen and J. Schweitzer (2011). Late stages of the Storfjorden, Svalbard, aftershock sequence. NORSAR Sci. Rep., **1-2011**, 43-52.

6.4 Test of new hybrid seismometers at NORSAR

6.4.1 Introduction

In the framework of the recapitalization of the NORSAR arrays NOA and ARCES (primary stations PS27 and PS28, respectively) and a potential modernization of the SPITS array (auxiliary station AS72) we wish to install new digitizers and sensors. One of our goals was to specify one sensor type suitable for all our arrays. Having a uniform sensor at all sites will simplify maintenance and data processing as well as improve the operational readiness, because of the interchangeability of spare parts.

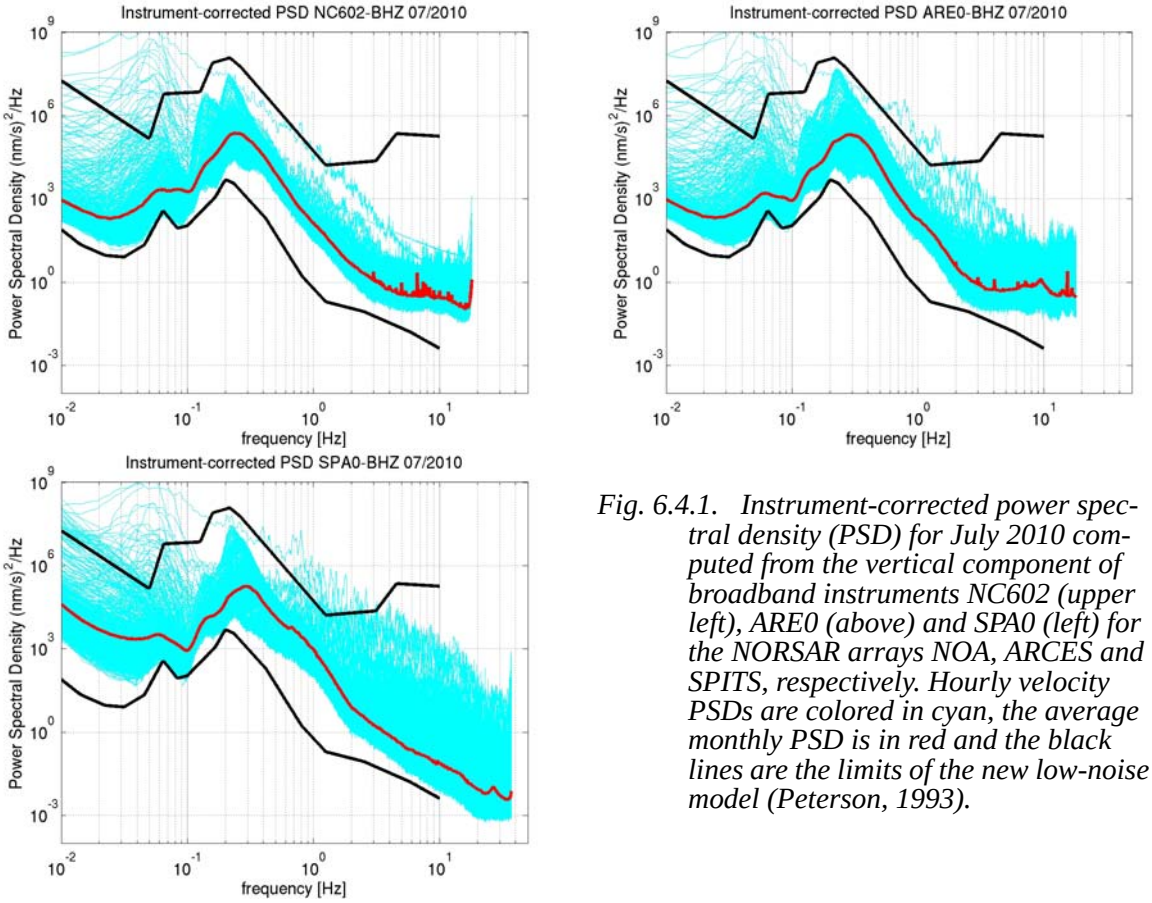

Fig. 6.4.1. Instrument-corrected power spectral density (PSD) for July 2010 computed from the vertical component of broadband instruments NC602 (upper left), ARE0 (above) and SPA0 (left) for the NORSAR arrays NOA, ARCES and SPITS, respectively. Hourly velocity PSDs are colored in cyan, the average monthly PSD is in red and the black lines are the limits of the new low-noise model (Peterson, 1993).

Figure 6.4.1 gives an overview on conditions for three sites NC602, ARE0 and SPA0 (broadband sites in NOA, ARCES and SPITS, respectively) for July 2010. For each hour we computed the power spectral density for the vertical components, corrected for instrument response and plotted the 744 curves on top of each other. The red curve is the average PSD for the month and the black lines are the bounds of the Peterson (1993) new low-noise model. We did not sort out time periods that contained seismic events, which contributes to the broad variation in the set of curves and causes a certain bias of the average curve. However, we clearly can determine the lower noise limit for the sites. For NOA and ARCES the ambient noise during quiet conditions is close to or even touches the low-noise Peterson model for frequencies below 0.2 Hz. At SPITS we have higher noise-levels for very low frequencies (<0.05 Hz), but in the high-fre-

quency range (> 4 Hz) the site is very quiet due to the absence of any industrial and man-made noise.

Figure 6.4.2 shows the transfer function of seismic sensors (digitizer response/gain included) in use at the NORSAR arrays. Most of the instruments are proportional to velocity (Guralp 3T NOA, Guralp 3T ARCES, STS2 NOA test bed, STS2 JMIC, Teledyne T20171 (for f < 1 Hz)), but two of them (Guralp 3T SPITS and KS5400) are proportional to acceleration. In order to decide on a new sensor type we were taking into account the ambient noise conditions and the experiences with our existing systems. In our opinion the current system at SPITS has too high gain for high-frequencies. At ARCES the sensor gain is fine for high frequencies, but it is too high for frequencies below 1 Hz. The KS5400 at NOA lacks sensitivity for very low frequencies and for frequencies higher than 10 Hz.

Eventually we decided to go for a seismic sensor with a newly designed hybrid response. We specified the desired shape and Guralp Systems designed and fabricated the sensor. The sensor has a sensitivity of 2x20 000 V/m/s at 5 Hz and it is proportional to velocity for 1/360 Hz - 1/3 Hz, proportional to acceleration for 1/3 Hz - 2 Hz and again proportional to velocity for 2 Hz - 50 Hz. The Guralp 3T Hybrid response is shown in Figure 6.4.2 It is less sensitive than the Guralp 3T ARCES instrument at lower frequencies, it fits the Teledyne T20171, the KS5400 and the Guralp 3T SPITS at about 5 Hz and it has lower sensitivity than the Guralp 3T SPITS at high frequencies.

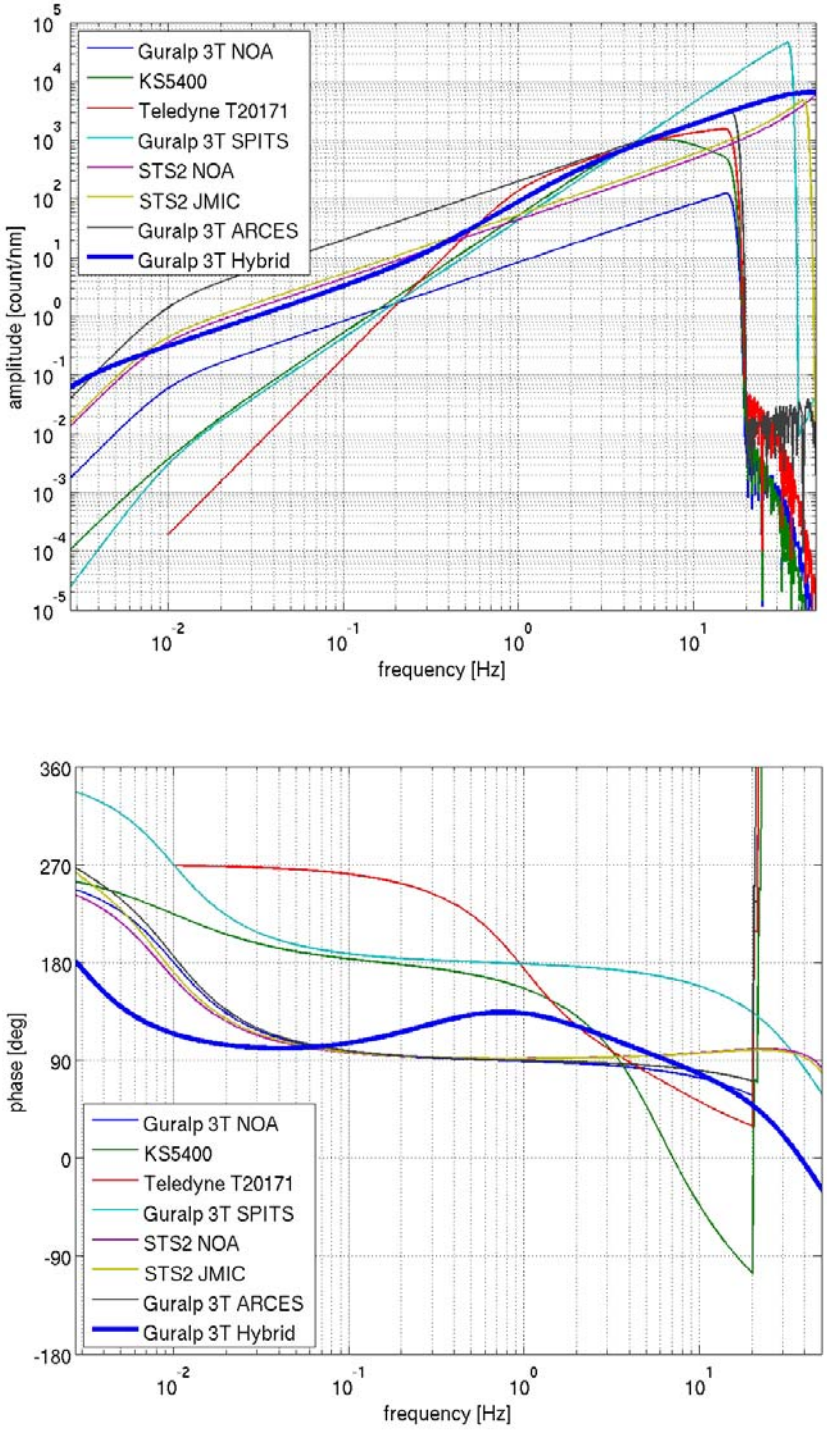

Fig. 6.4.2. Transfer functions for different sensors in use at the NORSAR arrays. Top: Amplitude response in units of counts/nanometer (site specific digitizer response/gain included). Bottom: Phase response.

6.4.2 Instrument tests

In the beginning of 2010 NORSAR received two prototypes of the new hybrid sensor. The sensors had the same instrument response but different sensitivity, i.e. 2x15000 V/m/s and 2x60000 V/m/s. Besides problems with reversed polarity we found undesirable high frequency noise bumps around 35-50 Hz. At the low frequency end we found incoherence between the sensors part of which could be associated with thermic convection and noise induced by the very stiff seismometer cables. In the following we discuss the tests on the second batch of instruments (5 Guralp 3T hybrid with 2x20000 V/m/s)

NORSAR has a test facility at the site NC602 of the NOA array. Figure 6.4.3 shows the central building at the site. About 20 m to the right of the building is a subsurface bunker that houses the IMS short-period Teledyne and Guralp instrument. The spacious bunker has three seismometer pits out of which two have been used for testing purposes. Figure 6.4.3 (bottom left) shows one of the pits with 7 instruments covered by thermal insulation tubes. The right side of Figure 6.4.3 shows an opened Guralp hybrid 3T.

Fig. 6.4.3. Top left: Central building of the NORSAR test facility. The subsurface vault containing the broadband site NC602 and the test instruments is to the right of the building. Bottom left: One out of three pits in the vault with thermically insulated Guralp instruments. Right: An open Guralp 3T hybrid instrument.

A main goal of the tests was to investigate the noise level of the sensors and the coherency between the instruments. The left hand side of Figure 6.4.4 shows PSDs for September 2010 for the IMS broadband sensor at NC602. Based on these types of displays (http:// www.norsardata.no/NDC/spectraplot/) we have been searching for quiet periods to analyze the test data. The right hand side of Figure 6.4.4 shows an 8-hour time window of raw data (Z, East and North component from top to bottom) recorded with 5 hybrid instruments located in one of the seismometer pits.

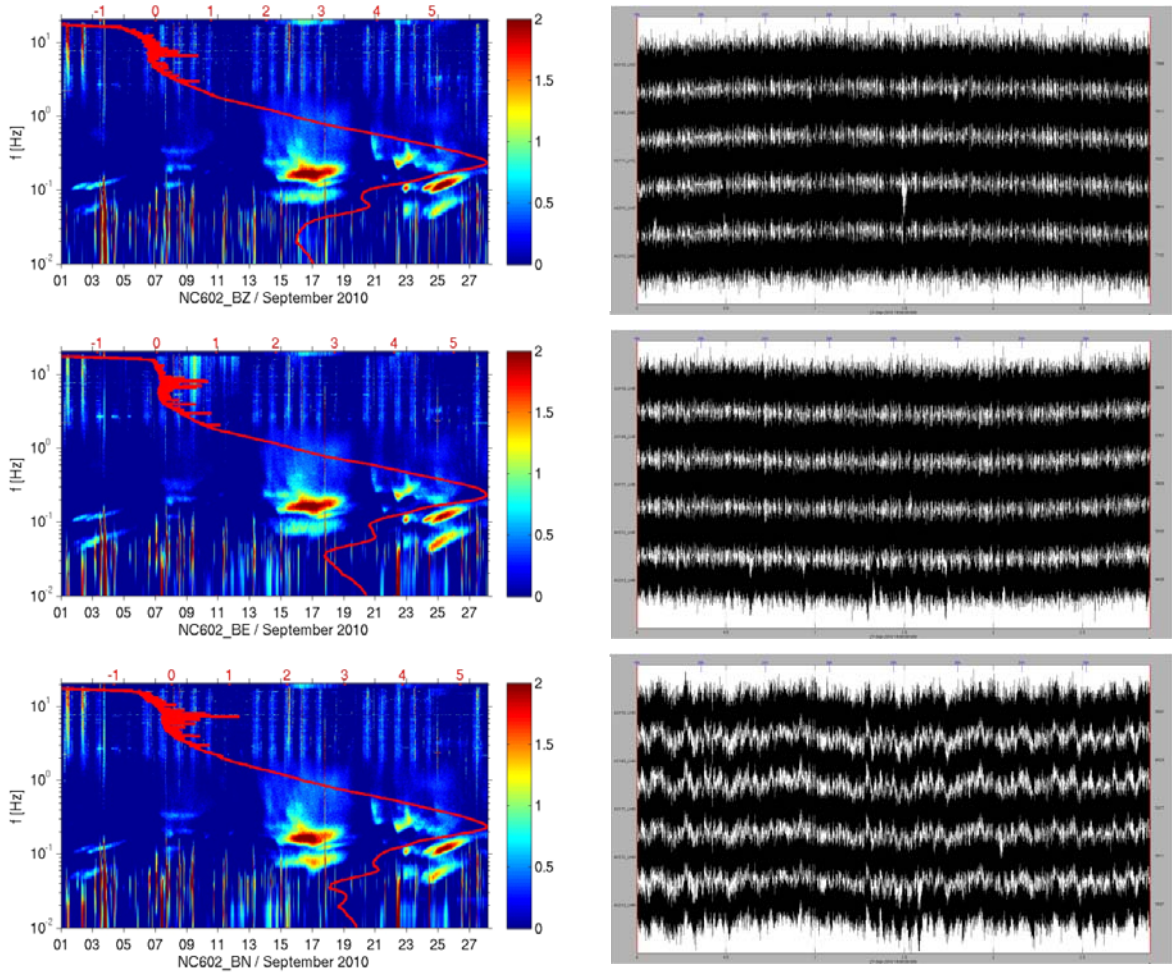

Fig. 6.4.4. Left column: Power spectral density (PSD) for the broadband instrument NC602 (Z, East and North component, raw data) for September 2010. The red curve shows the average PSD of the entire month and residuals from the average are color-coded. Right: Waveforms recorded with 5 colocated hybrid seismometers (Z, East and North component from top to bottom) for an eight-hour time window (start 27.09.2010 19:00). In each panel the traces from top to bottom correspond to digitizer/instrument A2118/T36307, A2149/T35728, A2171/T36340, A2212/T36344, and A2213/T36309, respectively.

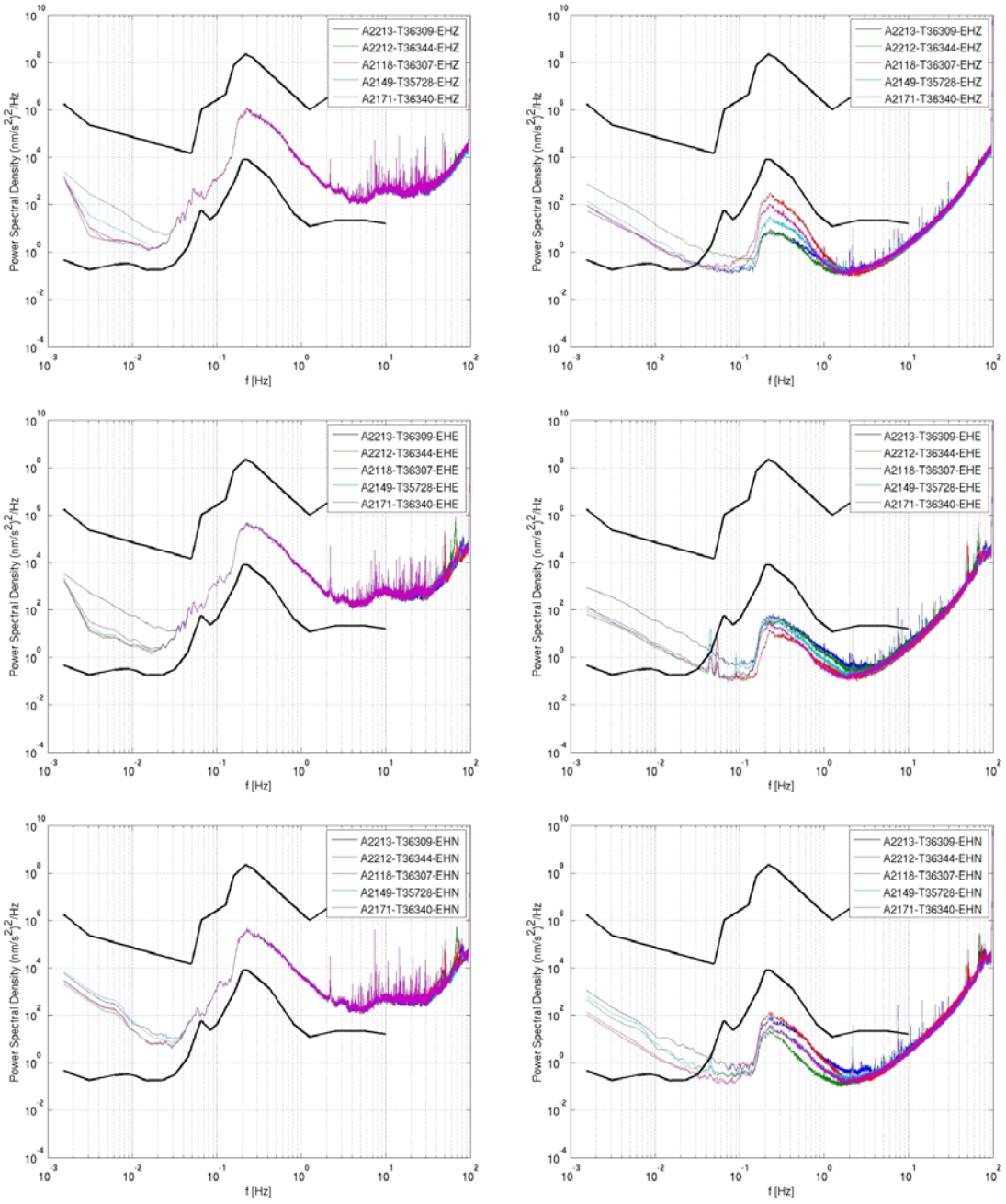

Fig. 6.4.5. Left: Instrument-corrected PSD (Z-, East and North component from top to bottom) computed for the eight-hour seismograms shown in Figure 6.4.1 We used 600 s windows with 300 s overlap and the PSD is for acceleration, i.e. in units of $(nm/s^2)^2$/Hz. Right: Instrument-corrected PSD of incoherent traces, i.e. we subtracted the average waveform and computed the PSD of the residual.

From the raw data in Figure 6.4.4 (right) we computed the power spectral density using Welch's method (1967) with time window lengths of 600 s and 300 s overlap. Figure 6.4.5 (left) shows the resulting PSDs corrected for the nominal acceleration instrument response. The PSDs for the different instruments coincide very well for frequencies above 0.03 Hz. All spectra have the identical noise peaks in the frequency range from about 2-50 Hz. These noise peaks are not related to the hybrid sensors (we see them also with other instruments at the site),

but are manmade (e.g. turbine of hydro-power plants) and electrical noise. For low-frequencies (< 0.03 Hz we see that some of the sensors deviate. This is partly due to settling effects or burps of the sensor. At very high frequencies (> 50 Hz) the spectra for the horizontal components exhibit differences, but this is outside of the frequency range of interest.

Since the instruments are co-located they should record the very same input signals (ambient seismic signals) and should produce the very same output. Differences in the output can be interpreted as instrument noise (intrinsic, but also settling events etc.). One approach to estimate the instrument noise is to compute an average output trace from all 5 instruments, subtract the average trace from the single recordings and compute the PSD of the residual traces. The results are displayed in Figure 6.4.5 (right column). The PSDs of the instrument noise is below the low-noise Peterson model for frequencies above 0.03 - 0.04 Hz. The higher instrument noise in the frequency range of the microseisms could be partly an artifact of the computational method, but it is anyway well below the low-noise model.

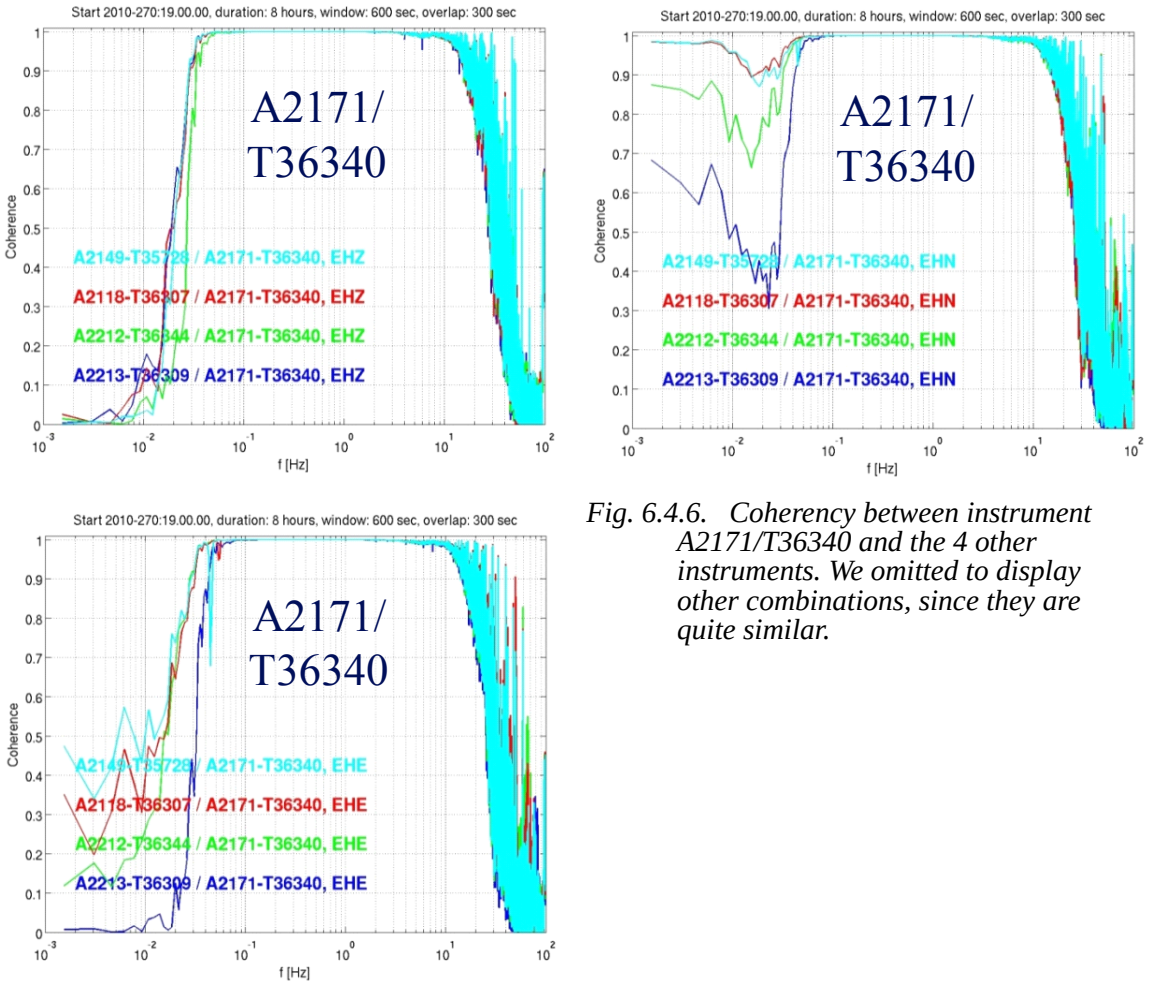

Fig. 6.4.6. Coherency between instrument A2171/T36340 and the 4 other instruments. We omitted to display other combinations, since they are quite similar.

Power spectral density is one way to compare instrument performance, but it does not give information on the signal coherency between the different instrument outputs. The coherency is defined as $C=|P_{12}|^2/(P_{11}P_{22})$, where P_{11}, P_{22} and P_{12} are the power spectral densities (PSD) for system 1 and 2 and cross-spectral density between the systems outputs, respectively (e.g.

Kay 1988). Representative for all results Figure 6.4.6 shows the coherency between A2171/ T36340 and the other 4 instruments. Coherency should be 1 for perfect trace alignment and this can be observed over a broad frequency range. At the low frequency end it starts to decrease at around 0.03 Hz (vertical components) and 0.04 Hz (horizontal components); at the high frequency end it starts to detoriate at 10 - 20 Hz. The coherency for the North component recovers again for low frequencies, which is an indication that there was coherent ambient seismic noise polarized in N-S direction. At that occasion it is important to mention that we observe nearly perfect coherence over the entire frequency range in the presence of a seismic event.

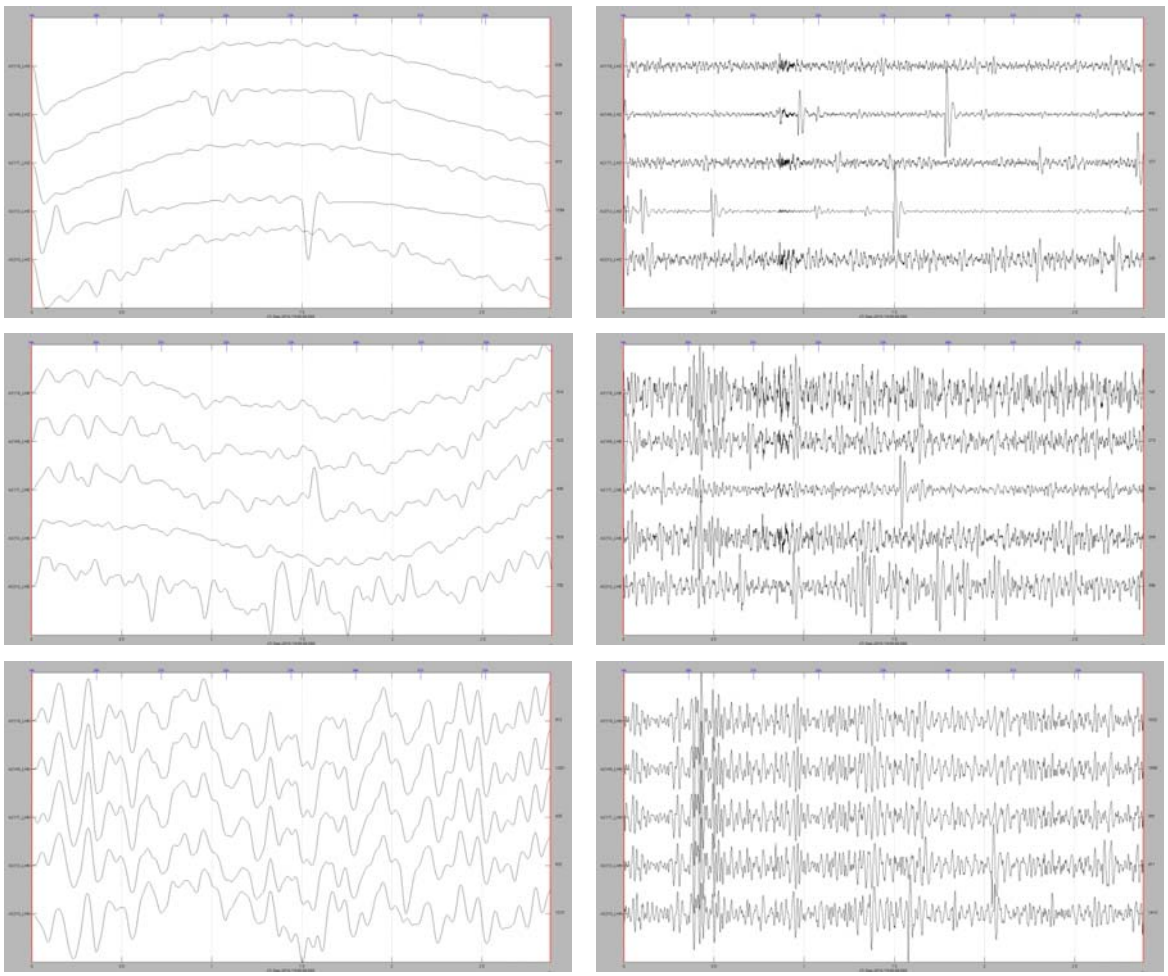

Fig. 6.4.7. Waveform comparison between the 5 hybrid instruments for different frequency bands. Left column: 8-hour time window and 1000 s low-pass. Right column: 8-hour time window and bandpass between 360 s- 50 s. The Z, East and North components are shown in the top, middle and lower panel, respectively. The trace order is the same as in Figure 6.4.4 (left).

A third way to compare the instruments is to compare directly the waveforms for different frequency bands. This is done in Figure 6.4.7 - Figure 6.4.9 For very low frequencies > 0.001 Hz (Figure 6.4.7 left column) one can see the earth tides on the Z and East component (confirmed also by observations with a Streckeisen STS2 at the test site); in addition, the vertical component also show settling events. On the North component we find coherent seismic signals with about twice the earth tide amplitudes. We do not know the reason for the of the relatively strong and coherent signals on the N components, but it is certainly not an instrumental feature

or caused by thermal convection, since we also see them on the STS2 in the neighbor pit. Figure 6.4.7 (right column) displays the waveforms for a filter band between 360 s - 50 s.We see again good coherency of the North-components due to the high amplitudes of the ambient seismic signal. The East and vertical components show weak coherency. The poor coherency of the vertical components is mainly caused by a number of settling events, which will cease in time.

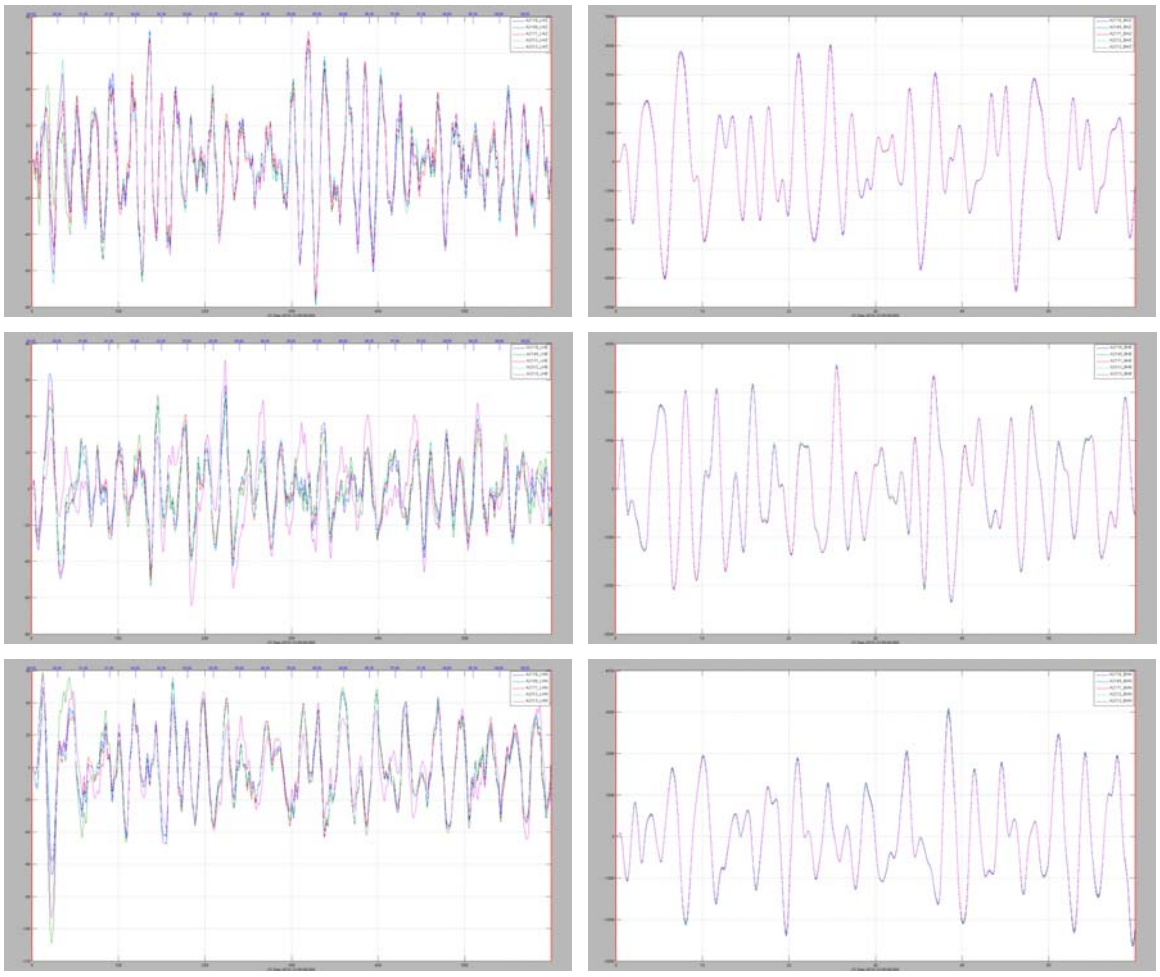

Fig. 6.4.8. Same as Figure 6.4.7, but for shorter time windows and higher frequency bands. The waveforms are now overlaid for better comparison. Left: 10-minute time window and bandpass between 0.02 Hz - 0.05 Hz. Right: 1-minute time window and bandpass between 0.05 Hz - 1 Hz.

Figure 6.4.8 shows the trace overlaid for better comparison. For a bandpass between 0.02 Hz - 0.05 Hz (left column) we see deviations between the horizontal components and very minute differences of between the vertical traces. For a bandpass 0.05 Hz - 1 Hz (Figure 6.4.8 right column) and 1 Hz - 20 Hz (Figure 6.4.9 left column) we observe perfect alignment of all traces. In the very high frequency band 20 Hz - 40 Hz (Figure 6.4.9 right column) the similarity between the traces starts to decrease again. The phase coherency is still ok for most of the wavelets, but we can observe differences in the amplitudes.

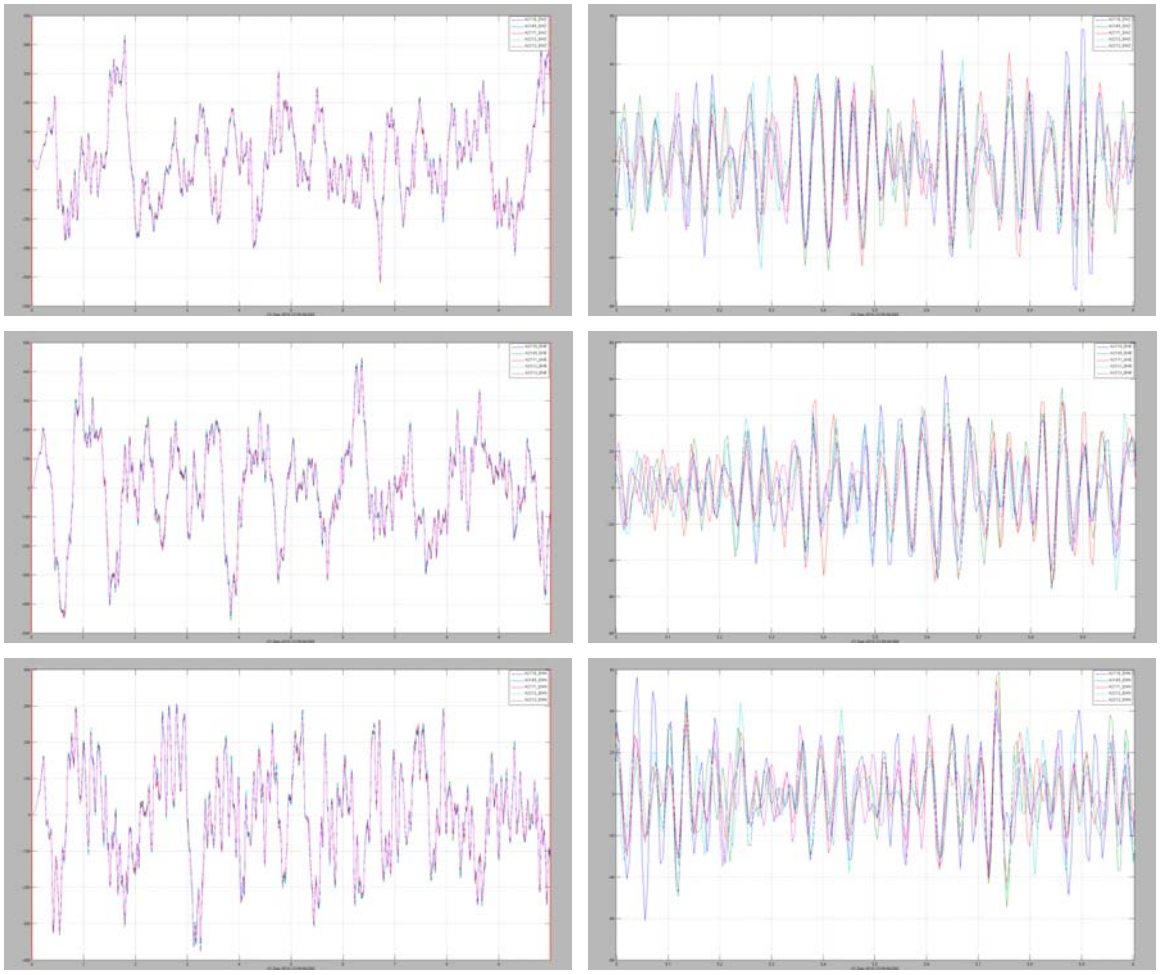

Fig. 6.4.9. Same as Figure 6.4.8, but for shorter time windows and higher frequency bands: Left: 10-second time window and bandpass between 1 Hz - 20 Hz. Right: 1-second time window and bandpass between 20 Hz - 40 Hz.

6.4.3 Conclusions

In the framework of the recapitalization of the NORSAR arrays we intend to install new seismic sensors with a hybrid response function. The transfer function of the instruments was designed to be suitable for the ambient noise conditions of our sites and to deliver similar or higher data quality than the existing systems are doing. The instrument noise of the new hybrid sensors is below the Peterson model for frequencies above 0.03 Hz. The coherency is very good (> 0.9) for frequencies between 0.03 Hz and 20 Hz under quiet ambient noise conditions. From direct waveform comparisons we can conclude that we can expand these frequency limits (especially in the high-frequency end) for practical applications, because the waveform similarity is still good.

6.4.4 References

Kay, S. M. (1988) Modern Spectral Estimation. Englewood Cliffs, NJ: Prentice-Hall, 1988. pp.453-455.

Peterson, J. (1993). Observations and modeling of seismic background noise. USGS Open-File Report 93-322.

Welch, P. D. (1967). The Use of Fast Fourier Transform for the Estimation of Power Spectra: A Method Based on Time Averaging Over Short, Modified Periodograms", IEEE Transactions on Audio Electroacoustics, Volume AU-15 (June 1967), pages 70–73.

Michael Roth
Jan Fyen
Paul W. Larsen
Johannes Schweitzer